Optimization of furfural production processes simultaneous stripping

van Kampen, J.

Award date:
2016

Technische Universiteit
Eindhoven
University of Technology

Optimization of furfural production processes

Simultaneous stripping

Jasper van Kampen

July 2016

CONFIDENTIAL

Student: Jasper van Kampen
Student number: 0675099
Daily supervisor: V. Krzelj
Supervisor/ Graduation Professor: Dr. ir. J. van der Schaaf
Internal committee member: Dr. M.F. Neira d'Angelo
External committee member: Dr. F. Gallucci
Date: 8th of July 2016

Contents

Abstract

Given the importance of renewably-sourced feedstocks for the production of chemicals as alternative to using petrochemicals and therefor the importance of an improvement of the furfural production process, a promising process with simultaneous stripping is reported in this study.

A setup is constructed as an experimental platform to perform stripping experiments under various conditions, both in a semi-batch and continuous fashion. Kinetic experiments are done as well to account for the degradation loss of furfural.

In this study thermodynamic models for the sulfuric acid catalyzed dehydration of xylose to furfural are developed and reported as well. The key steps in this model are the conversion of xylose, both the dehydration towards furfural and loss reactions, the degradation of furfural and the stripping of the vapor phase. Vapor-liquid equilibria are described using the van Laar equations or NRTL models. For a multicomponent NRTL model binary interaction parameters are fitted from experimental data.

Stripping proves to be able to improve the furfural yield, which together with the productivity of the reaction could be optimized by altering the operating conditions. Furfural yields up to 70% are reported under the used conditions. Model predictions show even higher yields could be obtained and the production rate could be significantly increased.

Regarding the hydrogenation of furfural as the next step in biomass valorization, the use of hydrogen as stripping agent is a promising development for process intensification.

1. Introduction

There is an increasing interest in using renewably-sourced feedstocks for the production of chemicals as alternative to using petrochemicals. Furfural is currently used as input material in production of various resins, herbicides and stabilizers, and it is also used as a solvent. [1] It is produced globally at about 300 kilotonnes per annum from pentosane rich biomass feedstocks such as corn cob and sugarcane bagasse. Furfural is considered to be a versatile platform chemical and one of the key renewably-sourced feedstocks for products that could compete with petroleum based chemicals. [2]

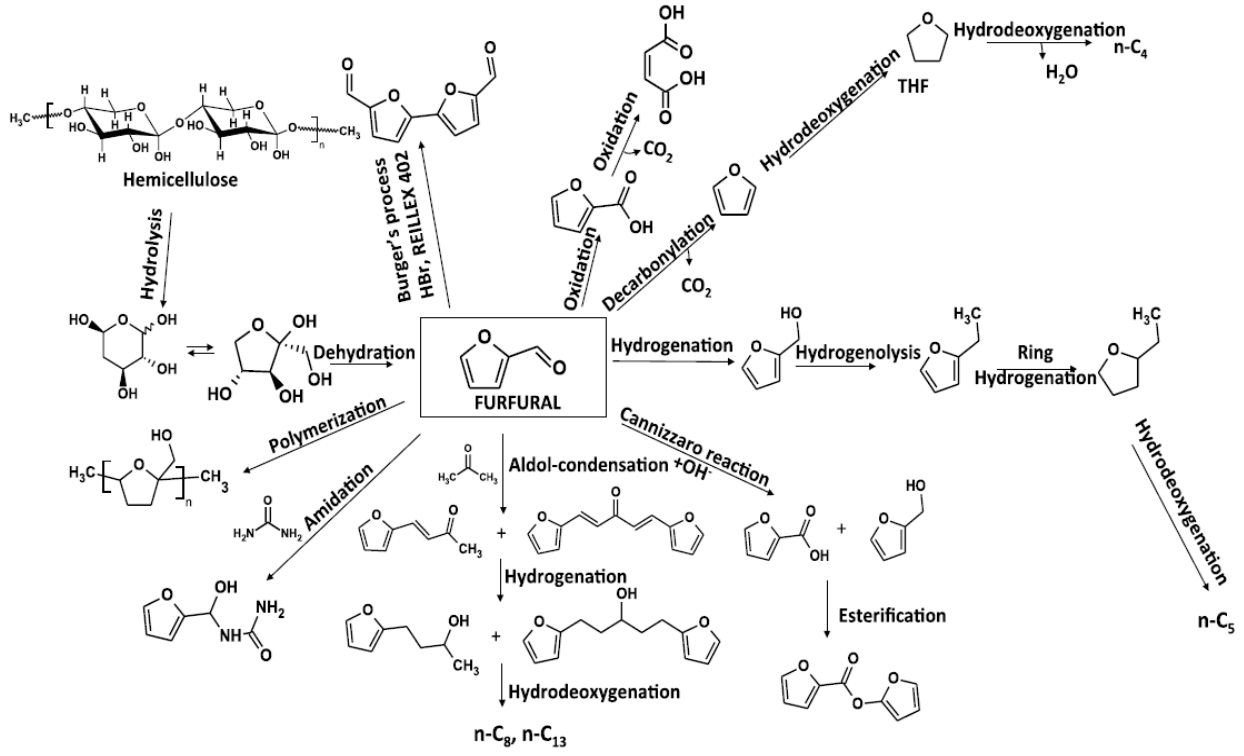

Figure 1: Furfural platform chemical

In the figure below the simplified mechanism for furfural synthesis from hemicellulose of biomass is shown. [3]

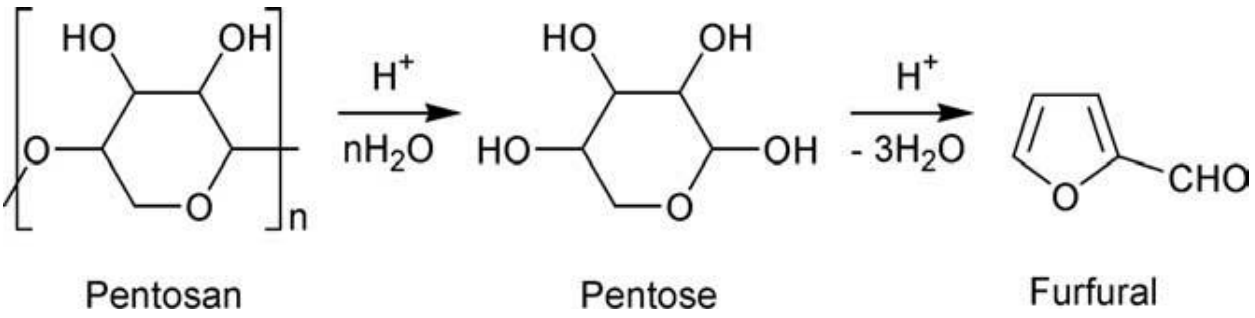

Figure 2: Simplified reaction pathway towards furfural

The majority of current production is still based on more or less modified versions of the original Quaker Oats process (1921). [4] For reason that can be related to their limited technological evolution, the production processes in use today generally suffer from low yields (around 50%), besides significant environmental concerns. The main reason for low furfural yields are consecutive reactions of furfural which are leading to formation of humins. [5] In current commercial processes steam is used as a stripping agent in order to remove furfural from the reactive mixture. However the steam consumption in this processes is very high (around 16 kg of steam per kg of furfural) and therefore furfural is obtained in low concentrated aqueous solutions. [1]

The integrated production of furfural within modern biorefineries is a big opportunity. [2] Since the next step in biomass valorization is hydrogenation of furfural, the idea is to use hydrogen as a stripping agent to remove furfural from the aqueous phase. Additional benefit, compared with current industrial processes, would be that higher furfural concentrations could be obtained. However, due to safety reasons, in this project nitrogen will be used as a stripping agent.

Especially in the Chemelot InSciTe biobased materials project the goal is to go to a biobased C5/C6 monomer. The chosen platform molecule, furfural, could be hydrogenated to cyclopentanone. Which on its turn is a suitable monomer for polymerization reactions. [6] This hydrogenation step in an aqueous, acidic, environment makes the stripping of furfural with hydrogen an interesting process intensification step.

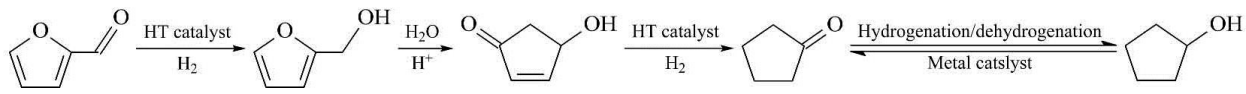

Figure 3: Hydrogenation pathway of furfural

The use of nitrogen as a stripping agent for optimizing furfural production processes will be investigated under different conditions. Xylose will be used as model (biomass) compound to simplify the reaction mechanism. The study is done by experimental procedures in an autoclave setup at elevated temperatures and pressures, and by modeling the furfural production process using Matlab as a programming platform.

2. Theory

Furfural formation from biomass/ xylose

As already stated before furfural is mainly produced from pentosane rich biomass feedstocks. Universally raw agricultural materials, mainly hemicellulose, so rich in pentosane, are used for the production of furfural. [1] Aqueous acid catalysis is used to hydrolyze the hemicellulose stream into pentoses, such as xylose. In the following step, the dehydration of pentose to furfural, again aqueous acidic conditions are used.

Regarding the mechanism of furfural production from xylose contradictory theories exist in literature. [2] Various schemes have been proposed to explain the dehydration mechanism and no real consensus is reached of the advantage of one scheme over another. The main differences conclude the formation of aliphatic or aromatic intermediates in the dehydration reaction. Knowledge of the mechanism is necessary to reduce the formation of side/loss products by designing new/ different reaction systems. Danon et al. investigated the mechanistic and kinetic aspects of furfural formation using homogeneous catalysis. They suggest the plausible mechanism that could be seen in Figure 4. The complex set of side and loss reactions, involving most likely intermediates, remain largely unknown. [5]

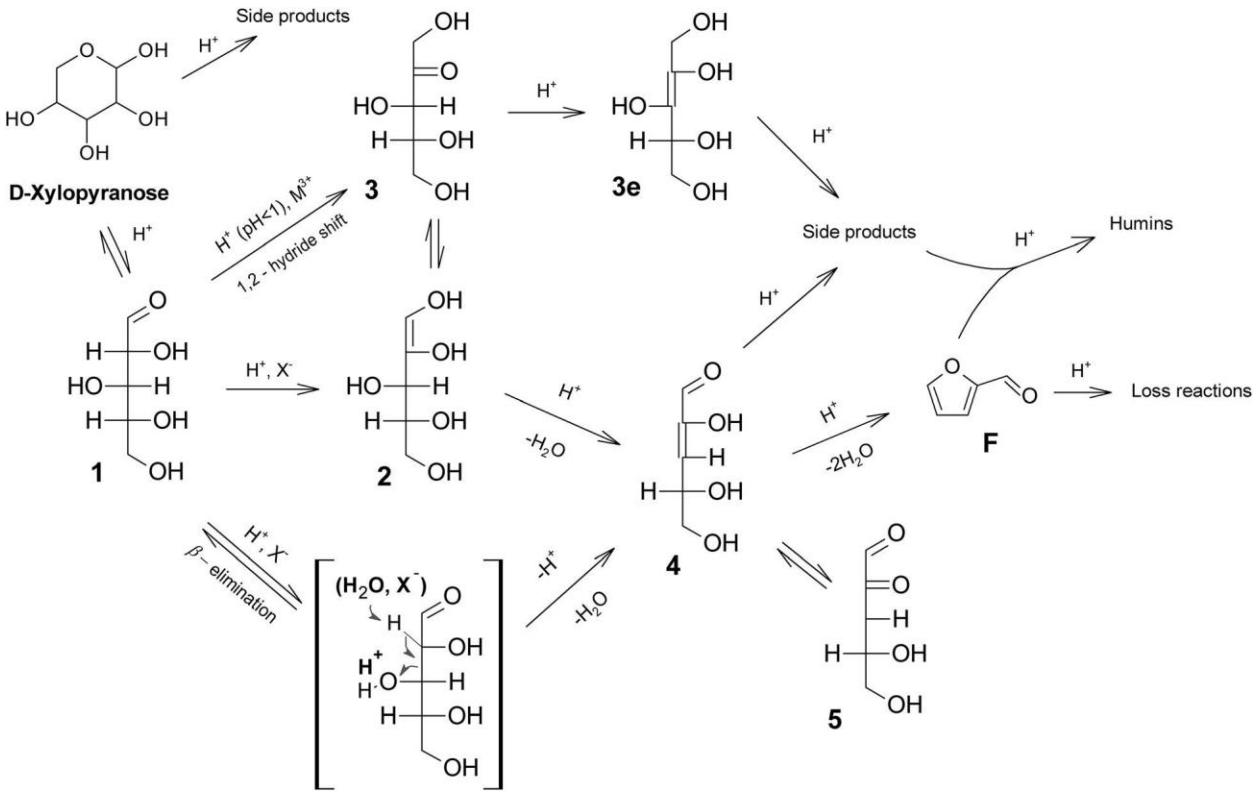

Figure 4: Furfural reaction mechanism

The production of furfural knows several side reactions, one of these is the formation of humins. Humins are basically black, resinous loss products and therefor already could be imagined as undesired. These losses can be attributed by reactions of furfural with itself, also often called resinification and of furfural with intermediates in the xylose to furfural reaction. [2] Furfural resinification is considered to be a first order reaction in the concentration of furfural, and is also dependent on the concentration of the used acid as several authors reported for various homo- and heterogeneous catalysts. [1] [3] [7] [8] The kinetics of this furfural loss are studied by Marcotulio et al. They conclude that the rate constant of this reaction is lumped with the ion activity of sulfuric acid. [7]

The condensation reactions leading to losses are harder to investigate. Upon addition of furfural to a solution of xylose the conversion rate of the xylose does not change. This clearly indicates that furfural has no loss reaction with xylose itself. This combined with the observation that furfural yields decrease when adding furfural to a xylose solution, indicates that furfural reacts with one or more intermediate products. It is unclear if furfural reacts in first and/or second order reactions with the intermediates. The only way which is used to determine these condensation losses is to look at the actual yields from experimental data and compare them to (possible) yields with only resinification loss. [9] [1]

By increasing the temperature the loss by resinification decreases strongly compared to the conversion of xylose. The explanation by Zeitsch for this is considered to be an entropy effect. Depending on the used conditions, but especially in this case the condensation reactions are considered the main loss.

Furfural is not the only product that could be obtained by the acid catalyzed conversion of biomass. Typical products from the conversion of biomass include furfural (from pentose from hemicellulose), levulinic acid (from hexose from cellulose), acetic acid, glycolic acid and lignin and lignin degradation products. [10] When focusing on the conversion of hemicellulose several organic acids, such as pyruvic, glycolic, lactic, formic and acetic acid, could be formed besides furfural by acidic, alkaline or hydrothermal degradation. [11] These acids are formed in relatively small amounts and there reaction is favored in mild conditions. Under more harsh temperature and acidic conditions conversion of pentoses to furfural would be the main reaction taking place.

The production of furfural from biomass is already a relatively old process and suffers among other issues from low yields. Various approaches have been investigated to improve the yield of furfural, produced from xylose or pentosane rich biomass. Multiphase systems, heterogeneous catalysis, microwave reactors, addition of salts are some of these investigations. Most of them are based on the reduction of the loss reactions that produce humins.

Several studies focus on new catalysts compared to the traditional used sulfuric acid, or sometimes hydrochloric acid, as homogeneous catalyst. Rackemann et al. made use of methanesulfonic acid (MSA) as a heterogeneous catalyst to form levulinic acid and furfural. Which showed no significant differences between sulfuric acid and MSA for the formation of levulinic acid, but sulfuric acid showed to be better for the production of furfural. [10] Micro-mesoporous sulfonic acid catalysts are investigated by Dias et al. Which only gave reasonable yields in biphasic/ organic solvent mixtures (10-70%). [3] Metkar et al. investigated solid acid catalysts in combination with reactive distillation. A combination of solid catalyst,

organic solvent (biphasic) and steam stripping resulted in the highest furfural yield. [12] Amberlyst was used as a heterogeneous catalyst by Agirrezabal-Telleria et al. They studied the production of furfural using this solid catalyst with simultaneous stripping and showed some improvements compared to the current production processes. [8]

Co-catalysis with acetic acid was proven to enhance lignin removal from residue biomass. Where high $FeCl_3$ concentrations caused improved cellulose degradation in corncob. [13] This synergy effect between solid acid catalysts and carboxylic acids was also investigated by Doiseau et al. Suggesting contributive effect of Lewis acid sites to the Brønsted acidity. [14] Chaudhary et al. also investigated the conversion of xylose to furfural using the combination of Lewis and Brønsted acid catalysts, improving the yield towards furfural. [15]

As already mentioned Agirrezabal-Telleria et al studied the production of furfural using solid catalyst with simultaneous stripping. [8] An increased yield and almost 100% selectivity in the condensate were achieved. Also the formation of water-furfural phase separation was seen at high xylose loadings. It was also shown that the use of simultaneous stripping has even more potential in increasing furfural yield than using a biphasic (toluene) system, both with xylose single feed and xylose and glucose feeding combined. [16] An economic evaluation of stripping by steam or nitrogen, done by Telleria et al., showed that a cost reduction of 60% could be achieved if the current furfural production process would be replaced by N_2-stripping. [17]

The majority of the current furfural production is still based on more or less modified versions of the original Quaker Oats process from 1921. [4] [18] The Quaker Oats process is traditionally a batch process in which the raw material is mixed with sulfuric acid. Steam is applied for several hours to heat the reaction. 50% of the theoretical possible yield of furfural could be obtained.

Later on a continuous variation on the original process was developed. Steam and sulfuric acid are added to pretreated material and the residue could be discharged. A yield of 55% could be obtained with a residence time of 1 hour.

Zeitsch himself has developed the SupraYield process. In this process the produced furfural is continuously removed from solution by slow depressurization of the reactor. The idea behind this process is that there is no furfural present in the liquid phase, where it could undergo loss reactions. Yields of 50 to 70% have been reported for this commercialized process. [1] [2]

Another process developed is the Biofine process. This process is designed for the production of levulinic acid, but produces furfural as a byproduct with high yield (~70%).

Besides low yields there are also significant environmental concerns with the current production processes. Many authors suggest the use of solvents in multiphase systems to improve furfural production. [3] [12] [19] The investigations of these systems remain on lab scale and are mostly done in batch till the present day. Unfortunately solvents bring cost issues and the need for additional recovery/ purification steps. In addition, many industrial solvents have issues of health, flammability and environmental effects around them.

The consumption of steam, that is used as a stripping agent in order to remove furfural from the reactive mixture, is very high (around 16 kg of steam per kg of furfural). Therefore furfural is also obtained in low concentrated aqueous solutions.

Hydrogenation of furfural

In the valorization of biomass the hydrogenation of furfural is often the next step. Hydrogenation is also a method used to avoid undesired reactions of furfural [20], as described before. Furfural could be hydrogenated to different products, such as furfuryl alcohol, cyclopentanone and cyclopentanol, which is shown in Figure 5. [21]

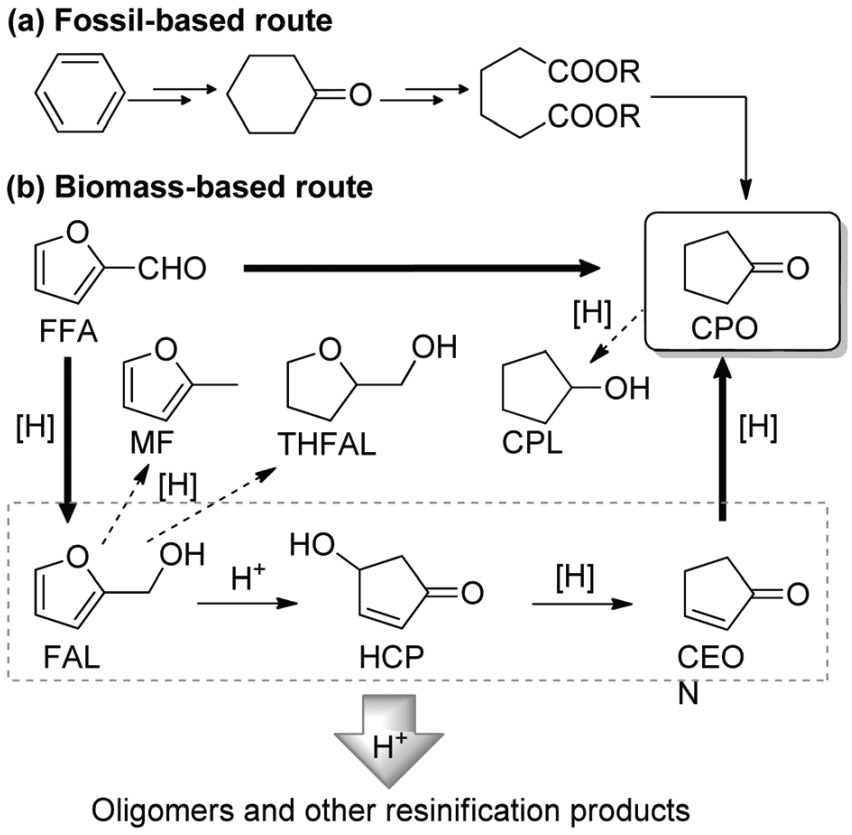

Figure 5: Furfural hydrogenation routes

Furfural could be hydrogenated to furfuryl alcohol (FAL), which is mainly used for the production of resins. This hydrogenation could be done in liquid or in vapor phase. Amongst others Vargas et al. show furfuryl alcohol could be produced with high selectivity and yield in the vapor phase. [20]

Other hydrogenation products of interest are cyclopentanol (CPL) and cyclopentanone (CPO). These are versatile compounds used in the preparation of fungicides, flavors, pharmaceuticals, rubber chemicals and materials. [21] Potentially it could be used for the preparation of polymers (polyamides). [6] Currently the production of these chemicals is still based on fossil based feedstocks, as could be seen in Figure 5, while they could be formed from furfural (biobased) as well.

Hronec et al. showed that furfural can be selectively converted to cyclopentanone in aqueous media, depending on the specific reaction conditions. [6] Later Zhu et al. and Zhou et al. show selective formation of cyclopentanol and cyclopentanone using copper derived catalysts in aqueous condtions. [22] [23] Recently Zhang et al. proposed a supported gold catalyst which showed over 99% selectivity towards cyclopentanone with full conversion.

Compared to the hydrogenation towards furfuryl alcohol, the hydrogenation towards cyclopentanol/cyclopentanone is only achieved in aqueous phase.

Modeling of the furfural production process

Kinetics

Several authors who investigated the production of furfural from biomass/xylose also tried to model their experimental data. [19] [8] The models vary by the mono-/multiphase systems used and the loss reactions that are assumed. It is widely accepted that the rates of reaction are depending on the acid or acidic catalyst concentration. Further kinetic parameters (and distribution coefficients) are estimated by fitting the proposed models to obtained experimental data.

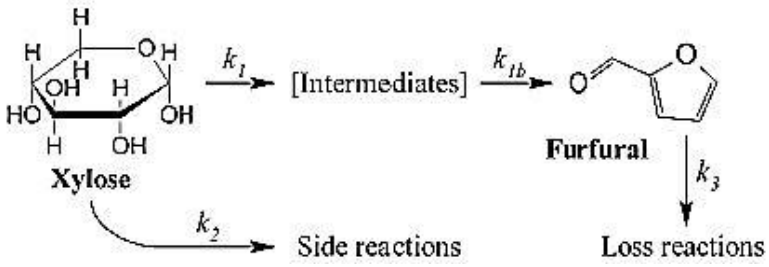

Figure 6: Furfural production

The main reaction is the dehydration of xylose towards furfural, in which three water molecules are formed. As could be seen from Figure 6 there are two more reactions for the system, a side reaction for xylose and product loss. Using a steady state approximation for the intermediates, the reaction rates could be defined as follows:

$$r_{X,1} = -k_1 C_{acid} \gamma_{acid} C_X \quad \text{(Eq. 1)}$$

$$r_{X,2} = -k_2 C_{acid} \gamma_{acid} C_X \quad \text{(Eq. 2)}$$

$$r_{F,3} = -k_3 C_{acid} \gamma_{acid} C_{Fur} \quad \text{(Eq. 3)}$$

Marcotulio et al. show kinetic correlations for the conversion of xylose, as well as for the destruction of furfural. [7] [24] They conclude that the rate constant of these reactions are lumped with the ion activity of sulfuric acid, not merely the concentration. The correlations described by Marcotulio et al. are shown below:

$$\ln(k_x^*) = 31.86 - \frac{133.3\ 10^3\ [\frac{J}{mol}]}{RT} \quad \text{(Eq. 4)}$$

$$\ln(k_3^*) = 26.64 - \frac{125.1\ 10^3\ [\frac{J}{mol}]}{RT} \quad \text{(Eq. 5)}$$

$$k = k^*\ C_{acid}\ \gamma_{acid}\ [s^{-1}] \quad \text{(Eq. 6)}$$

In these equations k_x is the kinetic rate constant for the conversion of xylose, k_3 is the rate constant for the degradation of furfural and γ is the activity coefficient of the acid. In an ideal solution the amount of H^+ ions that are dissociated, are equal to the acid concentration. In several cases there is (strong) deviation from ideality and γ is an indication of this deviation.

To conversion of xylose to furfural (k_1) and byproducts (k_2) are not described separately by Marcotulio et al. The constant k_x describes the total conversion of xylose, both towards furfural (k_1) and byproducts (k_2).

$$k_x = k_1 + k_2 \quad \text{(Eq. 7)}$$

Activity coefficients

To describe vapor-liquid equilibria that do not show ideal behavior, activity coefficients are necessary. Activity coefficients of components in a mixture could be calculated with several methods. Among these are the use of the so-called van Laar equations and the use of Non Random Two liquid composition models (NRTL).

Van Laar equations

To implement the binary interactions between the components in the reactor the van Laar equations could be useful solutions. [25] Van Laar already derived his equations, based on the van der Waals equation, from a thermodynamic study early in the 20th century. Van Laar's equations for a binary mixture are shown below:

$$\log(\gamma_1) = \frac{Bx_2^2}{(x_2+\frac{B}{A}x_1)^2} \quad \text{(Eq. 8)}$$

$$\log(\gamma_2) = \frac{Ax_1^2}{(x_1+\frac{A}{B}x_2)^2} \quad \text{(Eq. 9)}$$

In this method A and B are the van Laar constants. Derived from these equations A and B are equal to the theoretical value of the logarithm of the activity coefficient at mass fraction/ concentration of zero:

$$A = [\log(\gamma_2)]_{x_2=0} \quad \text{(Eq. 10)}$$

$$B = [\log(\gamma_1)]_{x_1=0} \quad \text{(Eq. 11)}$$

The van Laar coefficients have to be obtained by regression of experimental VLE data. [26] [27]

NRTL

The non random two liquid model (NRTL) was first described by Prausnitz et al. [28] They derived a new equation, based on a local compositions concept. The local compositions are given by [29]:

$$x_{ji} = \frac{x_j \exp(-\alpha_{ji}\tau_{ji})}{\sum_{k=1}^{c} \exp(-\alpha_{ki}\tau_{ki})} \quad \text{(Eq. 12)}$$

The local mole fraction of a component is given as x. τ is a parameter that is based on the energies of interaction between components. α is an constant, determined by the nonrandomness of the mixture. Especially the nonrandomness parameter makes it applicable to a variety of mixtures.

The molar excess Gibss energy is the sum of the changes in residual Gibss energy. The NRTL equation is expressed as:

$$\frac{g^E}{RT} = \sum_{i=1}^{c} x_i \left[x_{ji}\tau_{ji}\right] \quad \text{(Eq. 13)}$$

The expressions for the activity coefficients for the NRTL model could be found by differentiation of this equation:

$$\ln(\gamma_i) = \frac{\sum_{j=1}^{c}(\tau_{ji}G_{ji}x_j)}{\sum_{k=1}^{c}(G_{ki}x_k)} + \sum_{j=1}^{c}[\frac{(x_jG_{ij})}{\sum_{k=1}^{c}(G_{kj}x_k)}(\tau_{ij} - \frac{\sum_{k=1}^{c}(x_k\tau_{kj}G_{kj})}{\sum_{k=1}^{c}(G_{kj}x_k)})] \quad \text{(Eq. 14)}$$

For a binary mixture this could be rewritten to:

$$\ln(\gamma_1) = x_2^2(\tau_{21}\left(\frac{G_{21}}{x_1+x_2G_{21}}\right)^2 + \left(\frac{\tau_{12}G_{12}}{(x_2+x_1G_{12})^2}\right)) \quad \text{(Eq. 15)}$$

$$\ln(\gamma_2) = x_1^2(\tau_{12}\left(\frac{G_{12}}{x_2+x_1G_{12}}\right)^2 + \left(\frac{\tau_{21}G_{21}}{(x_1+x_2G_{21})^2}\right)) \quad \text{(Eq. 16)}$$

In the equations the parameter G is defined as follows:

$$G_{ji} = \exp(-\alpha_{ji}\tau_{ji}) \quad \text{(Eq. 17)}$$

The parameter τ is defined slightly different by various authors.

Among others Sunder et al. describe this parameters as [30]:

$$\tau_{ji} = \frac{\Delta g_{ji}}{RT} \quad \text{(Eq. 18)}$$

Fele et al. use a more practical/ mathematical definition [31]:

$$\tau_{ji} = a_{ji} + \frac{b_{ji}}{T} \quad \text{(Eq. 19)}$$

Others, such as the databases of ASPEN, even extend this expression depending on empirical data:

$$\tau_{ji} = a_{ji} + \frac{b_{ji}}{T} + e_{ji}\ln(T) + f_{ji}T \quad \text{(Eq. 20)}$$

$$\alpha_{ji} = c_{ji} + d_{ji}(T - 273.15) \quad \text{(Eq. 21)}$$

The NRTL activity coefficient model has shown great capabilities in predicting vapor-liquid phase equilibria. A major drawback is the availability of the required molecular interaction parameters though. For a lot of chemical systems these are unknown/unavailable. [29] [30] [31] [32]

3. Experimental section

Setup

To perform stripping experiments a setup was designed. In Figure 7 a schematic overview of the setup is shown. Kinetic and stripping test were performed in a 300 mL autoclave reactor (Autoclave Engineers). The temperature was controlled by electric heating and extreme heat loss to the surrounding was prevented by isolation and extra heat tracing. A backpressure regulator controlled the reactor pressure.

Xylose solutions of different concentrations could be fed from the top of the reactor using a Gilson HPLC pump. Depending on the configuration of the setup, the stripping agent could be fed from the bottom or top of the reactor where it was bubbled into the reactor liquid. The Bronckhorst mass flow controllers could go up to 1000 ml/min at normal conditions. By adjusting the setup to feed the gas from the bottom of the reactor clogging of the reactor sample line could be prevented and better gas distribution was possible. To recover the stripped vapor stream a condenser was designed by the use of a small vessel in an ice bath. Samples for analysis could be taken from the reactor and condensate vessel respectively.

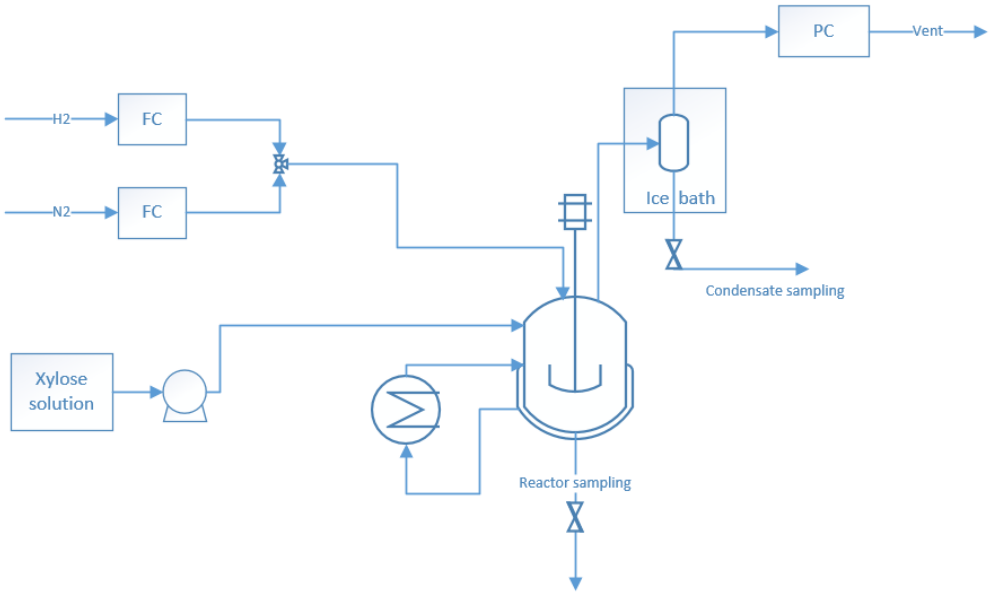

Figure 7: Schematic overview of the first experimental setup

Figure 8: Experimental setup

Kinetic and stripping tests

Furfural (99%), D-Xylose (+99%) and sulfuric acid (99%), purchased from Sigma-Aldrich, were used for the experiments.

Experiments were carried out in a 300 mL titanium reactor (Autoclave Engineers), with controlled electric heating and stirred at 200 rpm. A typical experiment was performed at 170°C and 10 bar pressure. The reactor was first loaded with the corresponding amount of sulfuric acid and demineralized water, then pressurized with nitrogen. After pressurization the reactor was heating to the desired temperature (170°C). A xylose solution of fixed concentration was then fed to the reactor to get the initial concentrations and start the reaction. By this procedure the initial degradation was minimized. A nitrogen flow was bubbled into the reaction liquid with flow rates from 150-1000 ml/min (normal conditions). The stripped vapor stream was led to the condenser, where gas and liquid streams were separated again. Reactor and condensate samples were taken for analysis. Reactor samples were always filtered before analysis to prevent possible solid deposition during the analysis.

For tests under continuous operation the xylose feed rate and feed concentration were adjusted to set the reactor volume constant, inlet flow in respect to stripping rate was adjusted.

Analysis

Components in the reactor and condensate samples were quantified using High Pressure Liquid Chromatography (HPLC) (Shimadzu LC-20AD) with a refractive index (RI) detector (Waters 2414) and Photodiode Array Detector (PDA) (Shimadzu SPD-M20A). The primary column used was a MetaCarb 67C column. A Biorad Animex HPX-87C (sugar) column was used as well for some analysis. New methods were made for the different columns and new calibrations to quantify the concentrations of the components were performed. The column oven was set to 85°C and HPLC graded water was used as mobile phase at 0.5 mL min^{-1}.

Xylose was detected using the RI detector. Furfural was detected both using the refractometer and the PDA detector at 254 nm wavelength. Other components could be detected as well using both detection methods.

Conversion of xylose (X_x), selectivity towards furfural (S_{Fur}) and furfural yield (Y_{Fur}) were calculated as follows:

$$X_X = 1 - \frac{amount\ of\ xylose\ at\ time\ t}{initial\ amount\ of\ xylose} \quad \text{(Eq. 22)}$$

$$S_{Fur} = \frac{amount\ of\ furfural\ at\ time\ t}{amount\ of\ xylose\ converted} \quad \text{(Eq. 23)}$$

$$Y_{Fur} = X_X\ S_{Fur} = \frac{amount\ of\ furfural\ at\ time\ t}{potential\ of\ furfural\ at\ time\ t} = \frac{amount\ of\ furfural\ at\ time\ t}{initial\ amount\ of\ xylose} \quad \text{(Eq. 24)}$$

Modeling

Experimental data were collected and rate parameters were obtained to compare with the proposed kinetic correlations by Marcotulio. [24]

With the use of these kinetic correlations for the dehydration of xylose, thermodynamic models were developed (see Appendix C). The model for the production of furfural consists of a set of non linear ordinary differential equations (ODEs). With Matlab as computational environment the set of ODEs were solved by numerical integration.

In the model it was assumed that degradation only occurs in the aqueous liquid phase, as are all the reactions. Furfural and xylose degradation are only dependent on their own concentration and not on each other or other possible byproducts, see equation 1 till equation 3.

Separate experiments with furfural as feed were performed to determine the rate of furfural degradation and check the proposed kinetic correlation (equation 5).

A steady state approximation is made for possible intermediate products, not including them in the material balances and assuming xylose conversion to furfural or loss products.

4. Results & Discussion

Reaction kinetics

Furfural loss

The loss of furfural could be described as is stated in equation 3. This loss has been investigated in a batch experiment at the general used operating conditions of 170°C and 10 bar and an initial acid concentration of 0.5 w%.

In Figure 9 the results are shown.

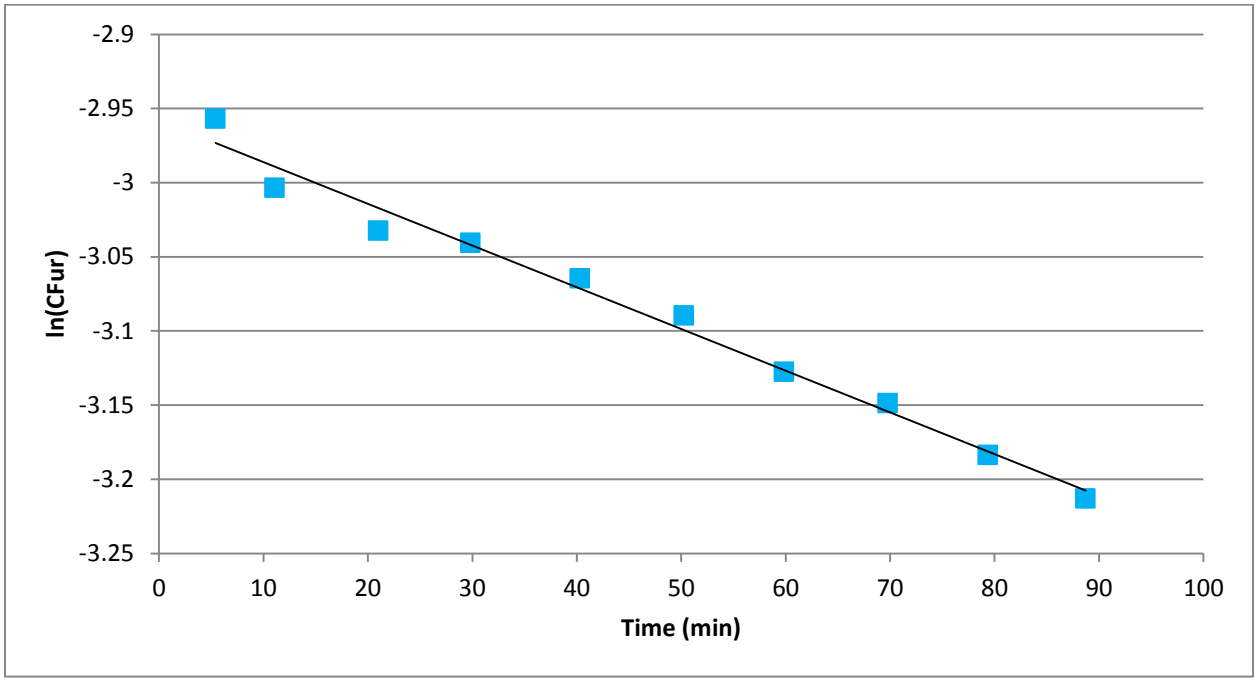

Figure 9: kinetic data for the degradation of furfural; 170°C, 10 bar, 0.5 w% H_2SO_4 and 0.5 w% initial furfural.

The logarithm of the furfural concentration is plotted as a function of the time, whereas the analytical solution of the furfural loss reaction is:

$$C_{Fur}(t) = C_{Fur,0}e^{-k_3 t} \qquad \text{(Eq. 25)}$$

From the slope of the plotted data the average kinetic rate constant k_3 could be determined and was found to be 0.0028 min^{-1}. This is in accordance to the average value of 0.00274 min^{-1} found using the description of this kinetic constant by Marcotulio without including the activity coefficient. [7] In Figure 10 the experimental and calculated concentrations are shown in good correspondence.

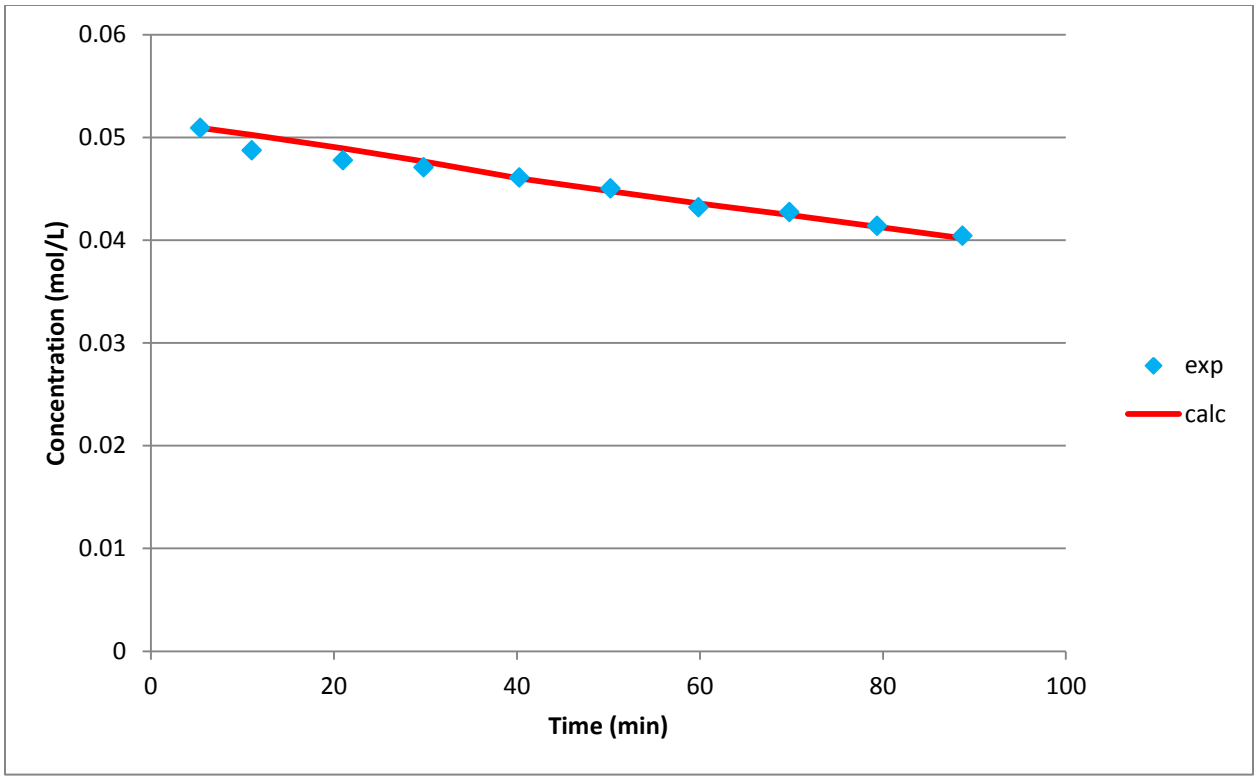

Figure 10: Comparison of experimental and calculated furfural concentrations for furfural degradation; 170°C, 10 bar, 0.5 w% H_2SO_4 and 0.5 w% initial furfural.

Xylose conversion

The conversion of xylose to both furfural and byproducts could be described as the combination of equation 1 and equation2. Where k_1 is the kinetic rate constant for the formation of furfural and k_2 the kinetic rate constant resulting in the formation of byproducts.

As explained before the formation of acids from furfural is favored under mild conditions. So for the used conditions these could be neglected as possible (side) products. k_2 describes loss of xylose to other by-products.

Corresponding to the conversion of furfural, in Figure 11 the logarithm of the xylose concentration is shown as a function of time.

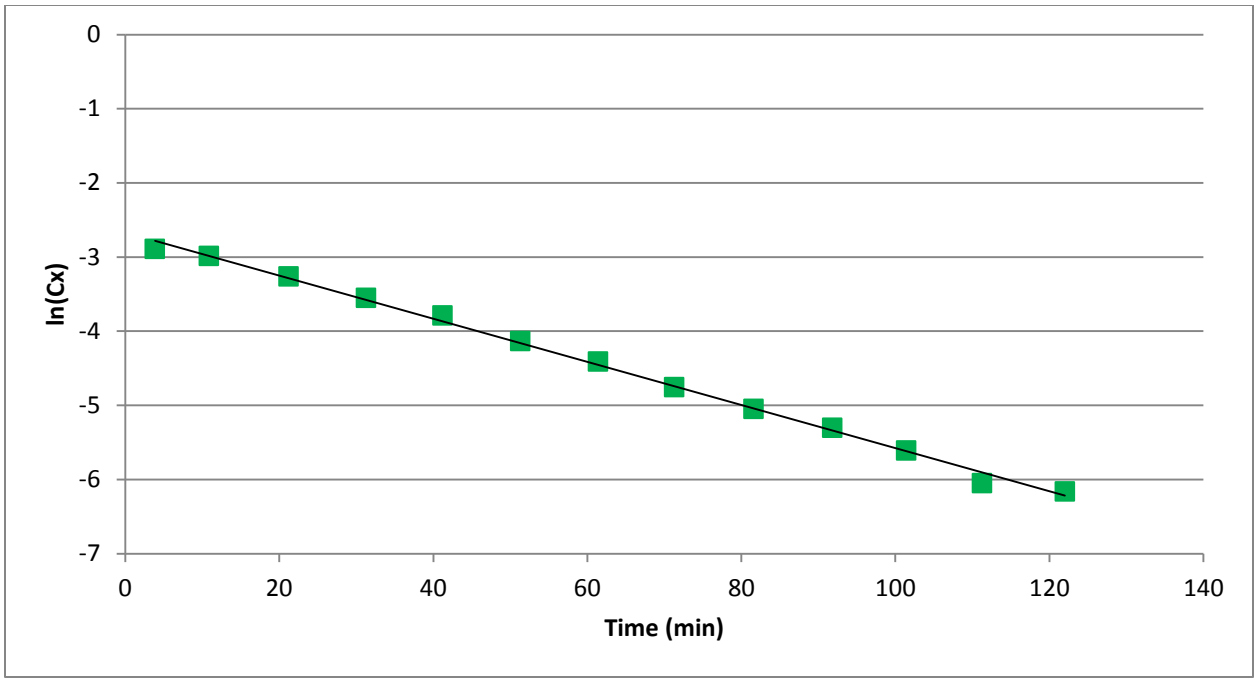

Figure 11: Kinetic data for the conversion of xylose; 170°C, 10 bar, 0.5 w% H_2SO_4 and 1 w% initial xylose.

From Figure 11 an average value for k_x of 0.0291 min^{-1} could be found. This is somewhat less than the calculated average value of 0.033 min^{-1} using the correlation defined by Marcotulio. [24]

It could be concluded that the correlations defined by Marcotulio describe the kinetics of furfural and xylose well under the used experimental conditions, henceforward they are used to describe the kinetics in the furfural production process.

The value of k_x consists of k_1 and k_2, respectively for the conversion towards furfural and byproducts. With all the other values known the exact value of k_1, and with that k_2, could be determined by fitting the experimental data.

The analytical solution for the formation of furfural is (batch):

$$C_{Fur}(t) = C_{X,0}\left(\frac{k_1}{k_3 - k_1 - k_2}\right)\left(e^{-(k_1+k_2)t} - e^{-k_3 t}\right) \quad \text{(Eq. 26)}$$

$$k_x = k_1 + k_2;\ k_1 = f_k k_x \quad \text{(Eq. 27)}$$

In this formulation k_x is divided into k_1 and k_2 by a fraction parameter f_k. The best fit for this fraction parameter f_k is found to be 0.77.

From these kinetic results it could be seen that the loss reaction of furfural is at least ten times slower than the conversion of xylose and about three times slower than the loss reaction(s) of xylose.

Stripping experiments

HPLC

As already mentioned in the experimental section, both reactor and condensate samples are quantified using HPLC. In Figure 12 and Figure 13 typical spectra for a condensate and a reactor sample are shown.

Figure 12: PDA-spectrum for a typical condensate sample

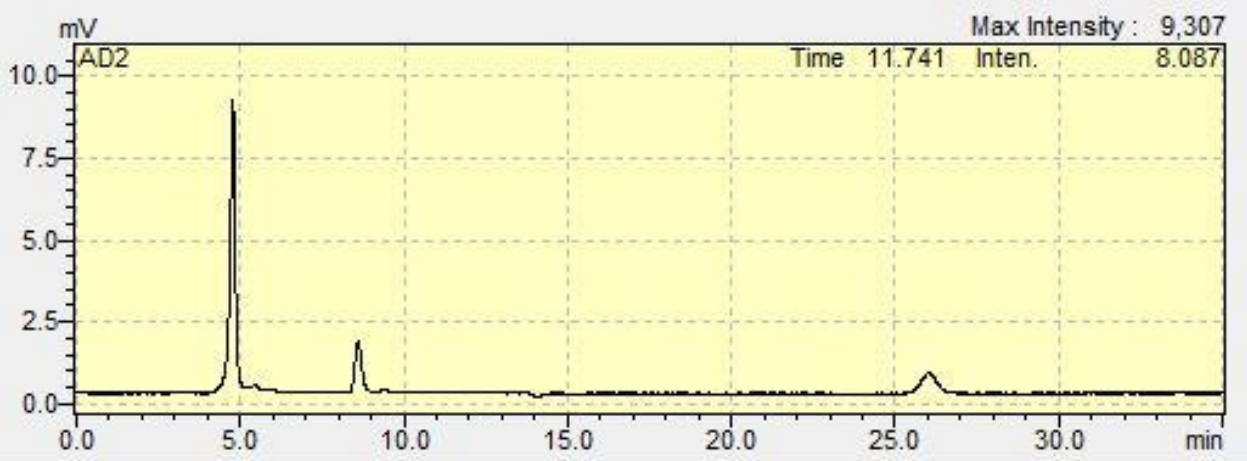

Figure 13: RI-spectrum for a typical reactor sample

As could be seen from Figure 12 only furfural is detected in the condensate samples. So the stripping process is (almost) 100% selective for furfural.

Reactor samples show three clear components, namely sulfuric acid, xylose and furfural. (Figure 13) Also some possible intermediates could be observed.

Stripping rates

For the reaction of xylose to furfural several flowrates of the stripping agent are investigated. An operating temperature of 170°C is chosen at an operating pressure of 10 bar. Initial acid and xylose concentrations were respectively 0.5 w% and 1.0 w%.

Figure 14 shows the conversion of xylose as a function of time. In Figure 15 the corresponding yields are shown. The furfural yield is calculated with the total amount of furfural, both in the reactor and in the condensate.

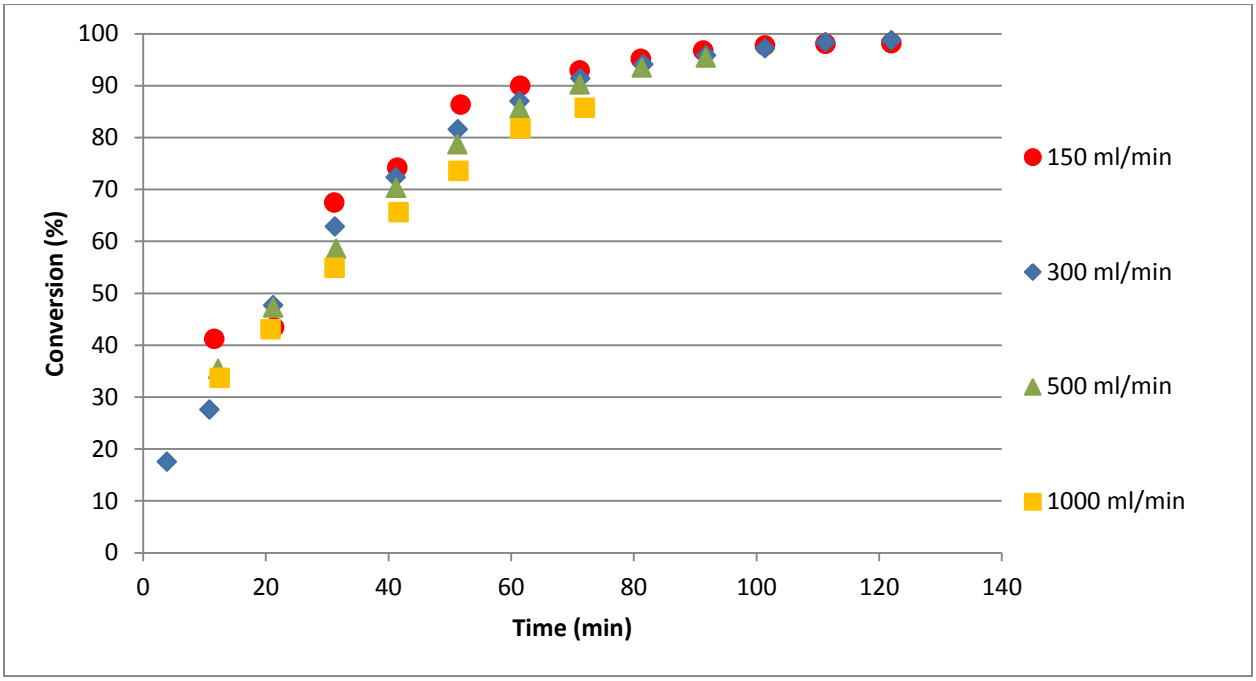

Figure 14: Conversion of xylose as a function of time for stripping rates from 150 to 1000 ml/min; 170°C, 10 bar, 0.5 w% H_2SO_4 and 1 w% initial xylose.

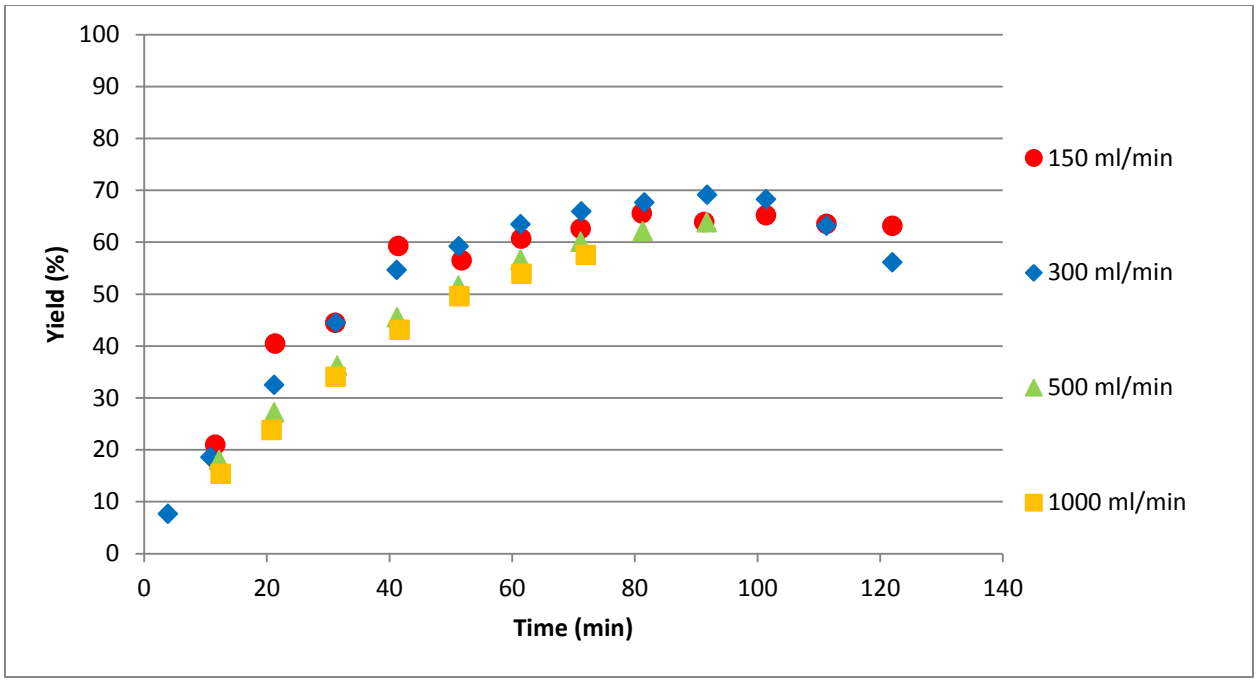

Figure 15: Furfural yield as a function of time for stripping rates from 150 to 1000 ml/min; 170°C, 10 bar, 0.5 w% H_2SO_4 and 1 w% initial xylose.

The initial reaction rate for the lower rate conditions are higher, resulting in a higher initial conversion of xylose. Due to the stripping the acid concentration increases, more for the higher rates than the lower. Therefor the higher stripping rates show a steeper increase in conversion. The difference in initial reaction rates is due to a temperature effect. The stripping stream, N_2, is not preheated and therefore the reactor is slightly cooled down at higher rates.

Concerning the yields no significant differences are seen between the different stripping rates. The corresponding selectivity's vary only between 67 and 72%. This is in contrast to the expectation that a higher furfural concentration in the reactor, which increases with lower rates, would lead to more furfural loss and therefor a lower selectivity/ yield. The low rate of furfural loss, as is determined before, confirms the minimal loss effect though. In Appendix B the amount of furfural in both reactor and condensate are shown for the various stripping rates, from which this effect could be seen clearly as well.

Reproducibility

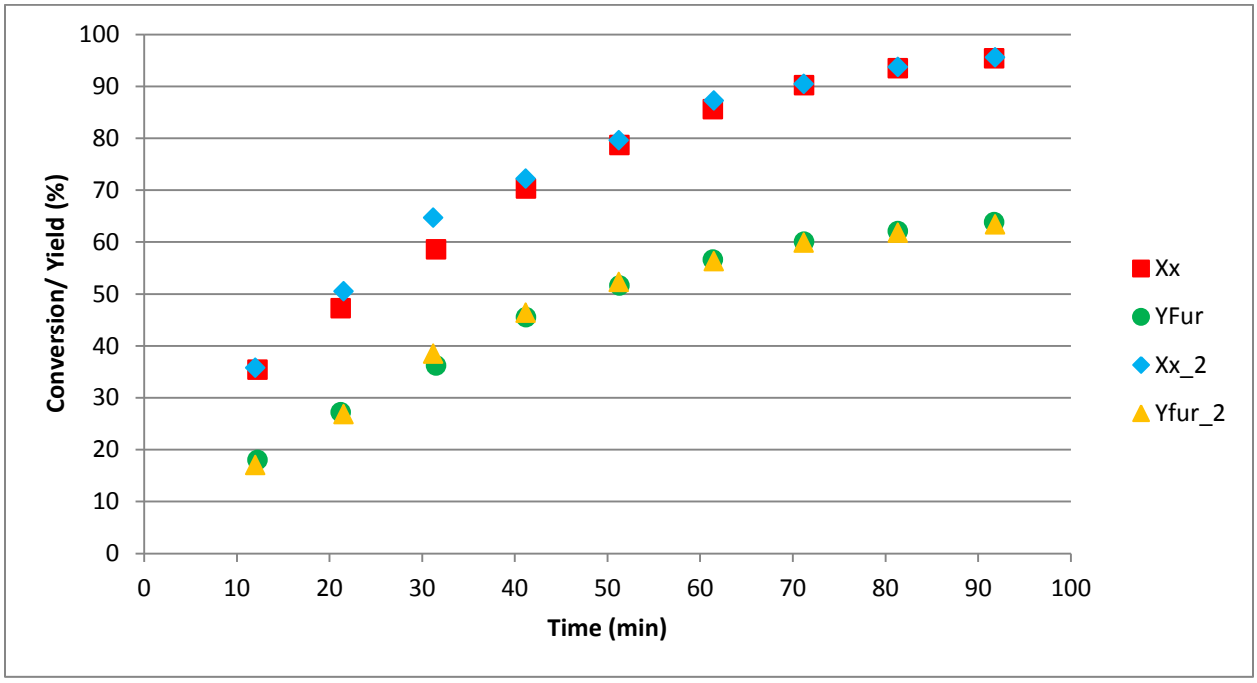

Figure 16: Conversion and yield for 500 ml/min stripping experiments; 170°C, 10 bar, 0.5 w% H_2SO_4 and 1 w% initial xylose.

It is important to validate results, so conclusions are not made without cause. Reproducibility of the experiments is checked by performing duplicate experiments. The results of these match each other well within the expected experimental error, as could be seen in Figure 16.

Continuous operation

Compared to the semi-batch experiments, where the reactor volume decreases due to the stripping, it is interesting to consider continuous operation. By adjusted feed rate and concentration steady state conditions can be achieved at different operating conditions.

In Figure 17 the furfural (FurC and FurR) and xylose (XR) concentrations are shown for continuous operating with a stripping rate of 500 ml/min.

First a xylose solution of 0.25 g/ml is fed at a rate of 4 ml/min to reach an 'initial' xylose concentration of 1 w%. During continuous operation 1.47 ml/min of a 0.05 g/ml xylose solution is fed to maintain a steady state concentration.

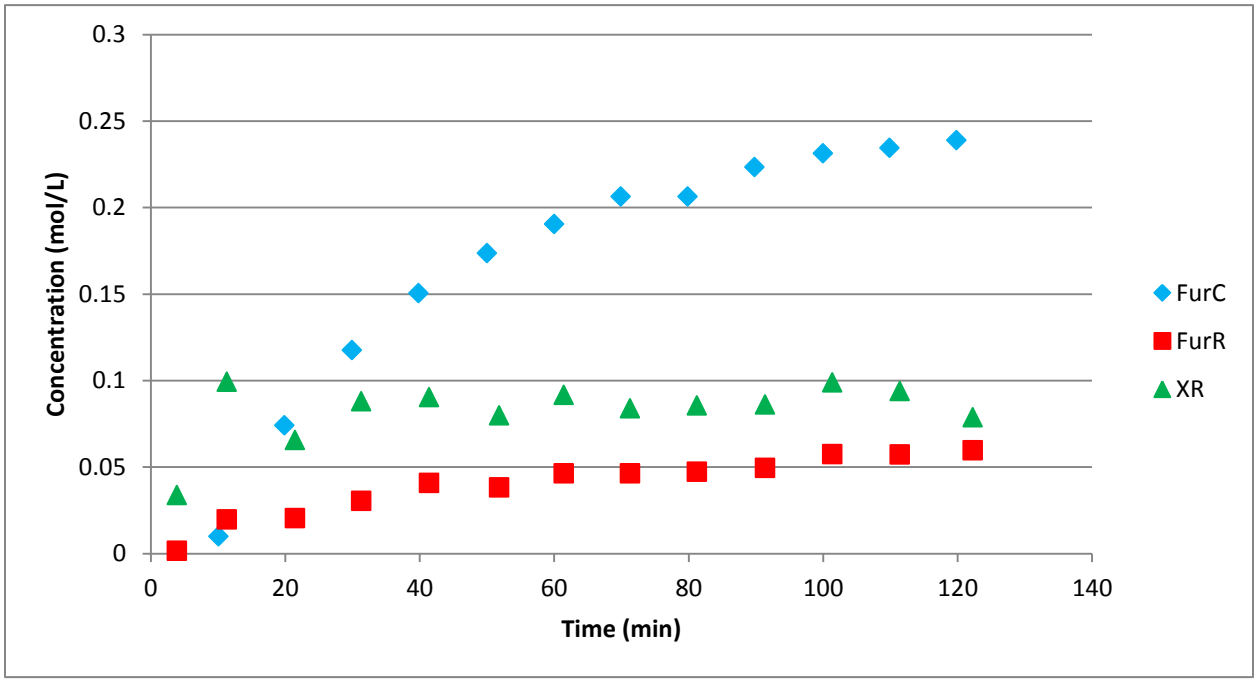

Figure 17: Continuous operation with 500 ml/min stripping rate; 170°C, 10 bar, 0.5 w% H_2SO_4 and 1.47 ml/min 0.05 g/ml xylose feed.

As could be observed from Figure 17 steady state conditions could be reached resulting in a 55% yield at a conversion of 75%.

Model

To describe the furfural production process a model was made using Matlab as programming environment.

The kinetic correlations discussed before are implemented in the model and as could be seen in Figure 18 the conversion of xylose is modeled well.

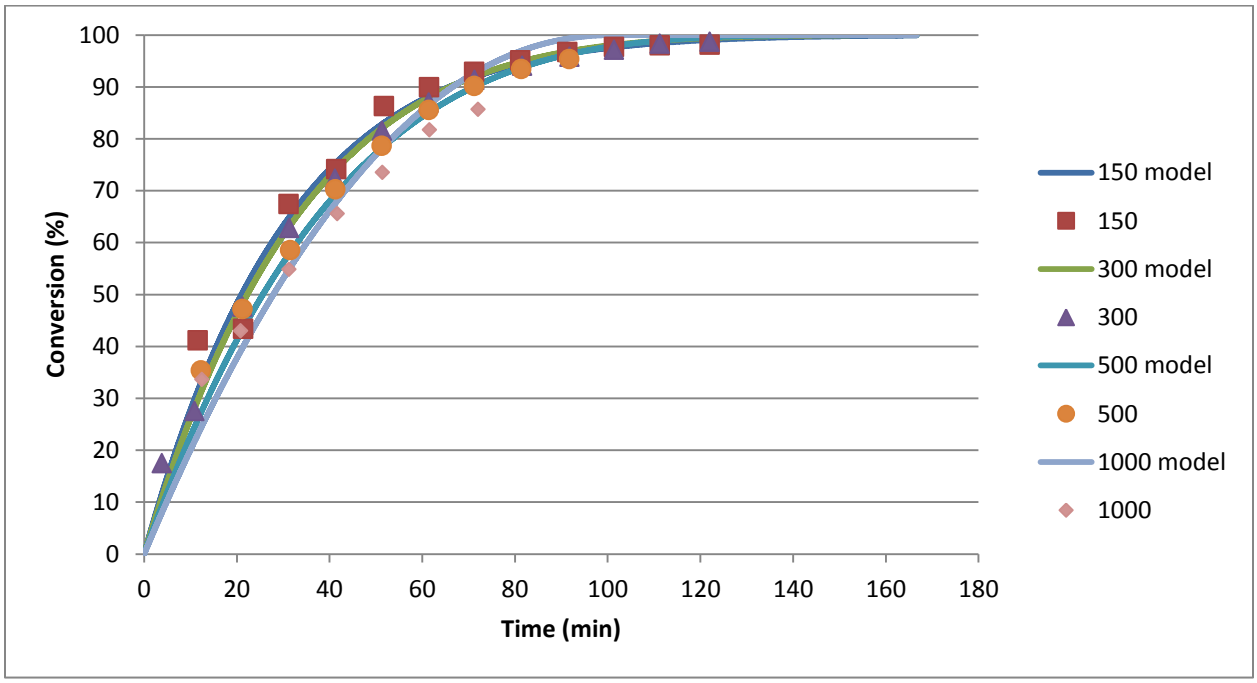

Figure 18: Predicted model conversion compared to the experimental results at different stripping rates; 170°C, 10 bar, 0.5 w% H_2SO_4 and 1 w% initial xylose.

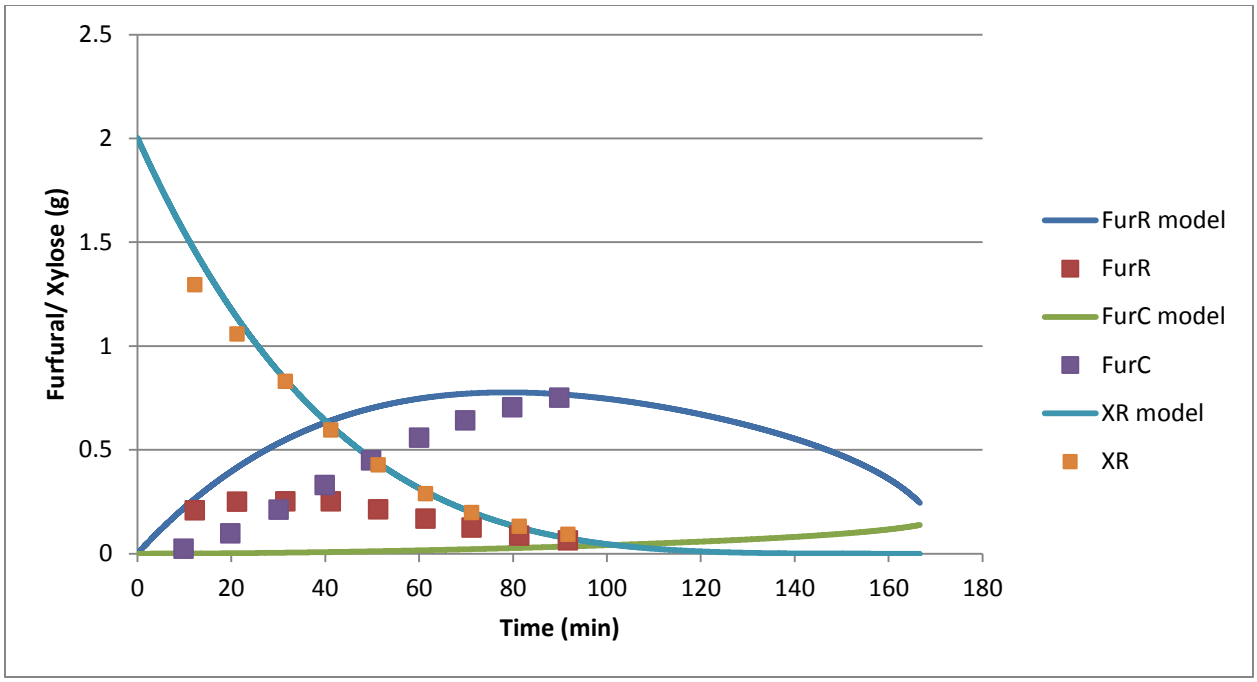

Figure 19: Comparison of model prediction and experimental results for the amounts of xylose and furfural for simple vapor-liquid equilibrium assumption.

As could be seen in Figure 19 simple vapor-liquid equilibrium assumptions do not account for the amount of furfural stripped from the reactor. Assuming ideal behavior the equilibrium (and maximum) gas phase concentration is modeled as:

$$N_{i,G,eq} = \frac{x_i P_i V_G}{RT} \qquad \text{(Eq. 28)}$$

In Figure 20 the mole fraction of furfural in the vapor phase is plotted as a function of the mole fraction of furfural in the liquid phase. These experimental data from Curtis&Hatt show the same trend as the data from Mains and make clear that activity coefficients have to be taken into account. [36] Activity coefficients for furfural, 26.68, and water, 0.999, are taken from literature as estimates for the used conditions. [26] The necessity, but also the possible good model description using activity coefficients could be observed from the results, as are shown in Figure 21.

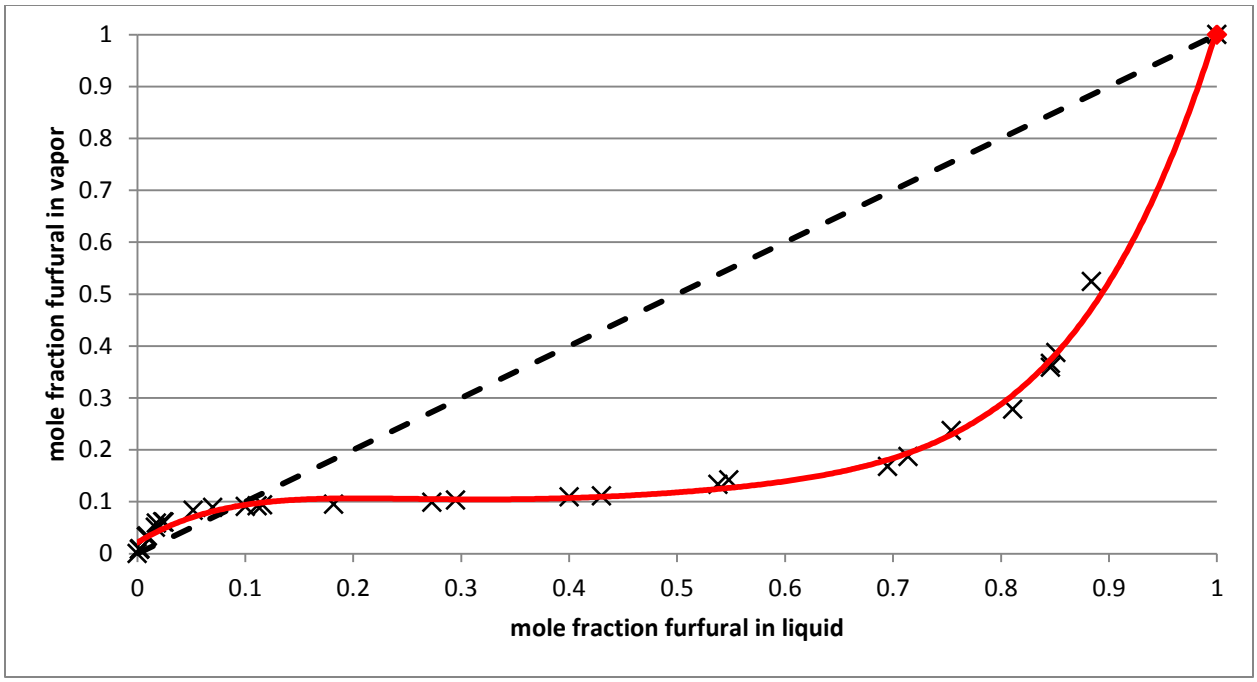

Figure 20: Vapor fraction of furfural as a function of the liquid fraction; Experimental data from Curtis&Hatt at 6.05 bar.

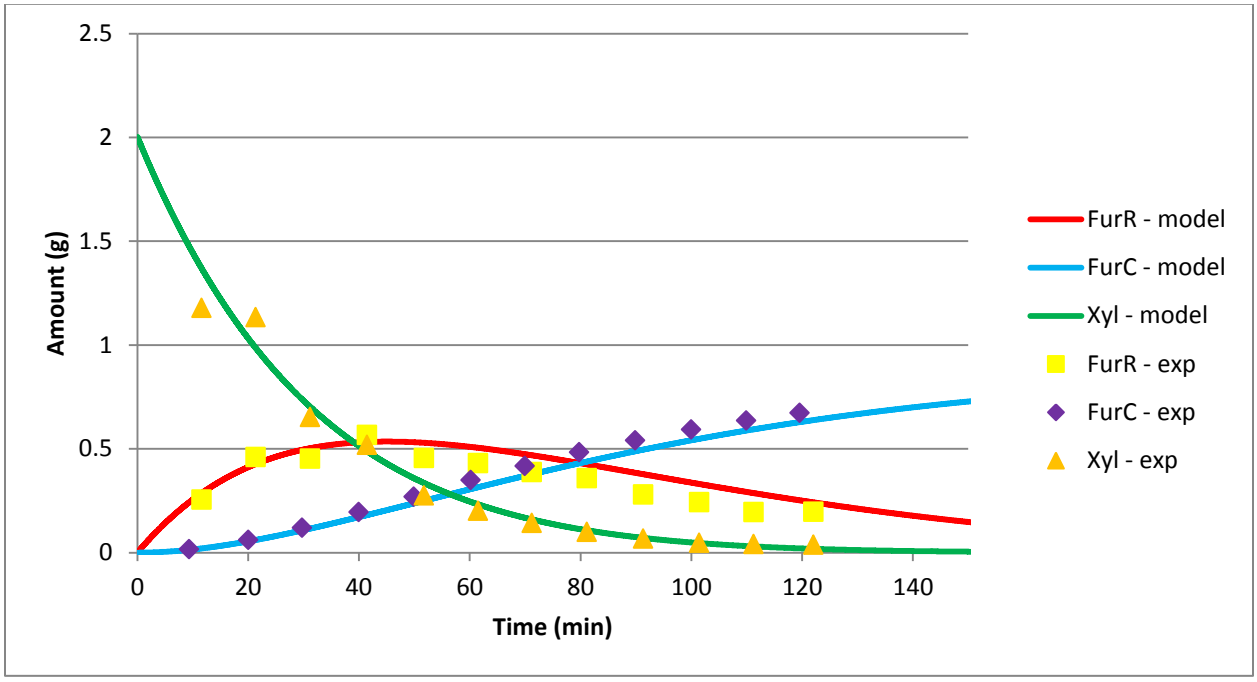

Figure 21: Model predictions for the amount of xylose and furfural using activity coefficients from literature; 170°C, 10 bar, 0.5 w% H_2SO_4, 1 w% initial xylose and 150 ml/min N_2 stripping stream.

The activity coefficients of components in a mixture could be calculated with several methods. The focus in this study is on model descriptions using the van Laar equations and Non Random Two Liquid (NRTL) equations.

Van Laar parameters

One way to include interaction parameters between components into the model is by using van Laar parameters. Van Laar's equations are shown in equation 8 and equation 9.

Using the experimental data from Curtis and Hatt temperature dependent correlations for A and B could be defined for a mixture of furfural and water. [26] The used parameters/ parameter correlations are given in Table 1.

	van Laar parameter A	**van Laar parameter B**
Harris et al.[ref] (10 atm)	0.4504	1.392
Harris et al.[ref]	$\frac{-0.20505 * 1000}{T_{sat} + 273.15} + 0.9017$	$\frac{0.9091 * 1000}{T_{sat} + 273.15} - 0.60886$
van Laar parameter correlation	$\frac{-85.62}{T_{sat} + 273.15} + 0.6229$	$\frac{799.73}{T_{sat} + 273.15} - 0.3366$

Table 1: van Laar parameters

Model results are shown for using van Laar parameters [27], parameters correlations [27] and own correlations (given in Table 1).

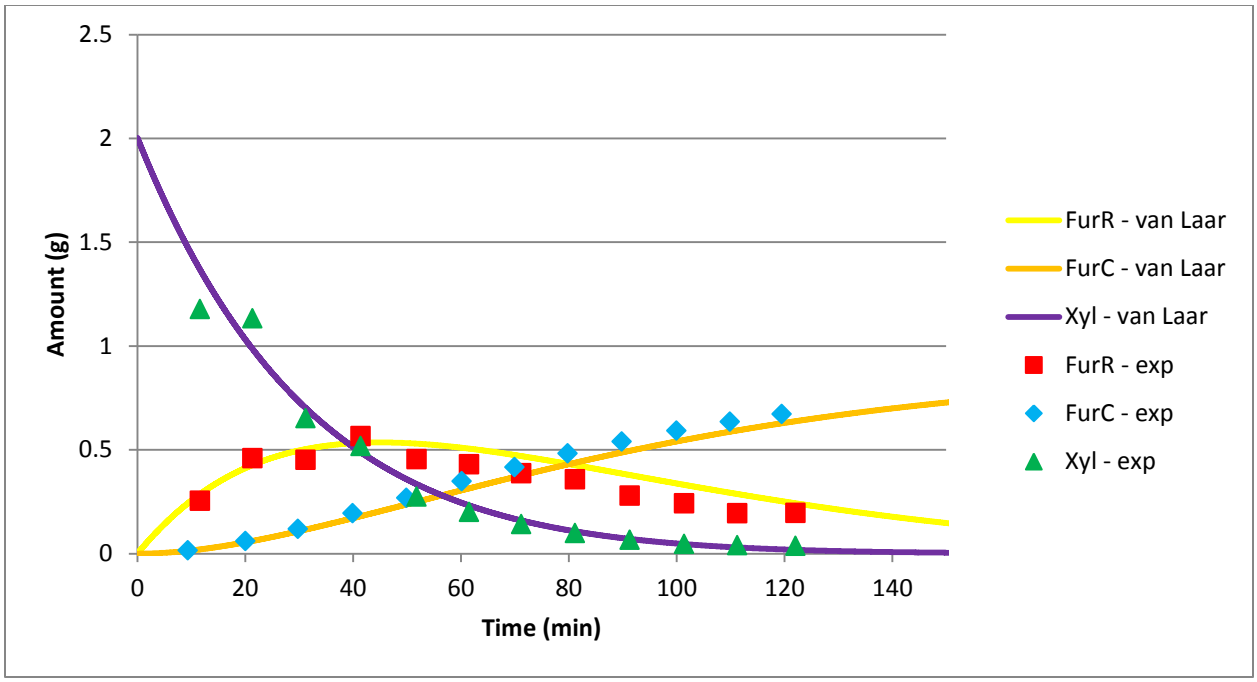

Figure 22: Model predictions for the amount of xylose and furfural using own van Laar parameters correlations; 170°C, 10 bar, 0.5 w% H_2SO_4, 1 w% initial xylose and 150 ml/min N_2 stripping stream.

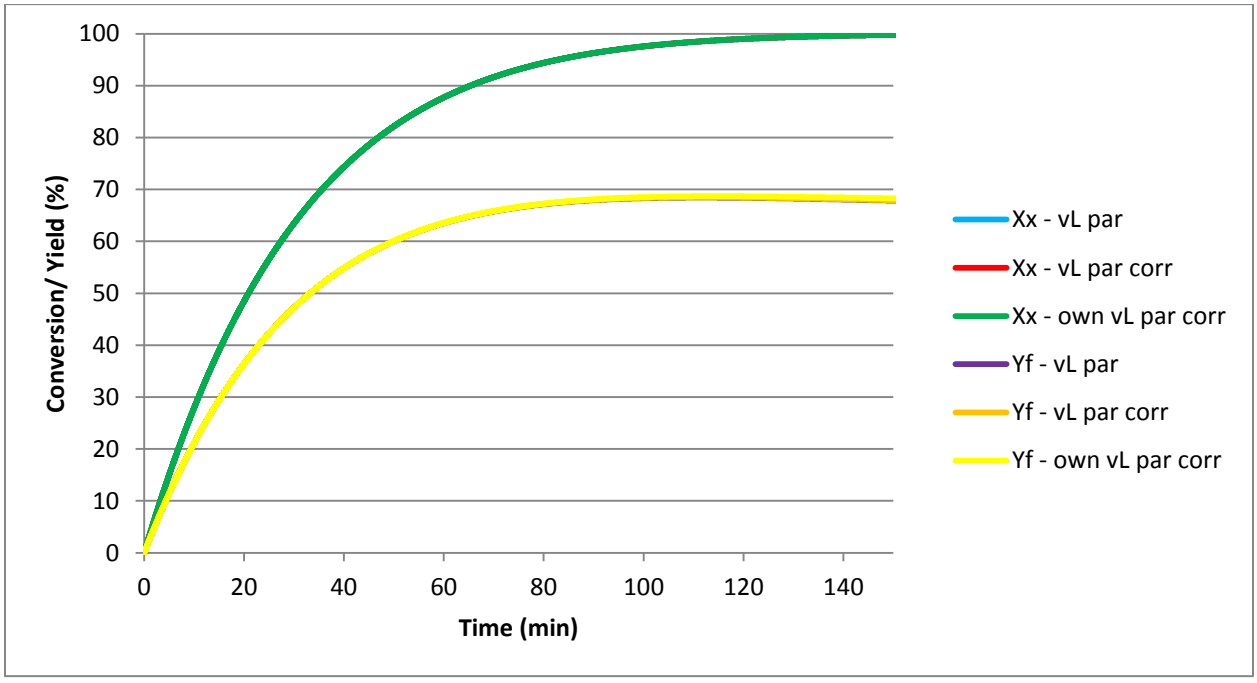

Figure 23: Comparison of different van Laar parameter (correlations); 170°C, 10 bar, 0.5 w% H_2SO_4, 1 w% initial xylose and 150 ml/min N_2 stripping stream.

In Figure 22 the modeled results using the self-defined correlation for the van Laar parameters are shown. It shows that the model describes the experimental data well, although there is some small derivation in furfural at later timescales (overestimation furfural in the reactor and underestimation condensate furfural). From Figure 23 the differences between the use of the van Laar parameters from literature, correlations from literature or own correlations could be seen. The differences are minimal with a predicted yield increase from 67.5% to 68% from literature values to own correlation.

Non random two liquid (NRTL) model

First described by Renon and Prausnitz [28] non random two liquid local composition models are another option to determine activity coefficients for VLE data. It is based on an expression for the Gibbs free energy for local compositions.

The expressions for the activity coefficients for the NRTL model could be found by differentiation and are given in equation 14. Equation 15 and 16 are rewritten for a binary mixture.

The different binary interaction parameters, as defined in equation 18 till equation 21, for a mixture of furfural and water are given in Table 2. Results for these different binary interaction parameters are shown in Figure 24 till Figure 28.

	a_{ij}	a_{ji}	b_{ij}	b_{ji}	c_{ij}	e_{ij}	e_{ji}
Sunder et al.	-	-	1683.3 (g)	-463.5 (g)	0.12	-	-
Fele et al.	4.4233	-3.1078	-95.0897	964.0374	0.2	-	-
VLE-RK	4.2744	-4.7587	-273.1076	1910.4714	0.3	-	-
LLE_ASPEN	52.8289	112.55	-2808.5376	-4131.4375	0.2	-6.902	-17.3004
VLE-HOC	4.2362	-4.7563	-262.2408	1911.4222	0.3	-	-
VLE-IG	7.1079	-5.8732	-1265.8367	2335.0493	0.3	-	-
VLE-LIT	-	-	1309.6942	219.8905	0.3958	-	-
Binary interaction parameters	-0.0619	31.91	1468.8	-8114.8	0.3	-	-

Table 2: Binary interaction parameters for the NRTL model. Water (i) and Furfural (j)

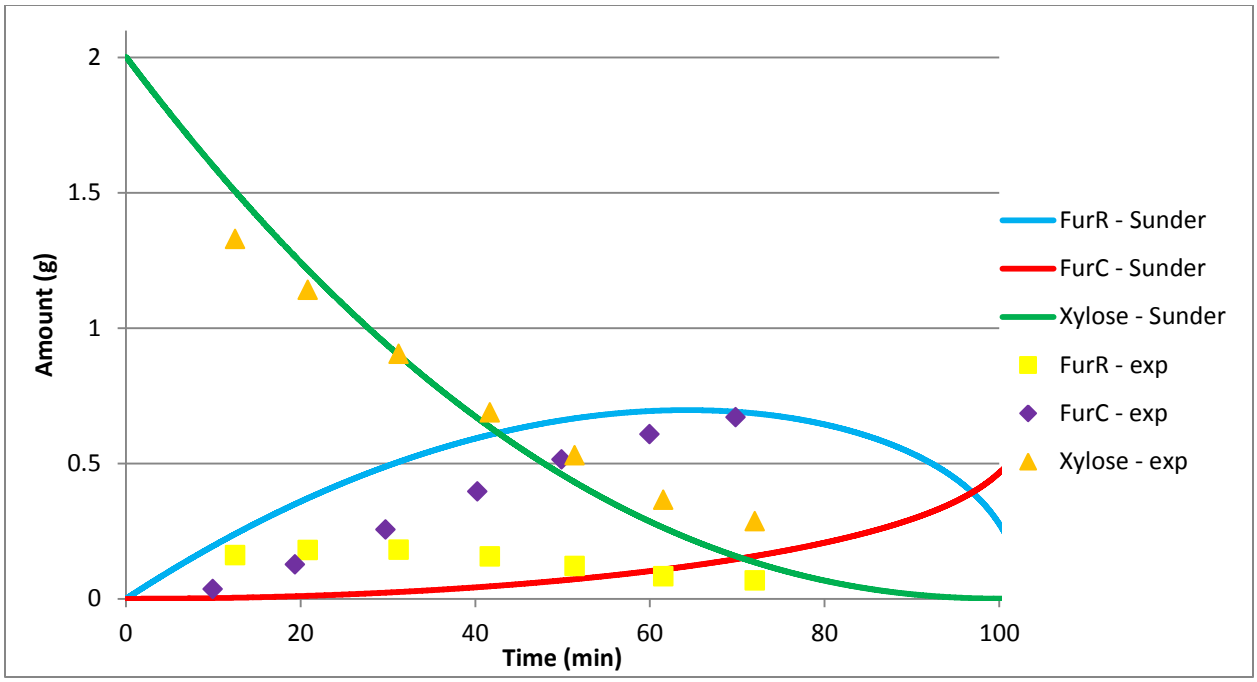

Figure 24: Model predictions using the parameters from Sunder et al; 170°C, 10 bar, 0.5 w% H_2SO_4, 1 w% initial xylose and 1000 ml/min N_2 stripping stream.

As could been seen in Figure 24 the binary interaction parameters from Sunder et al. [30] do not give a correct description of the furfural production process.

The parameters from Fele et al. [31] give a better description of the production and stripping of furfural. (see Figure 25) As is shown in Figure 26 compared to the van Laar model, the NRTL model with the binary interaction parameters from Fele et al. result in slightly less stripping of furfural, but a similar yield is obtained.

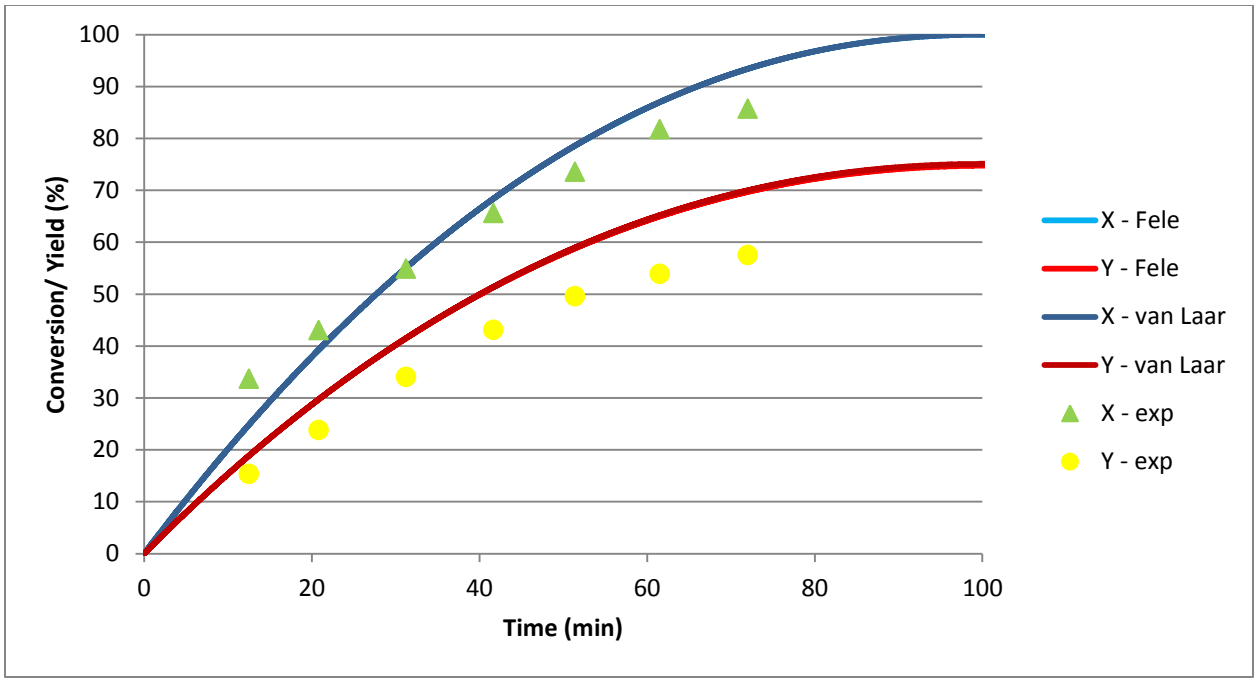

Figure 25: Conversion and yield comparison NRTL (Fele) and van Laar models; 170°C, 10 bar, 0.5 w% H_2SO_4, 1 w% initial xylose and 1000 ml/min N_2 stripping stream.

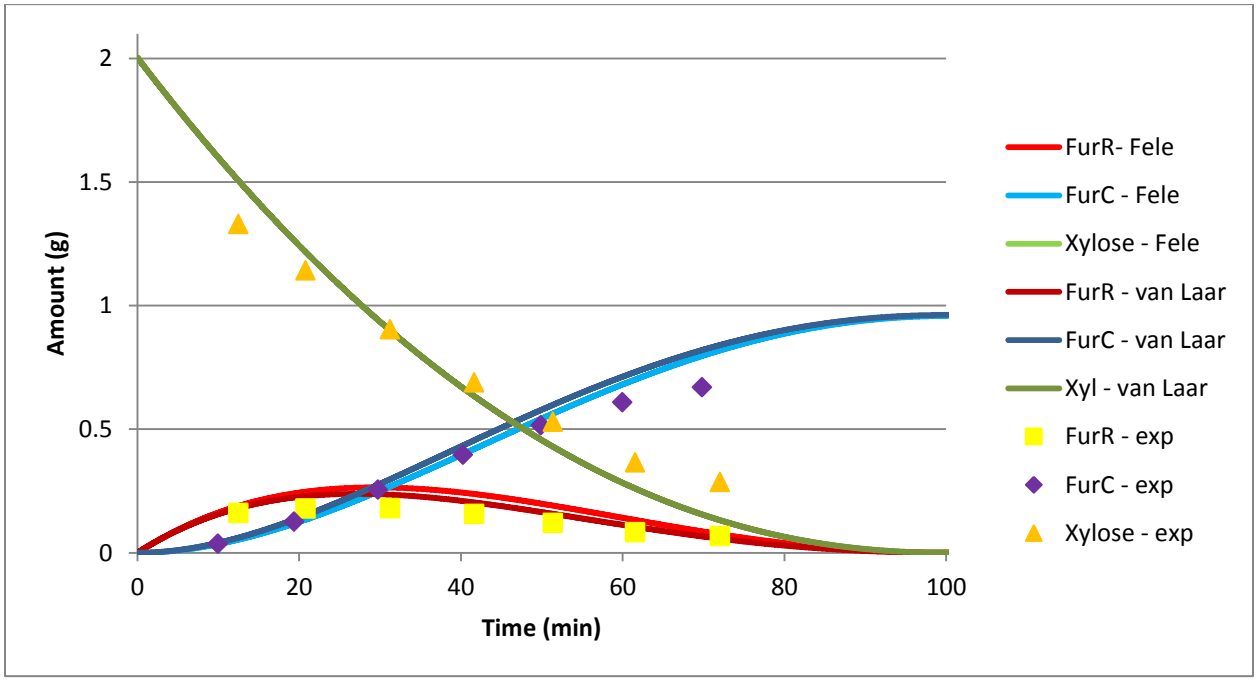

Figure 26: Comparison of NRTL (Fele) and van Laar models for the amount of xylose and furfural; 170°C, 10 bar, 0.5 w% H_2SO_4, 1 w% initial xylose and 150 ml/min N_2 stripping stream.

The binary interaction parameters between water and furfural are also obtained from several ASPEN databases. The comparison of these results are shown in Appendix B.

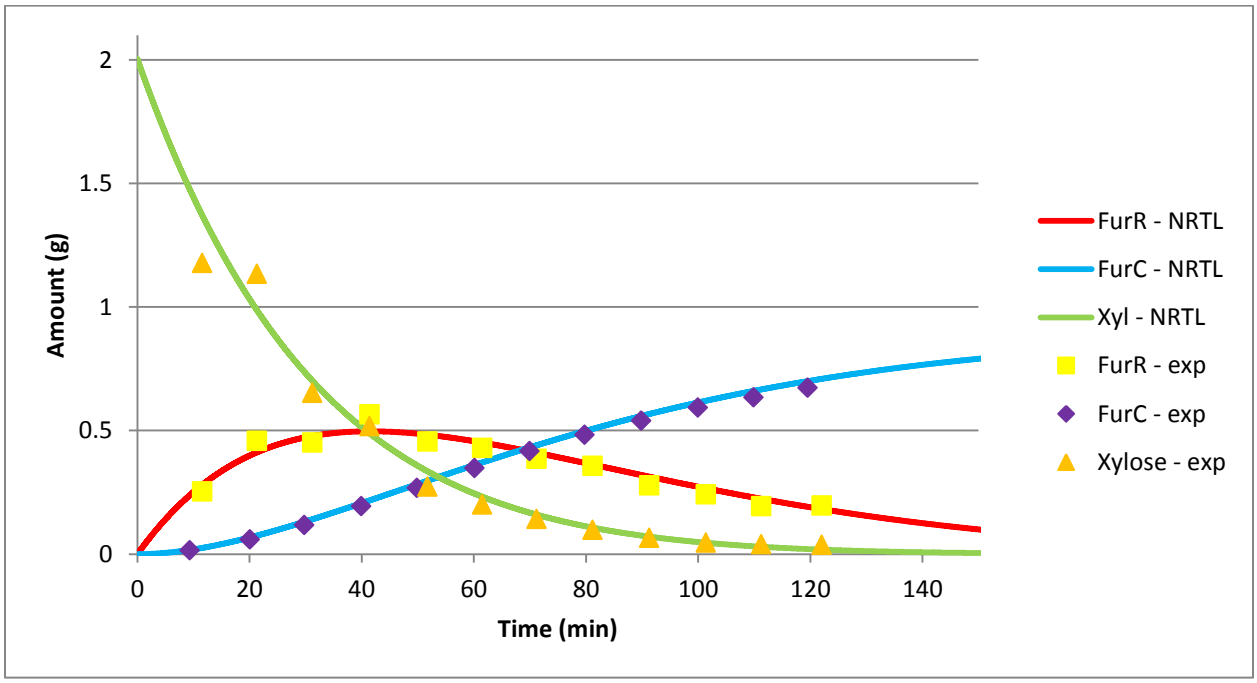

Figure 27: NRTL model predictions (VLE-IG) for the amount of xylose and furfural; 170°C, 10 bar, 0.5 w% H_2SO_4, 1 w% initial xylose and 150 ml/min N_2 stripping stream.

It could be observed that the parameters from the ASPEN VLE-IG source result in the best fit of the experimental results at a stripping rate of 150 ml/min (Figure 27), also better than the parameters from Fele et al.

MT limitations

The results for the other stripping rates are showed in Appendix B. From these results it could be observed that the model derives more from the experimental data at higher stripping rates. Where the liquid phase in the reactor could be considered as a batch operation, the gas phase could be considered as plug flow. With increasing the stripping rate the residence time of the vapor phase decreases from 4 minutes to only 0.6 minutes, giving the reaction mixture less time to restore vapor-liquid equilibrium. At these lower residence times mass transfer from the liquid to the gas phase will limit the stripping concentrations.

Using the data from Curtis&Hatt [26] own binary interaction parameters are fitted for the interaction between furfural and water as well. Using a least squares method and fixing the nonrandomness parameter α at a value of 0.3, the obtained results are shown in Table 2 and Table 3.

As could be seen from Figure 28 these modeled results even fit the experimental data slightly better than the previous mentioned parameters.

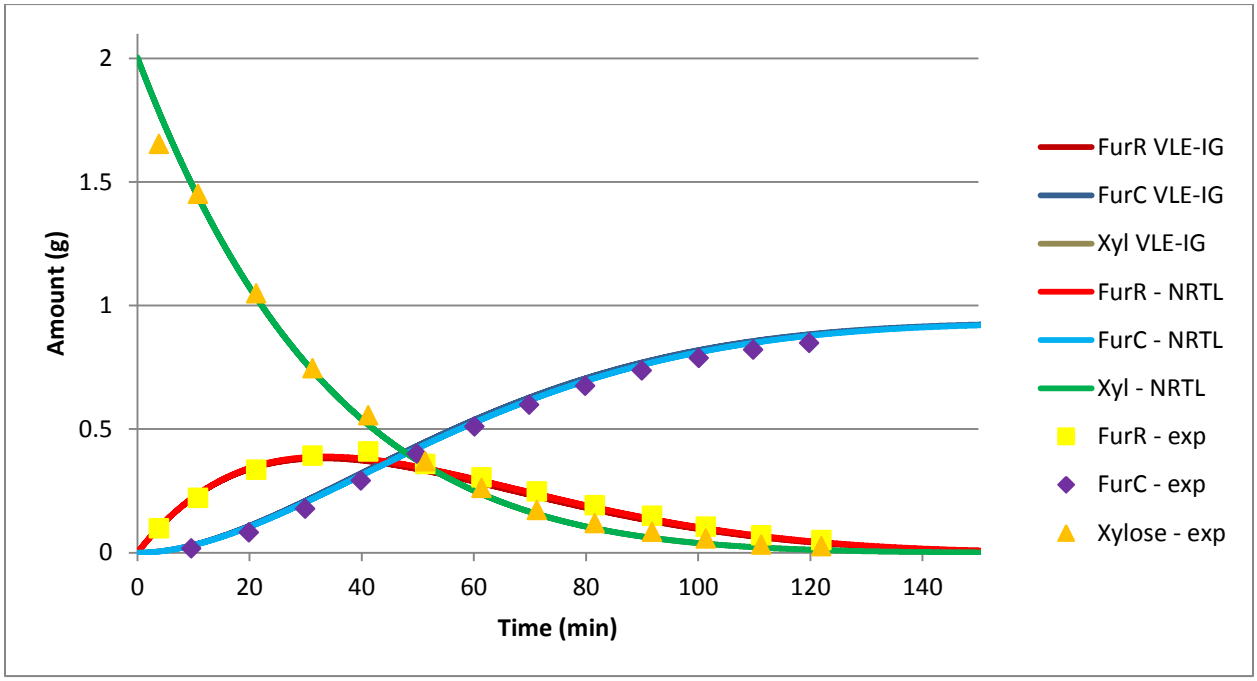

Figure 28: Comparison between binary interaction parameters (VLE-IG and fitted); 170°C, 10 bar, 0.5 w% H_2SO_4, 1 w% initial xylose and 300 ml/min N_2 stripping stream.

Multicomponents

Also a multicomponent NRTL model is made. In this model the interactions between the four components, water, furfural, xylose and sulfuric are taken into account.

The binary interactions parameters for water and furfural, water and xylose and water and sulfuric acid are determined by fitting the NRTL model to experimental data from literature. [26] [34] [35] The obtained results are shown in Table 3. Interactions between the other components are unfortunately unknown.

Component i	Component j	a_{ij}	b_{ij}	c_{ij}
1	**2**	-0.0619	1468.8	0.3
1	**3**	-8.514803317	-0.015817732	0.3
1	**4**	14.796	-6518.3	-0.059
2	**1**	31.91	-8114.8	0.3
3	**1**	53.42269308	-7999.912573	0.3
4	**1**	1.391	-2639	-0.059

Table 3: Fitted binary interaction parameters. Water (1), Furfural (2), Xylose (3) and sulfuric acid (4)

The results of these multicomponent interactions are shown in Figure 29. (The rest could be seen in Appendix B.)

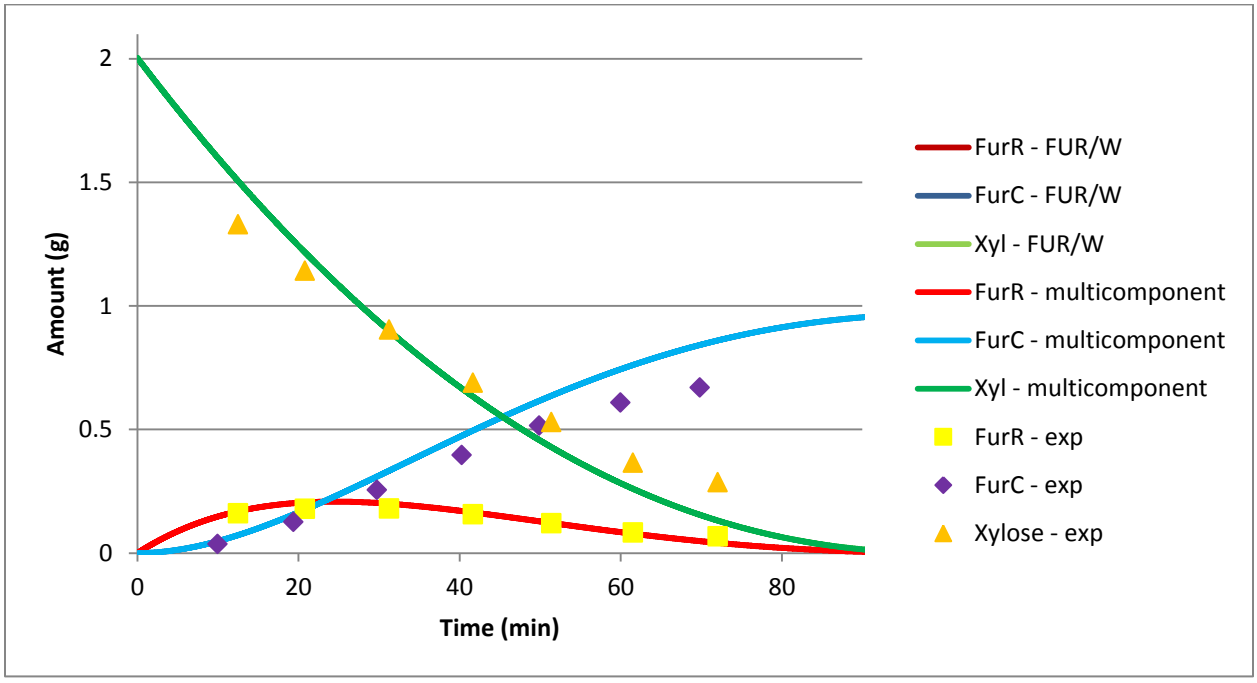

Figure 29: Multicomponent NRTL model predictions; 170°C, 10 bar, 0.5 w% H_2SO_4, 1 w% initial xylose and 1000 ml/min N_2 stripping stream.

From these results it could be observed that the effect of sulfuric acid and xylose (on water) is minimal under the used conditions.

Outlook

Recycle of hydrogenation gas stream

The reason to strip furfural from the reactor using hydrogen as a stripping agent, is the next step in the valorization process, hydrogenation. This would be especially advantageous for the hydrogenation of furfural to furfuryl alcohol. It is possible to perform this reaction in the vapor phase with relatively high yield. With pure furfural and hydrogen present in the stripped vapor stream this could be a direct consecutive reaction.

The hydrogenation of furfural to cyclopentanol/cyclopentanone takes place in acidic aqueous conditions under hydrogen pressure. For this a trickle bed reactor could be designed where the stripped vapor stream will be condensed. The transfer of furfural would be the limiting factor in such a reactor, which would result in a full direct conversion of furfural. Over the length of the reactor all furfural could be condensed and converted. To obtain higher concentrations of cyclopentanol/cyclopentanone in the liquid phase, this stream could be recycled for the hydrogenation reactor, making separation afterwards easier.

The vapor phase, consisting of some small amount of unreacted furfural (in the case of non-full conversion) and water, could be compressed and fed back to the stripping reactor as assisting stripping agent. A main advantage of this would be that the recycle stream would require less energy to heat up and evaporate mainly water. Using only dry hydrogen/ nitrogen a lot of energy is spend on evaporating mainly water, by using a recycle this would be reduced.

In Figure 30 and Figure 31 the conversion and furfural yield are shown with the steam recycle stream.

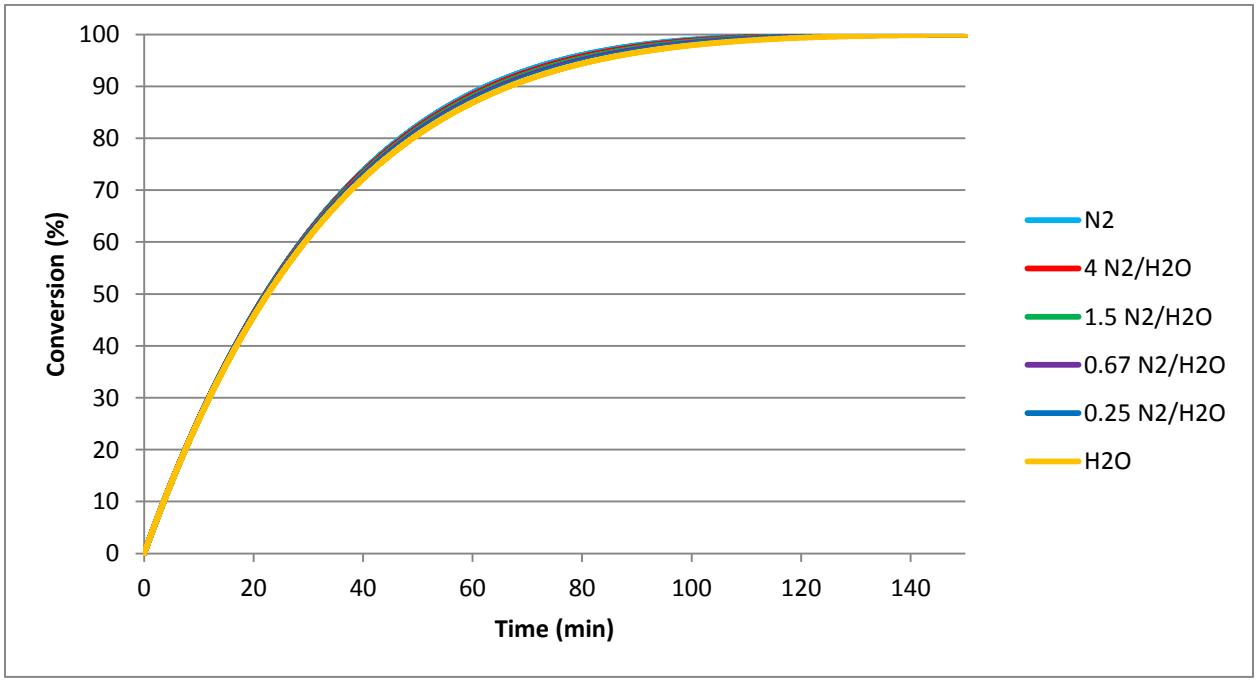

Figure 30: Predicted conversion for assisted stripping by recycle stream; ; 170°C, 10 bar, 0.5 w% H_2SO_4, 1 w% initial xylose and 500 ml/min stripping stream.

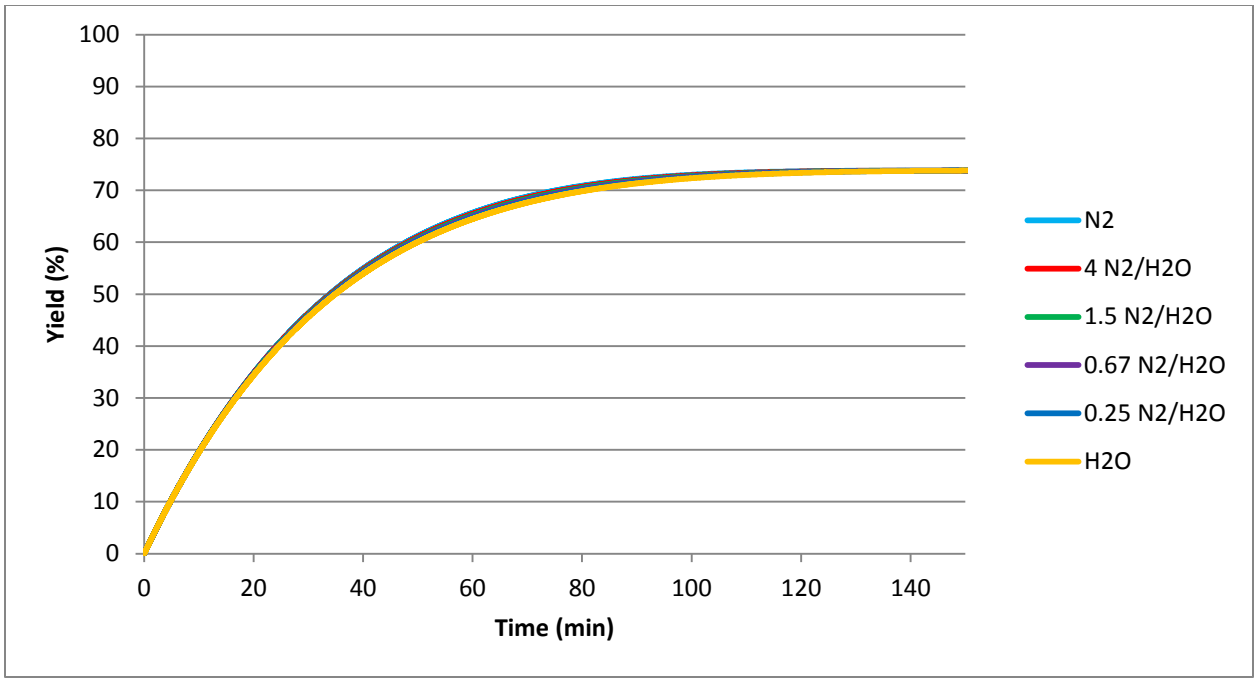

Figure 31:Predicted furfural yield for assisted stripping by recycle stream; 170°C, 10 bar, 0.5 w% H_2SO_4, 1 w% initial xylose and 500 ml/min stripping stream.

As could be seen from the conversion of xylose is slightly less at a higher steam to nitrogen ratio. By using recycle water vapor as stripping agent, less water in the reactor will be evaporated and stripped. This leads to slightly lower concentrations in the reactor and therefore lower conversion.

Increasing the amount of recycle stream will lead to less stripping of furfural and more furfural in the reaction. This evens out and result in a similar yield.

Using water vapor as assisting stripping agent will also decrease the furfural concentration in the stripped/ condensate stream, simply due to an increased amount of water in this stream.

The main advantage of the recycle stream would be the reuse of the energy. By using a preheated stripping agent, compared to the stripping agent at ambient temperature, the energy input of this stream increases 1.5 times. Going from a pure nitrogen/ hydrogen stripping stream to a pure steam stripping stream a heat reduction of 28% could be achieved due to the evaporation of water.

Higher acid concentrations

To validate if the model is still valid for higher acid concentrations, model results are compared to experimental data obtained at 1 and 2 weight percent of sulfuric acid. These results are shown in Figure 32 and Figure 33.

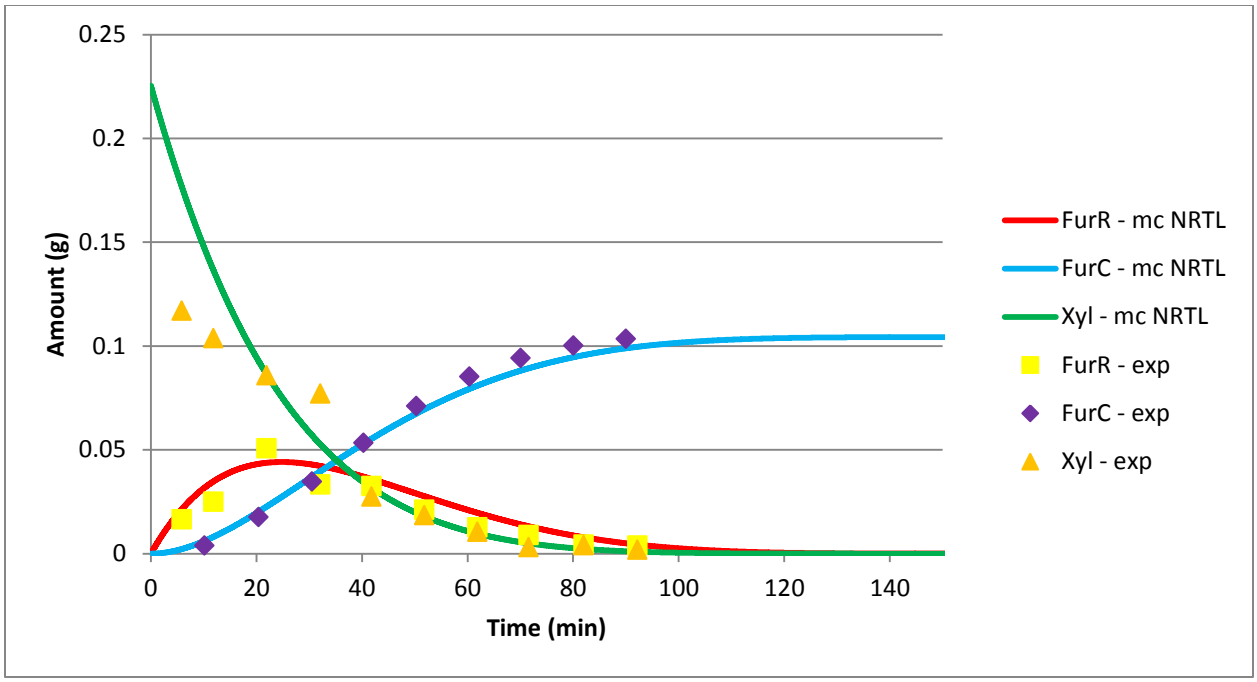

Figure 32: NRTL model validation for 1 w% sulfuric acid; ; 170°C, 10 bar, 1 w% initial xylose and 500 ml/min N_2 stripping stream.

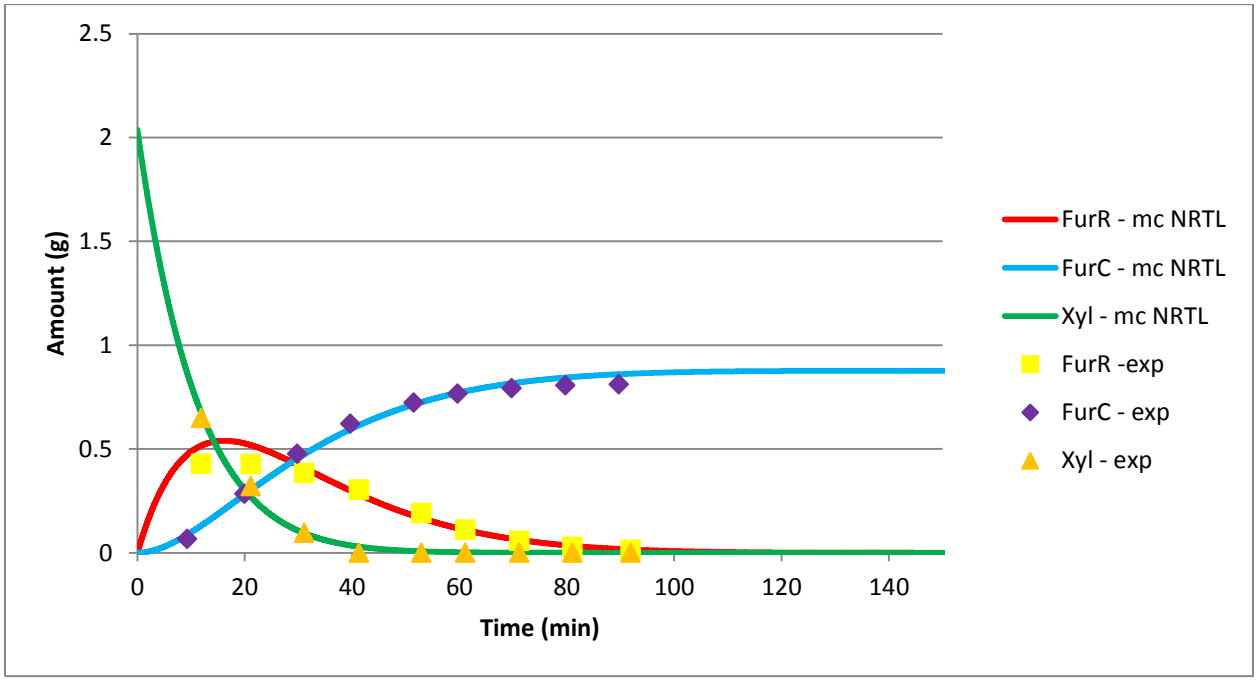

Figure 33: NRTL model validation for 2 w% sulfuric acid; 170°C, 10 bar, 1 w% initial xylose and 500 ml/min N_2 stripping stream.

These results show that the model is still valid for higher concentration of sulfuric acid, at least up to 2 weight percent.

To have a better understanding of the influence of the sulfuric acid concentration, the furfural production process is modeled for various concentrations of H_2SO_4. In Figure 34 the predicted final furfural yield and productivity of the reaction are shown.

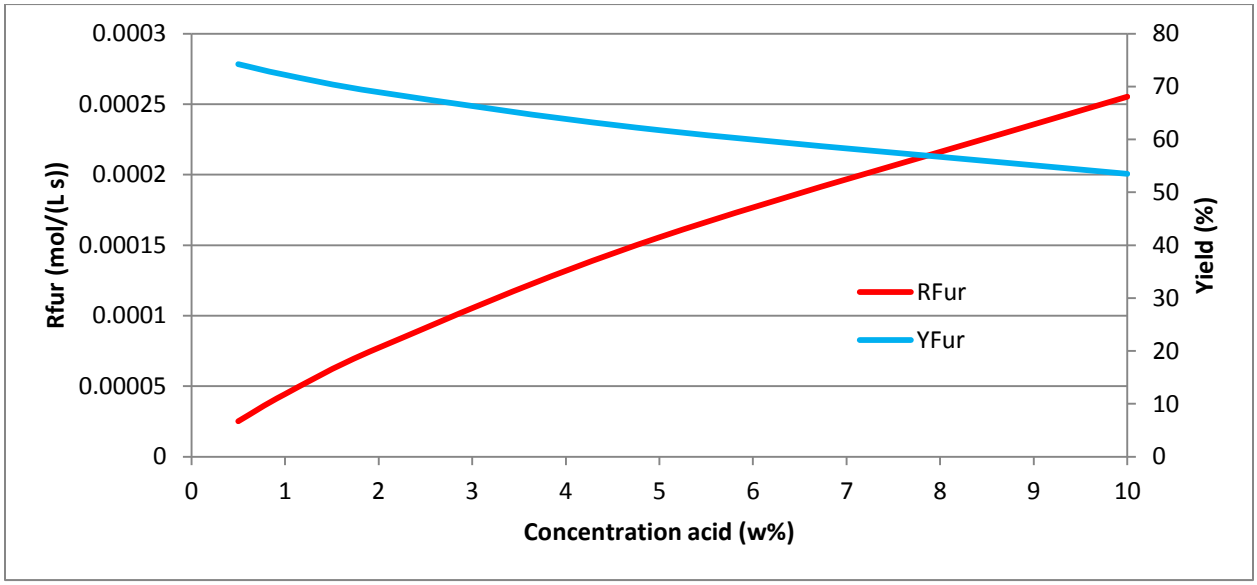

Figure 34: Prediction of final yield and productivity for sulfuric acid concentrations from 0.5 to 10 w%; 170°C, 1 w% initial xylose and 500 ml/min N_2 stripping stream.

As could be seen from Figure 34 higher acid concentrations increase the rate of conversion of xylose and production of furfural, as could be expected. The development of the conversion is shown in Appendix B. The rate of conversion increases simply because it is assumed to be first order dependent on the acid concentration. This is not the only effect though, increasing the acid concentration form 0.5 to 10 w% results in a lower apparent ion concentration, modeled with an H^+ activity coefficient (which decreases with concentration in this concentration range).

The reaction rate constant for the conversion of xylose increases 10 times with an increasing acid concentration form 0.5 to 10 w%, so leading to a significant higher productivity.

In Figure 34 it is also shown that the furfural yield (and therefor selectivity) drops with increasing acid concentrations. The final yield drops with from 74% to 53% for the acid concentration increase. Higher acidic conditions also show a clear maximum yield obtained after a relatively short time (see Appendix B). After this time more furfural is lost by the formation of humins than is stripped out due to the higher

amount of furfural in the reactor present at higher acid concentrations. At higher acid concentration less furfural is stripped from the reactor for this same reason. By increasing the stripping rate this effect could be prevented.

Different xylose concentrations

Model results are compared to experimental results with an initial xylose concentration of 0.5 w% as well. From these results, shown in Figure 35, it is plausible that the model is also valid for these conditions.

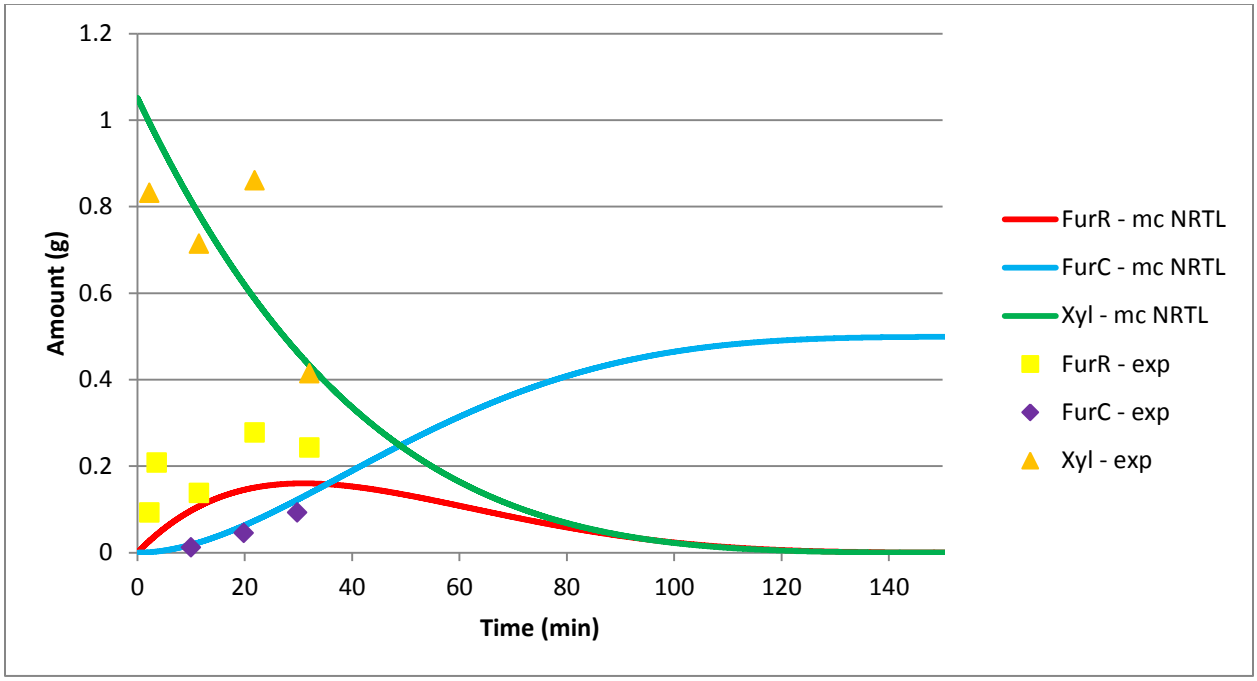

Figure 35: NRTL model validation for 0.5 w% xylose; 170°C, 10 bar, 0.5 w% H_2SO_4 and 500 ml/min N_2 stripping stream.

Different xylose concentrations are modeled as well and the results are shown in Figure 36.

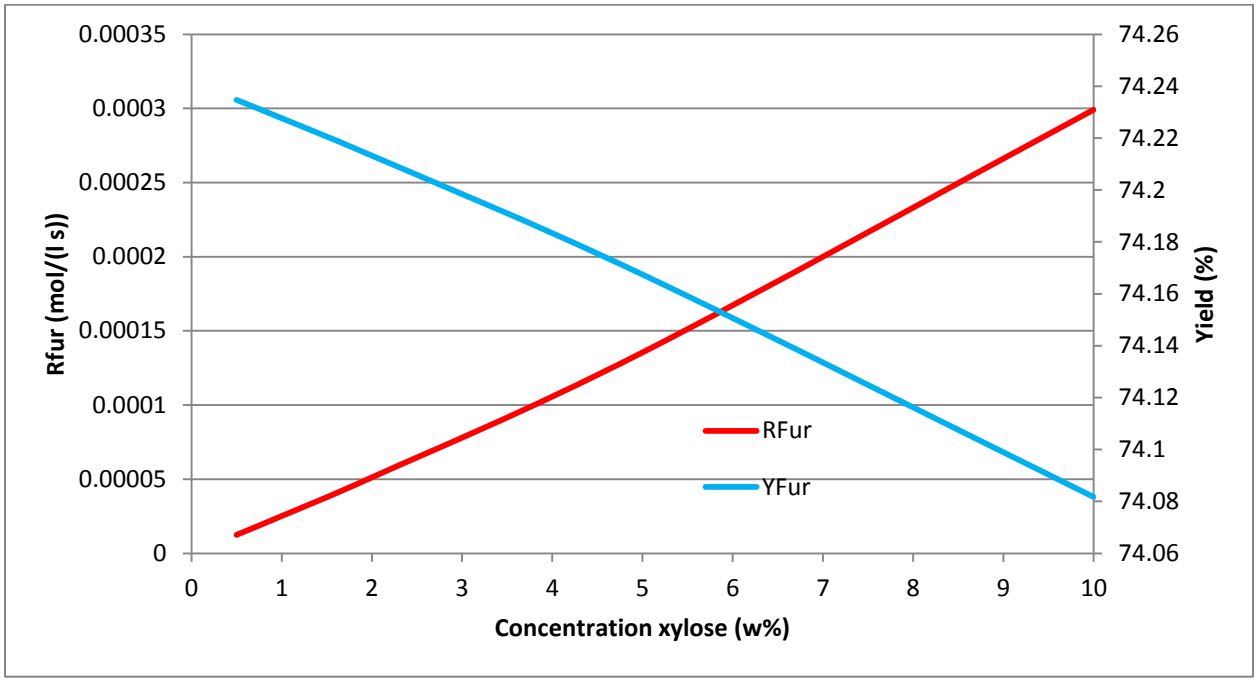

Figure 36: Yield and productivity predictions for 0.5 to 10 w% initial xylose concentrations; 170°C, 10 bar, 0.5 w% H_2SO_4 and 500 ml/min N_2 stripping stream.

As could be seen an increase in the xylose concentration only leads to a minimal decrease in the modeled furfural yield. This is in contradiction with experimental data that show a decrease in selectivity/ yield with increasing xylose concentrations. [1] [19] In the model only direct loss of furfural with itself (resinification) and xylose with itself are assumed, which seems valid under the used experimental conditions.

There are other possible loss reactions, so called condensation loss reactions, where furfural reacts with intermediates of xylose (first and/ or second order in furfural concentration). These losses will result in a lower furfural yield at higher xylose, and therefor also intermediate, concentrations. This negative effect on the yield will be decreased/ removed as well by the suggested stripping process compared to conventional furfural production.

Due to a steady state approximation for the intermediate(s) in the model, this is not taken into account.

From Figure 36 it could be observed that the rate furfural formation significantly increases with increasing xylose concentration. This rate increase is also quite simply due to a first order dependency on the xylose concentration.

Different temperatures

The developed model could predict the results for the furfural production process at different temperatures as well. In Figure 37 the results are shown for the temperature range 150°C-200°C.

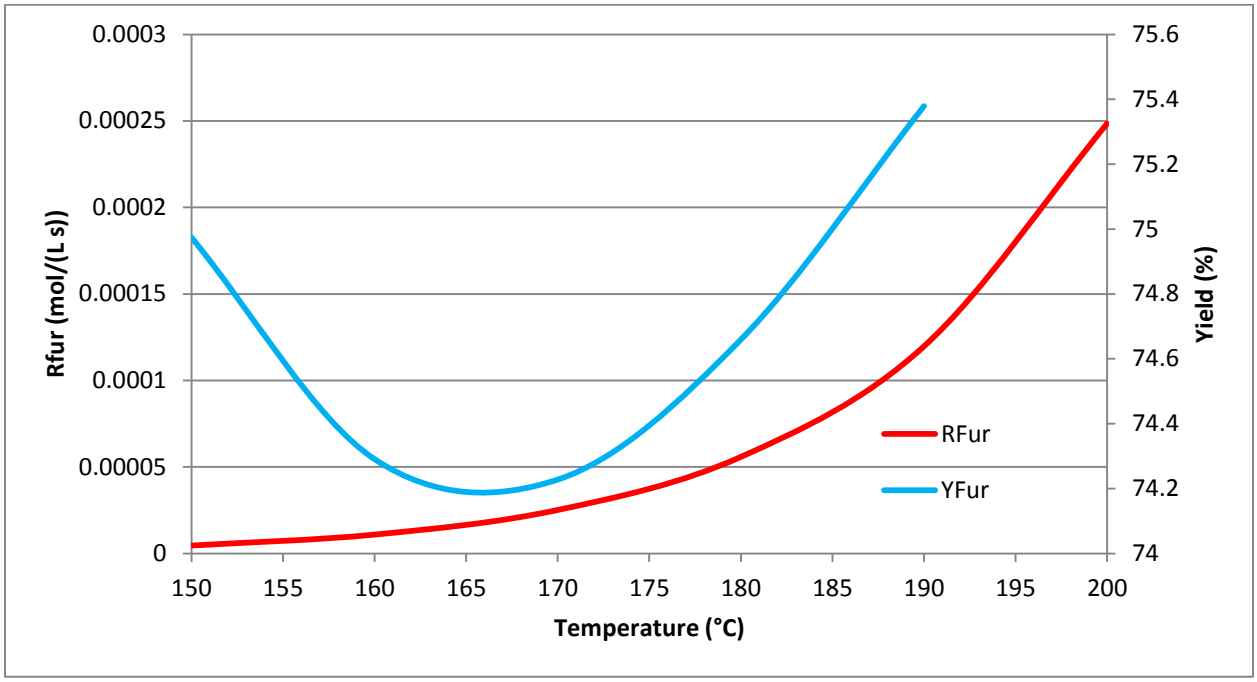

Figure 37: Predicted furfural yields and productivity for a temperature range of 150°C to 200°C; 10 bar, 0.5 w% H_2SO_4, 1 w% initial xylose and 500 ml/min N_2 stripping stream.

From Figure 37 it could be observed that the rate of conversion increases significantly with increasing temperature. (The conversions for all temperatures are shown in Appendix B.) This is due to the reaction rate kinetics which increase with increasing temperature. From 150 to 200°C the reaction rate constant for the conversion of xylose increases more than 50 times, causing a significant increased productivity.

In Figure 37 the predicted furfural yields for the temperature range are shown as well, with increasing temperature from 170°C to 200°C an increase in yield could be seen. For the higher temperatures a the maximum yield is observed in a short time period, at this point all possible furfural is stripped out of the reactor (see Appendix B).

It is predicted that the degradation of furfural will decrease compared to the conversion of xylose at higher temperatures. [1] This prediction could be clearly seen from the kinetic rate correlation, where the reaction rate constant for the conversion of xylose increases more than the degradation rate constant of furfural. The ratio k_3/k_x is shown in Figure 38 for the investigated temperature range.

With increasing temperature the partial pressures of furfural and water increase as well. The partial pressure of pure furfural increases more with temperature than the partial pressure of water, so it is possible to obtain a higher concentrated condensate stream (Figure 38). In the semi-batch experiments this could be seen in the beginning of the experiment, at a longer time scale the concentration for higher temperatures drops because (almost) all furfural is stripped and only water will be stripped.

The small yield effect at lower temperatures (150°C) is due to the fact that the used stripping rate is better able to remove the furfural formed in the reactor, at a lower rate.

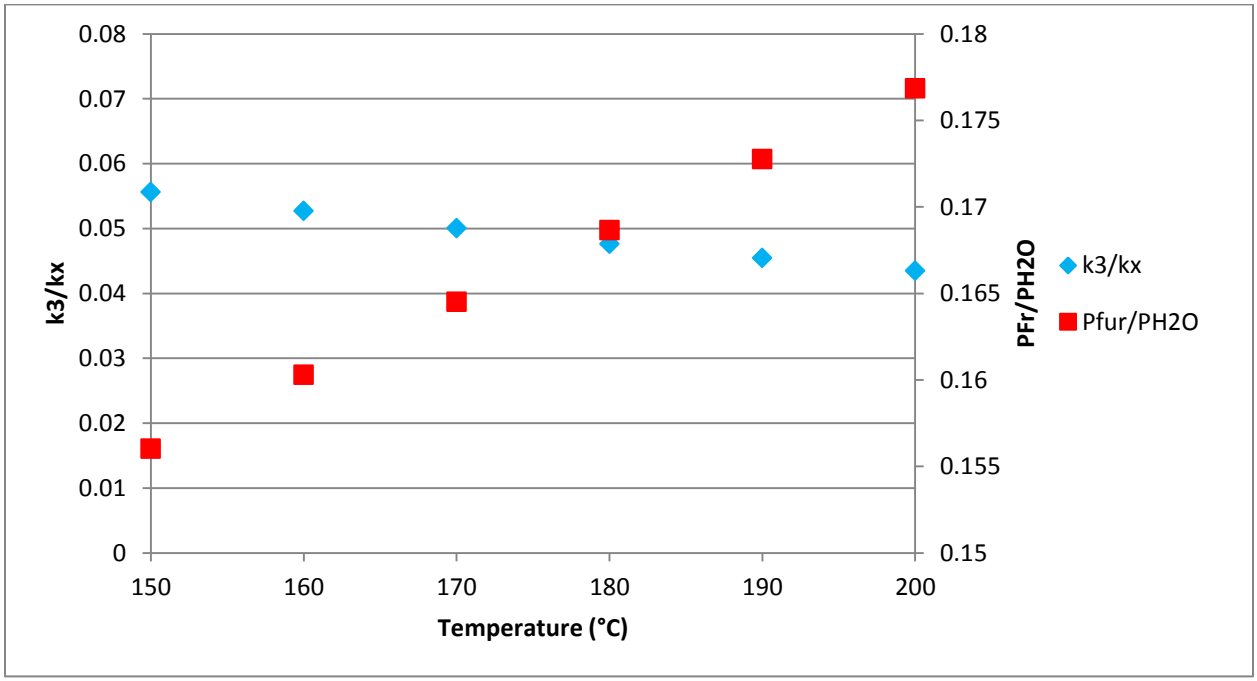

Figure 38: k3/kx and Pfur/PH2O as a function of temperature

Influence of pressure

Temperature is not the only operating condition, the pressure of the system influences the furfural production process as well. In Figure 39 and Figure 40 the conversion and yield are shown for 10 and 20 bar operating pressures at 170°C and 200°C.

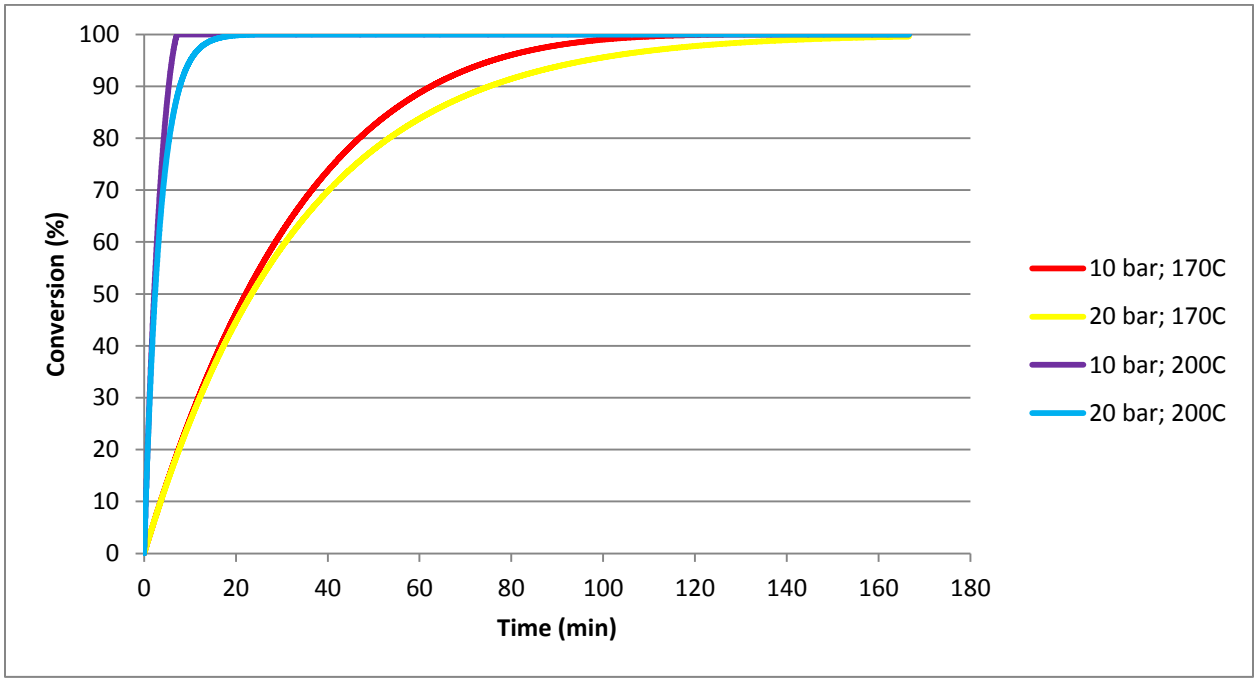

Figure 39: The influence of operating pressure on the conversion of xylose; 0.5 w% H_2SO_4, 1 w% initial xylose and 500 ml/min N_2 stripping stream.

From Figure 39 it could be seen that the conversion of xylose decreases slightly with increasing the pressure from 10 to 20 bar. At 20 bar a smaller fraction of the vapor phase is water/ furfural, so less of the reactor volume could be stripped out. The reaction rate constant for the conversion of xylose is dependent on concentration (of xylose and the acid). Due to reaction the concentration decreases, but stripping leads to an increase in concentration. At higher pressure this increasing effect is less, leading to a slower rate of conversion.

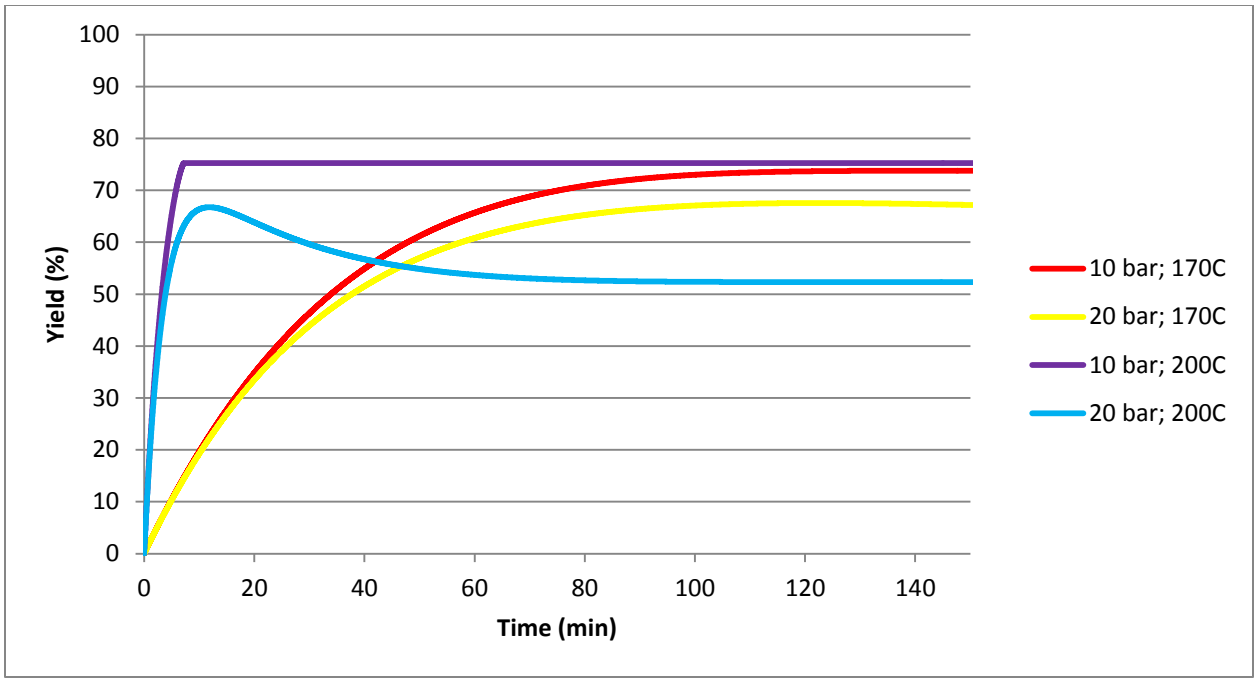

Figure 40: The influence of operating pressure on the predicted yield; 0.5 w% H_2SO_4, 1 w% initial xylose and 500 ml/min N_2 stripping stream.

In Figure 40 it could be seen that a higher pressure will also lead to a lower furfural yield. As already mentioned at higher pressure less furfural is stripped. This leads to a higher concentration of furfural in the reactor and therefore to more degradation loss.

At 200°C another observation could be made. Similar to higher acid concentrations a maximum yield is obtained, which thereafter drops to its lower final value. At 200°C the rate of formation of furfural is significantly increased, the stripping rate is not high enough to remove the furfural at a similar rate. This leads to high amount of furfural in the reactor and more furfural loss. At 10 bar the stripping rate is to remove the formed furfural almost instantaneous, resulting in minimal loss. This last observation is in accordance to experiments were the 'analytical' yield of furfural was obtained. [1] A boiling reaction medium, as is the case at 200°C and 10 bar, would lead to the instantaneous removal of furfural from the reactive liquid phase and therefore the maximum 'analytical' yield could be obtained.

The operating pressure also influences the furfural concentration in the condensate stream. Due to the reduced stripping rate more furfural will be present in the reactor, which also increases the fraction of furfural in the vapor phase. So at increased operating pressure a more concentrated vapor stream/ condensate stream will be obtained.

Continuous operation

The possibility of continuous operation is discussed before. The model is developed that it could describe continuous feeding of xylose as well. This is validated by comparison with experimental data, results are shown in Figure 41.

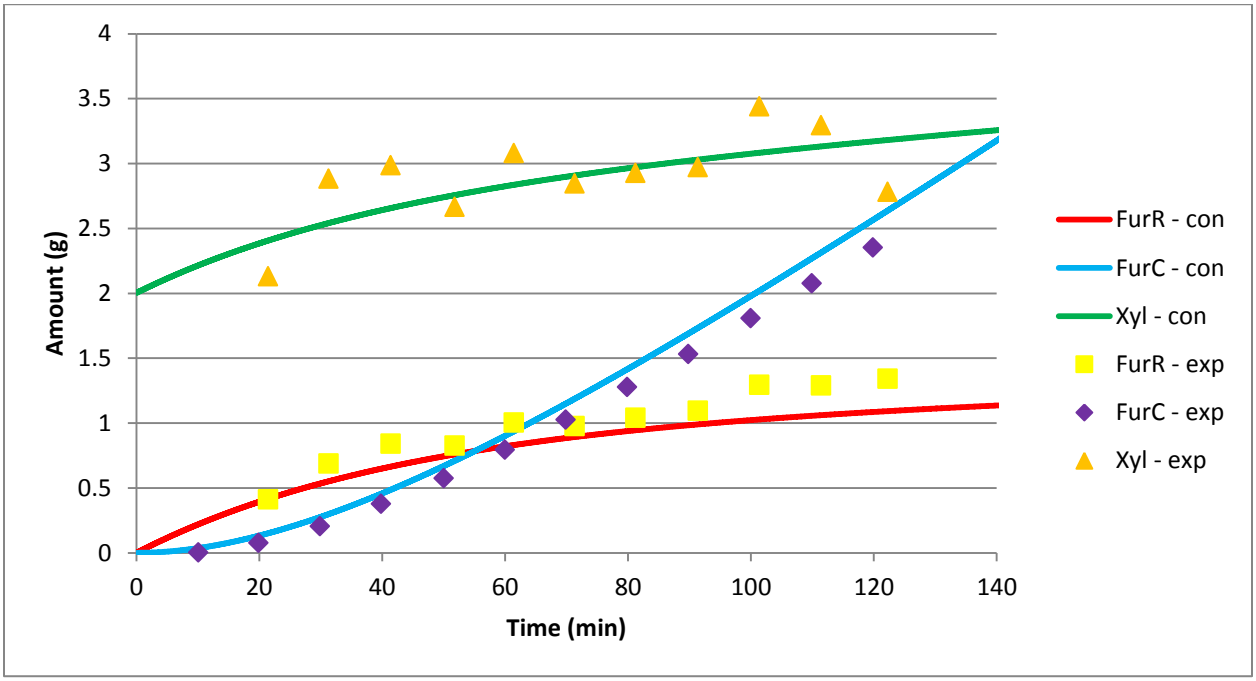

Figure 41: NRTL model validation for continuous operation; 170°C, 10 bar, 0.5 w% H_2SO_4, 1 w% initial xylose, 500 ml/min N_2 stripping stream and 1.47 ml/min 0.05 g/ml xylose-solution feed.

As could be seen from Figure 41 the model is able to describe continuous operation well. In the model results a starting concentration of xylose is present, in experiments this starting condition is reached by a high feed flow of a more concentration xylose-solution at the start of the experiment. In this way an initial condition of 1 w% xylose is reached as in semi-batch operation.

Advantageous of continuous operation would be that the xylose concentration could be kept constant in the reactor (at a relatively low value) by continuous feeding of a xylose solution. A low concentration of xylose would prevent significant losses, but to increase productivity higher acid concentrations could be used. Furfural is stripped out of the reactor at equal rate to its formation, preventing further losses.

Unfortunately loss reaction cannot be totally prevented. The formed byproducts, including humins will influence continuous operation. In general furfural is formed from raw biomass material, which is converted into pentoses (such as xylose) by aqueous acid catalyzed hydrolization. Residue of this starting material has to be removed/handled either way, so the formation of humins would only lead to some extra residue.

Optimized scenario

Model predictions show that significant productivity improvements could be made by adjusting operating conditions. Increasing the sulfuric acid concentrations, the xylose concentration and the temperature all led to a higher productivity without a major penalty for yield loss.

Using 10 w% of sulfuric acid, 10 w% of xylose and an operating temperature of 200°C a productivity rate of 0.0288 mol L^{-1} s^{-1} could be achieved (limited by investigated range). Even if a decreased yield of 60% is taken into account, which could be prevented, only 6 liters of reaction volume is necessary to produce 10 gram of furfural per second. This would be only 1-1.5% of the volume of conventional batch reactors used in industry. [1]

This is a hypothetical case, limitations for this process intensification could be expected. However it shows the amount of improvement possible.

5. Conclusion

From this study several conclusion could be made. Kinetic experiments for the degradation of furfural and conversion of xylose confirmed the correlations described by Marcotulio et al. under the used reaction conditions. Results also show that resinification of furfural is a relatively minor loss reaction.

Stripping experiments show 100% selectivity towards furfural for the stripped stream. No significant difference in furfural yield for stripping rates from 150 to 1000 ml/min are shown due to the minimal effect of furfural degradation. The corresponding selectivity's vary only between 67 and 72%.

Thermodynamic models for the production process of furfural are developed in this study. The model involves three main reactions and vapor-liquid equilibria. These consist of the dehydration of xylose to form furfural, the loss of xylose and the degradation of furfural. Activity coefficients are introduced to describe the amount of furfural and water that could be stripped from the reactive system.

The proposed model using the van Laar equations describes the experimental results well. Van Laar parameters and parameter correlations from literature have been used, also own temperature dependent parameter correlations have been developed using experimental data from Curtis&Hatt. The differences are minimal with a predicted yield increase from 67.5% to 68% from literature values to values obtained by own correlations.

Non random two liquid local composition models are another option to determine activity coefficients for VLE data. A NRTL model is proposed as well for binary interactions between furfural and water. Different binary interaction parameters from literature and ASPEN databases have been investigated and compared to each other and to obtained parameters by fitting the previously mentioned experimental data from Curtis&Hatt. With exception when using the values from Sunder et al. the model is consistent with the experimental data, where the fitted interaction parameters describe the experimental results best.

The NRTL model is developed as a multicomponent model. Interactions between all components in the reaction mixture could be included. Besides the water-furfural interactions, the binary interaction parameters for water-xylose and water-sulfuric acid are obtained by fitting of experimental data from literature. Interactions between the other components are unfortunately unknown. From the results it could be observed that the effect of sulfuric acid and xylose (on water) is minimal under the used conditions.

At higher stripping rates the model deviates more from the experimental data under these conditions, this suggest that mass transfer limitation is present at higher stripping rates.

The model is consistent with experimental data for continuous operation, where a xylose solution is fed in ratio to the stripping rate to maintain a constant reactor volume. This potential of the model could be used to design a continuous operating reactor.

The model is also validated for higher sulfuric acid conditions and model predictions are made up to concentrations of 10 w%. The reaction rate constant for the conversion of xylose increases 10 times with an increasing acid concentration from 0.5 to 10 w%, so leading to a significant higher productivity. The final yield drops with 21% to 53%.

It could be validated if the models is able to describe higher xylose concentrations well. So called condensation loss reactions could result in a lower furfural yield at higher xylose concentrations. With this remark made, the model predicts a significant increase in productivity for higher xylose concentrations, up to 10 w%, without noticeable loss in yield.

The effect of temperature on the furfural production process is investigated as well. For a temperature range from 150 to 200°C the reaction rate constant for the conversion of xylose increases more than 50 times, causing a significant increased productivity. Another beneficial effect is that the rate for conversion of xylose is increased more than the rate of furfural degradation at increasing temperatures. Also the saturation pressure of furfural vapor increases more than the same pressure for water at increasing temperatures.

The influence of an increased operating pressure is also predicted. Mainly due to a negative effect on the stripping rate a higher pressure leads to a decrease in conversion and yield. At higher operating pressure it is possible to obtain a more concentrated stripping/ condensate stream.

Combining the advantages predicted for the various operating conditions, a theoretical productivity rate of 0.0288 mol L^{-1} s^{-1} could be achieved. Exploiting such a rate could lead to an enormous process intensification compared to the conventional (batch) production process.

The desired next step in the biomass valorization is the hydrogenation of furfural. In the case of vapor phase hydrogenation towards furfuryl alcohol, the use of hydrogen as a stripping agent could be most beneficial. For the aqueous phase hydrogenation towards cyclopentanol/cyclopentanone a trickle bed reactor could be designed where the vapor phase furfural is condensed. The proposed model is able to predict output when a recycle stream of furfural and/or water from the hydrogenation reaction is used. The use of recycle heat already leads to a 1.5 times increased energy input. Going from a pure nitrogen/ hydrogen stripping stream to a pure steam stripping stream a heat reduction of 28% could be achieved due to the evaporation of water.

The proposed models are compared to models proposed in literature. It is showed to be impossible to reproduce the data from other models. Also the use of a stripping mass transfer constant, as suggested in literature, proves to be unable to describe the experimental data.

6. Recommendations

Based on the investigations done in this study several recommendations for future research could be made.

To improve the productivity of the furfural production process experiments with higher xylose, acid and/or temperatures should be performed. The use of different catalysts, such as HCl, and/or the addition of salts/halides could be studied as well for the improvement of productivity. Several authors showed different effects compared to sulfuric acid. [26] [24]

Going to more severe conditions hydrogen would not be the preferred stripping agent. The use of (unsaturated) steam could be a possibility, but more investigation for the optimization of this aspect should be done.

Mechanistic research to the intermediate and loss products is not included in this study and could be further investigated as well to optimize the process by the further prevention of loss reactions.

To obtain kinetics for condensation losses of furfural and binary interaction parameters between all the different components, experiments should be done.

The model could be improved by taking into account the possible condensation losses. This should lead to a better model description for higher xylose concentrations. It is only a small model adjustment, but new kinetic parameters are needed.

The next step in biomass valorization, the hydrogenation of furfural, could be investigated further. Both processes could be tuned to optimize the combined process for process intensification. A hydrogenation reactor could be designed (in place of the currently used condenser).

The experimental setup for the production of furfural used in this study could be improved to make it better suitable for the process and eventually possible scale-up.

Instead of using xylose as a model compound, biomass could be investigated as a starting material for this production process.

7. References

[1] K. Zeitsch, "The Chemistry and Technology of Furfural and its many By-Prodructs," in *Sugar series*, vol. 13, 2000.

[2] A. Mandalika and T. Runge, "Enabling integrated through high-yield conversion of fractionated pentosans into furfural," *Green Chem.,* vol. 14, pp. 3175-3184, 2012.

[3] A. Dias, M. Pillinger and A. Valente, "Dehydration of xylose into furfural over micro-mesoporous sulfonic acid catalysts," *J. Cat.,* vol. 229, pp. 414-423, 2005.

[4] A. Dunlop, "Furfural formation and behavior'," *Ind. Eng. Chem.,* vol. 40, no. 2, p. 204, 1948.

[5] B. Danon, G. Marcotulio and W. d. Jong, "Mechanistic and kinetic aspects of pentose dehydration towards furfural in aqueous media employing homogeneous catalysis," *Green Chem.,* vol. 16, p. 39, 2014.

[6] M. Hronec and K. Fulajtarova, "Selective transformation of furfural to cyclopentanone," *Cat. Comm.,* vol. 24, pp. 100-104, 2012.

[7] G. Marcotulio, M. Tavares Cardoso, W. de Jong and A. Verkooijen, "Furfural Destruction Kinetics during Sulphuric Acid-Catalyzed Production from Biomass," *Int. J. of Chem. Reactor Eng.,* vol. 7, 2009.

[8] I. Agirrezabal-Tellaria, A. Larreategui, J. Requies, M. Guemez and P. Arias, "Furfural production from xylose using sulfonic ion-exchange resins (Amberlyst) and simultaneous stripping with nitrogen," *Bioresource Technology,* vol. 102, pp. 7478-7485, 2011.

[9] D. Root, J. Saeman, J. Harris and W. Neill, *Forest Products Journal,* vol. 9, pp. 158-165, 1959.

[10] D. Rackemann, J. Bartley and W. Doherty, "Methanesulfonic acid-catalyzed conversion of glucose and xylose mixtures to levulinic acid and furfural," *Ind. Crops and Products,* vol. 52, pp. 46-57, 2014.

[11] P. Oefner, A. Lanziner, G. Bonn and O. Bobleter, "Qunative Studies on Furfural and Organic Acid Formation during Hydrothermal, Acidic and Alkaline Degradation of D-Xylose," *Monatshefte fur Chemie,* vol. 123, pp. 547-556, 1992.

[12] P. Metkar, E. Till, D. Corbin, C. Pereira, K. Hutchenson and S. Sengupta, "Reactive distillation process for the production of furfural using solid acid catalysts," *Green Chem.,* vol. 17, pp. 1453-1466, 2015.

[13] L. Mao, L. Zhang, N. Gao and A. Li, "FeCl3 and acetic acid co-catalyzed hydrolysis of corncob for improving furfural production and lignin removal from residue," *Bioresource Technology,* vol. 123,

pp. 324-331, 2012.

[14] A.-C. Doiseau, F. Rataboul, L. Burel and N. Essayem, "Synergy effect between solid acid catalysts and concentrated carboxylic acids solutions for efficient furfrual production from xylose," *Cat. Today,* vol. 226, pp. 176-184, 2014.

[15] V. Choudhary, S. Sandler and D. Vlachos, "Conversion of Xylose to Furfural Using Lewis and Bronsted Acid Catalysts in Aqueous Media," *ACS Cat.,* vol. 2, pp. 2022-2028, 2012.

[16] I. Agirezzabal-Tellaria, J. Requies, M. Guemez and P. Arias, "Furfural production form xylose + glucose feedings and simultaneous N2-stripping," *Green Chem.,* vol. 14, pp. 3132-3140, 2012.

[17] I. Agirrezabal-Tellaria, I. Gandarias and P. Arias, "Production of furfural from pentosan-rich biomass: Analysis of process parameters during simultaneous furfural stripping," *Bioresource Technology,* vol. 143, pp. 258-264, 2013.

[18] W. McKillip, G. Collin, H. Hoke and K. Zeitsch, "Furan and Derivatives," Wiley-VCH Verlag, 2005.

[19] R. Weingarten, J. Cho, W. Conner and G. Huber, "Kinetics of furfural production by dehydration of xylose in a biphasic reactor with microwave heating," *Green Chem.,* vol. 12, pp. 1423-1429, 2010.

[20] D. Vargas-Hernandez, J. Rubio-Caballero, J. Santamaria-Gonzalez, R. Moreno-Tost, J. Merida-Robles, M. Perez-Cruz, A. Jimenez-opez, R. Hernandez-Huesca and P. Maireles-Torres, "Furfuryl alcohol from furfural hydrogenation over copper supported on SBA-15 silica catalysts," *J. of Mol. Cat.,* vol. 383, pp. 106-113, 2014.

[21] G.-S. Zhang, M. Zhu, Q. Zhang, Y. Liu, H. He and Y. Cao, "Towards quantitative and scable transformation of furfural to cylcopentanone with supported gold catlaysts," *Green Chem.,* vol. 18, pp. 2155-2164, 2016.

[22] H. Zhu, M. Zhou, G. Xiao and R. Xiao, "Selective hydrogenation of furfural to cyclopentanone over Cu-Ni-Al hydrotalcite-based catalysts," *Korean J. Chem. Eng.,* vol. 31, pp. 593-597, 2014.

[23] M. Zhou, Z. Zeng, H. Zhu, G. Xiao and R. Xiao, "Aqueous-phase catalytic hydrogenation of furfural to cylcopentanol over Cu-Mg-Al hydrotalcites derived catalysts: Model reaction for upgrading bio-oil," *J. of Energy Chem.,* vol. 23, pp. 91-96, 2014.

[24] G. Marcotulio, "The Chemistry and Technology of Furfural Production in Modern Lignocellulose-Feedstock Biorefineries," 2011.

[25] H. Carlson and A. Colburn, *Ind. Eng. Chem.,* vol. 34, p. 581, 1942.

[26] R. Curtis and H. Hatt, "EQUILIBRIA IN FURFURAL-WATER SYSTEMS UNDER INCREASED PRESSURE

AND THE INFLUENCE OF ADDED SALTS UPON THE MUTUAL SOLUBILITIES OF FURFURAL AND WATER," pp. 213-235, 1948.

[27] J. Harris and J. Smuk, "Engineering for the distillation of the furfural-water system," 1959.

[28] H. Renon and J. Praustnitz, "Local Compostions in Thermodynamic Excess Functions for Liquid Mixtures," *AIChE Journal,* vol. 14, pp. 135-144, 1968.

[29] N. Bouneb, A.-H. Meniai and W. Louaer, "Introduction Of The Group Contribution Concept Into The Nrtl Model," in *20th European Symposium on Computer Aided Process Engineering*, 2010.

[30] M. Sunder and D. Prasad, "Phase Equilibria of Water + Furfural and Dichloromethane + n-Hexane," *J. Chem. Eng. Data,* vol. 48, pp. 221-223, 2003.

[31] L. Fele and V. Grilc, "Separation of Furfural from Ternary Mixtures," *J. Chem. Eng. Data,* vol. 48, pp. 564-570, 2003.

[32] A. Vetere, "The NRTL equation as a predictive tool for vapor-liquid equilibria," *Fluid Phase Equilibria,* vol. 218, pp. 33-39, 2004.

[33] B. Staples, "Activity and Osmotic Coefficients of Aqueous Sulfuric Acid at 298.15 K," *J. Phys. Chem. Ref. Data,* vol. 10, no. 3, pp. 779-798, 1981.

[34] J. Comesana, A. Correa and A. Sereno, "Water activity at 35 C in 'sugar' + water and 'sugar' + sodium chloride + water systems," *Int. J. of Food Science and Technology,* vol. 36, pp. 655-661, 2001.

[35] A. Bosen and H. Engels, "DESCRIPTION OF THE PHASE EQUILIBRIUM OF SULFURIC ACID WITH THE NRTL EQUATION AND A SOLVATION MODEL IN A WIDE CONCENTRATION AND TEMPERATURE RANGE," *Fluid Phase Equilibria,* vol. 43, pp. 213-230, 1988.

[36] G. Mains, *Chem. Metall. Eng.,* vol. 26, p. 779, 1922.

Appendices

Appendix A: Nomenclature

CPO	cyclopentanone
CPL	cyclopentanol
FA(L)	furfuryl alcohol
FFA	furfural
FurC	furfural in condensate
FurR	furfural in reactor
HMF	hydroxymethylfurfural
HPLC	high pressure liquid chromatography
NRTL	non random two liquid (model)
VLE	vapor-liquid equilibrium
Xyl	xylose (in reactor)
A	van Laar parameter
a	binary interaction parameter
B	van Laar parameter
b	binary interaction parameter
C	concentration, mol/ L
c	binary interaction parameter
d	binary interaction parameter
E_A	reaction energy, J/ mol
e	binary interaction parameter
f	binary interaction parameter
G	NTRL parameter
k	reaction constant, s^{-1}
N	amount of mole, mol
p	pressure, bar
R	gas constant, J/ (mol K)
r	reaction rate mol/ (L s)
S	selectivity
T	temperature, K (°C)
t	time, s (min)
w%	weight percentage
V	volume, m^3 (L)
X	conversion
x	mole fraction (liquid phase)
Y	yield
y	mole fraction (vapor phase)
α	nonrandomness parameter
γ	activity coefficient
τ	NRTL parameter (energy of interaction)

Appendix B: Experimental results

Concentrations of furfural in the reactor (FurR), furfural in the condensate (FurC) and xylose (Xyl) for the various stripping rates are shown; at 170°C, 10 bar, 0.5 w% H_2SO_4 and 1 w% initial xylose.

a) 150 ml/min

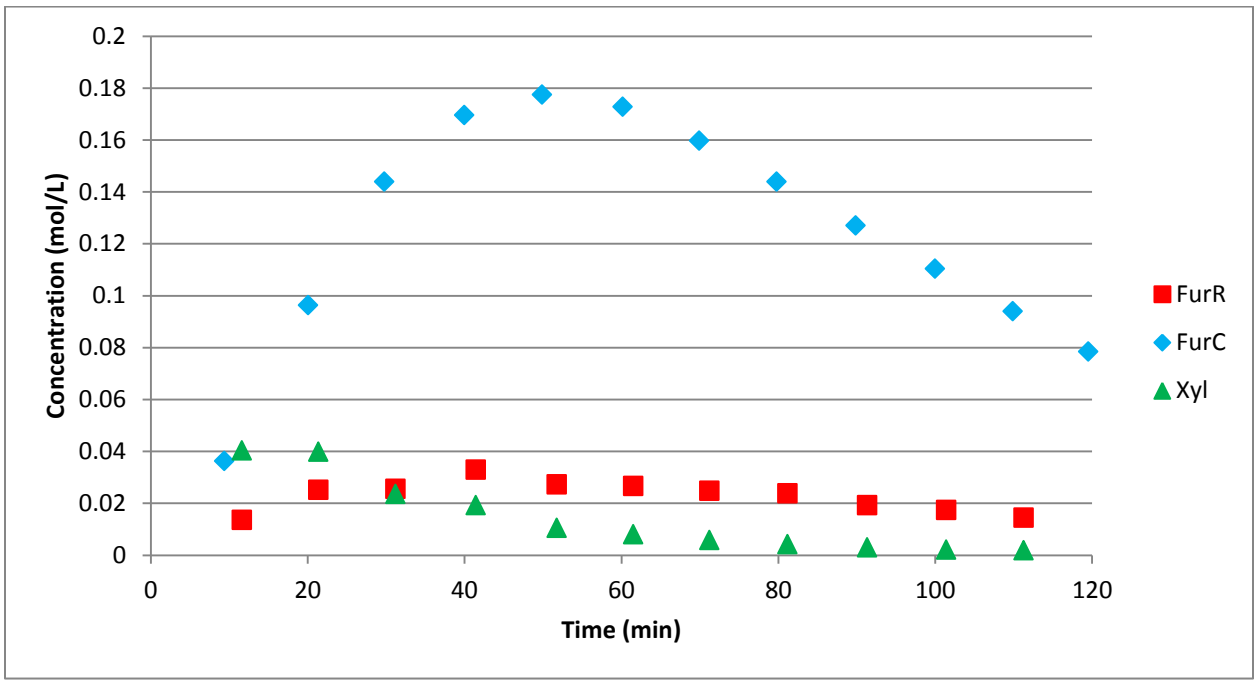

b) 300 ml/min

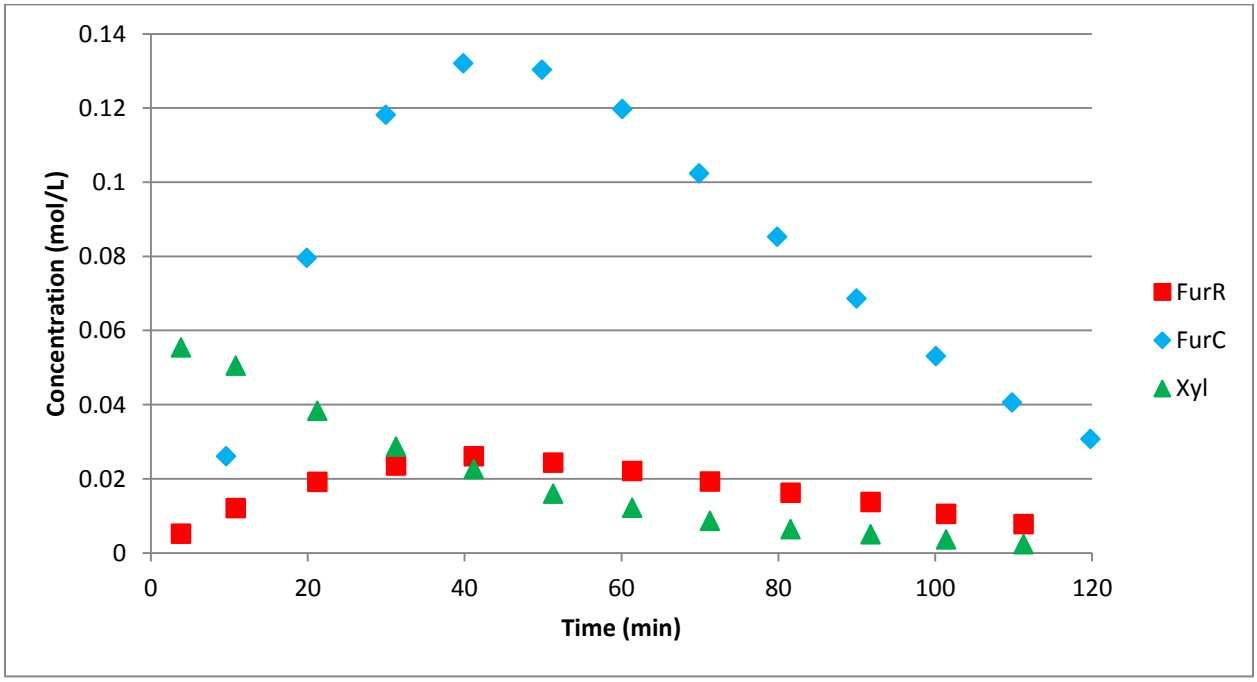

c) 500 ml/min

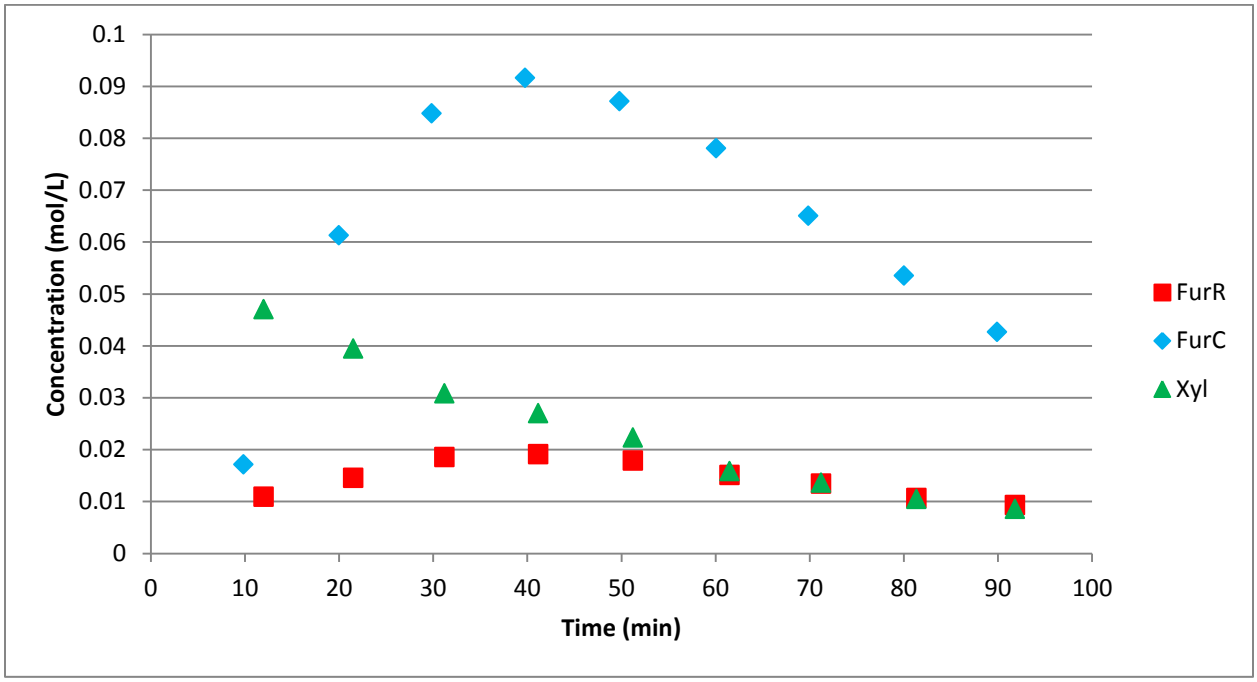

d) 1000 ml/min

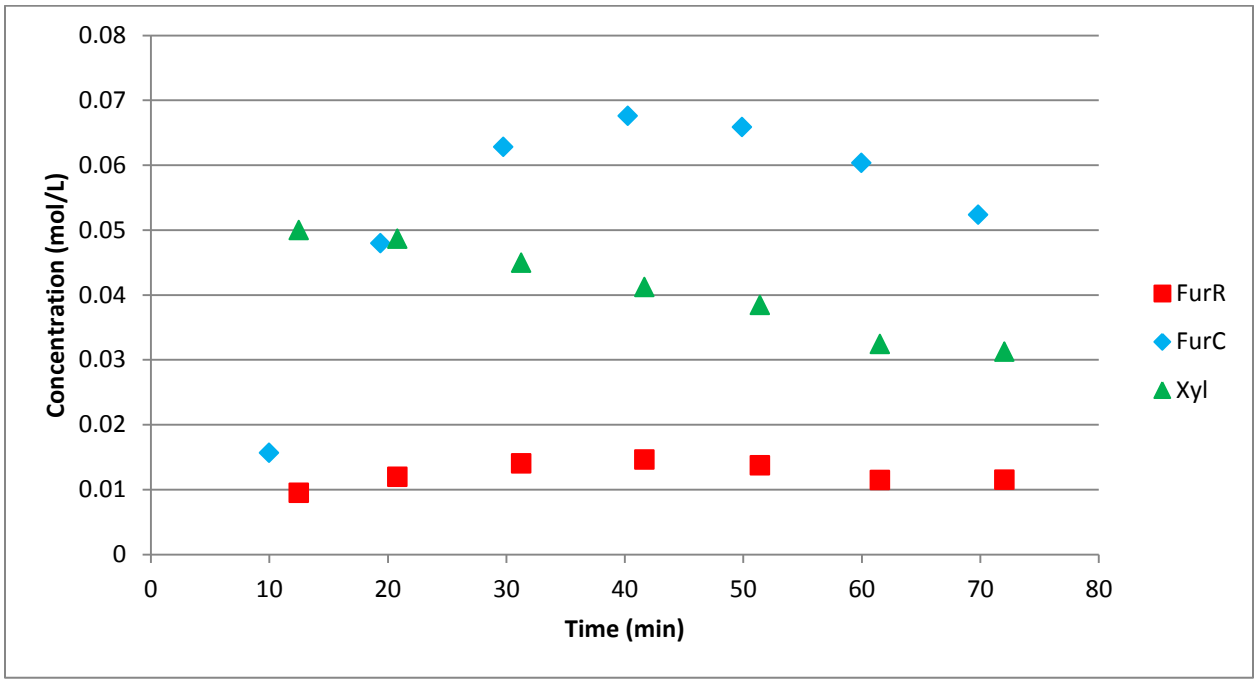

Concentrations of furfural in the reactor (FurR), furfural in the condensate (FurC) and xylose (XR) for the continuous operation are shown; at 10 bar, 0.5 w% H_2SO_4 and 1 w% initial xylose (2 min 4/ml/min 0.2504 g/ml).

a) 170°C and 1.47 ml/min 0.05 g/ml xylose feed

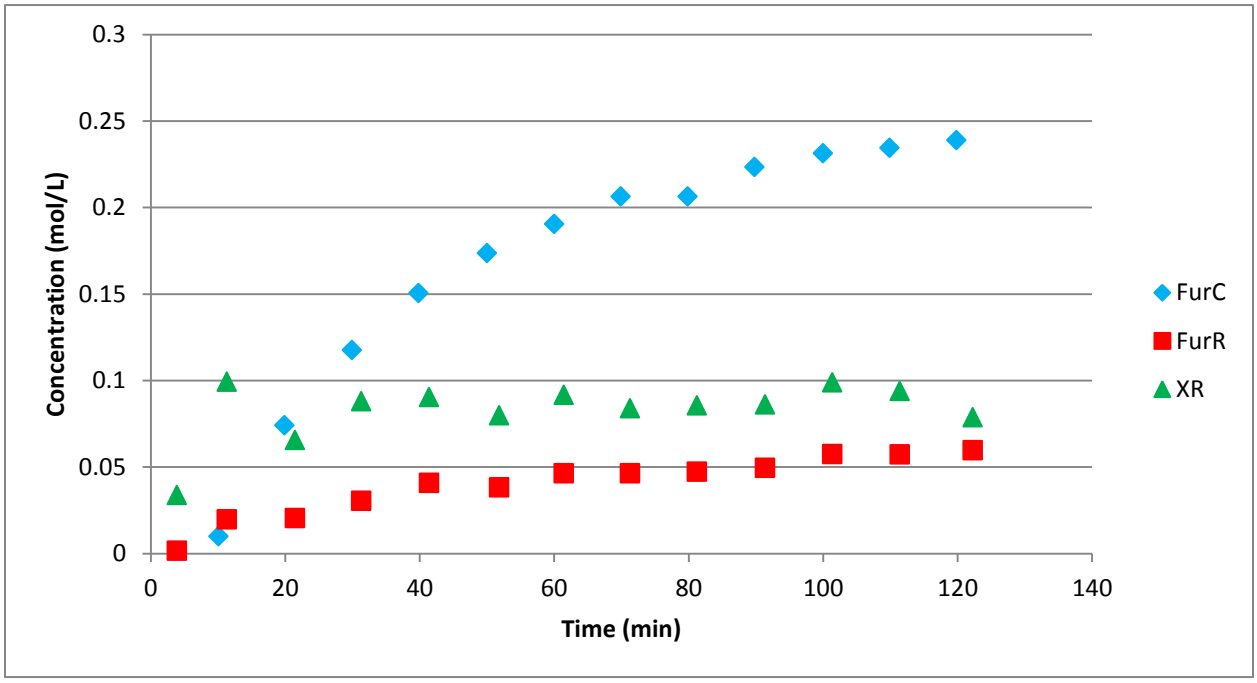

b) 177°C (200°C set) and 5 ml/min 0.03 g/ml xylose feed

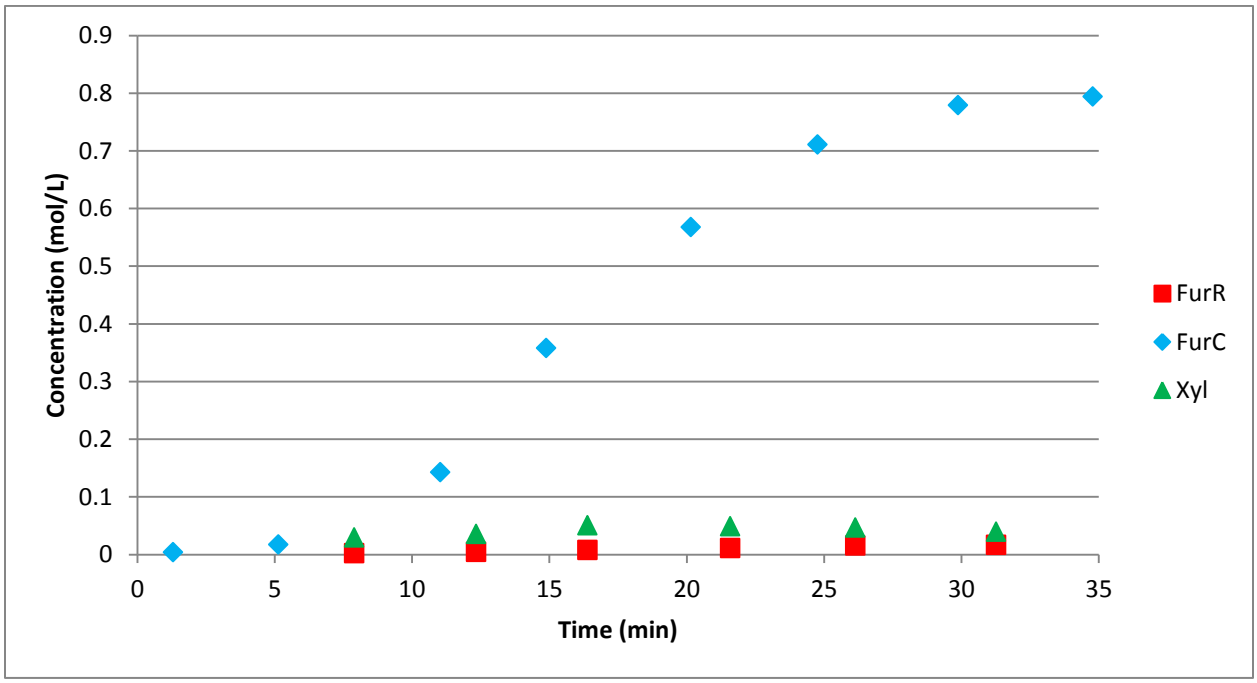

Comparison between different van Laar parameters/ parameter correlations on the amount of furfural in the reactor (FurR) and in the condensate (FurC) at 170°C, 10 bar, 0.5 w% H_2SO_4, 1 w% initial xylose and 150 ml/min N_2 stripping stream.

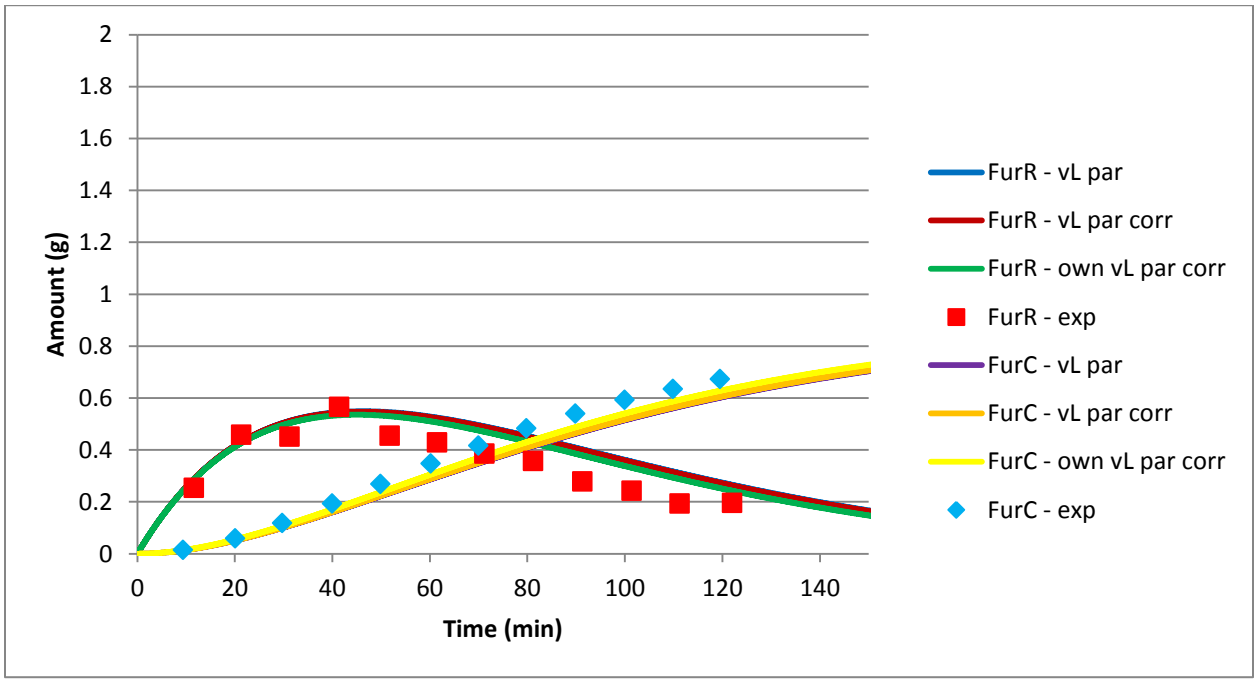

Amounts of furfural in the reactor (FurR), furfural in the condensate (FurC) and xylose (Xyl) for the other stripping rates are shown using the self-defined van Laar parameter correlations; at 170°C, 10 bar, 0.5 w% H_2SO_4 and 1 w% initial xylose. a) 300 ml/min

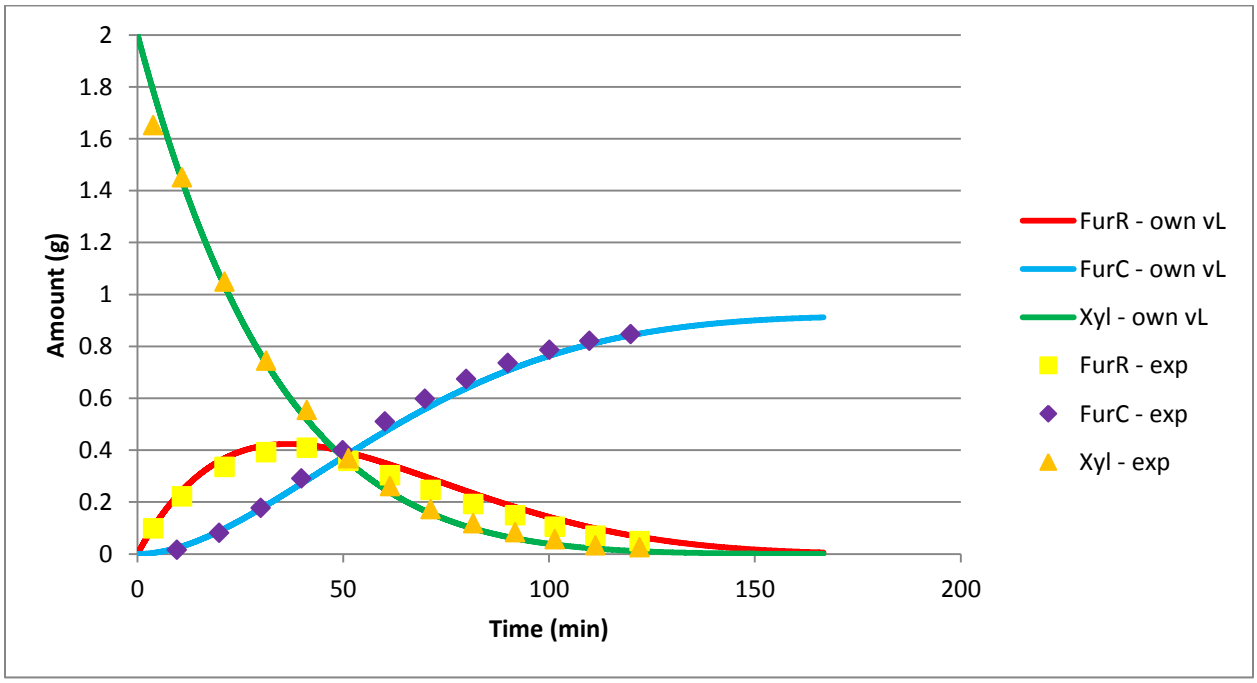

b) 500 ml/min

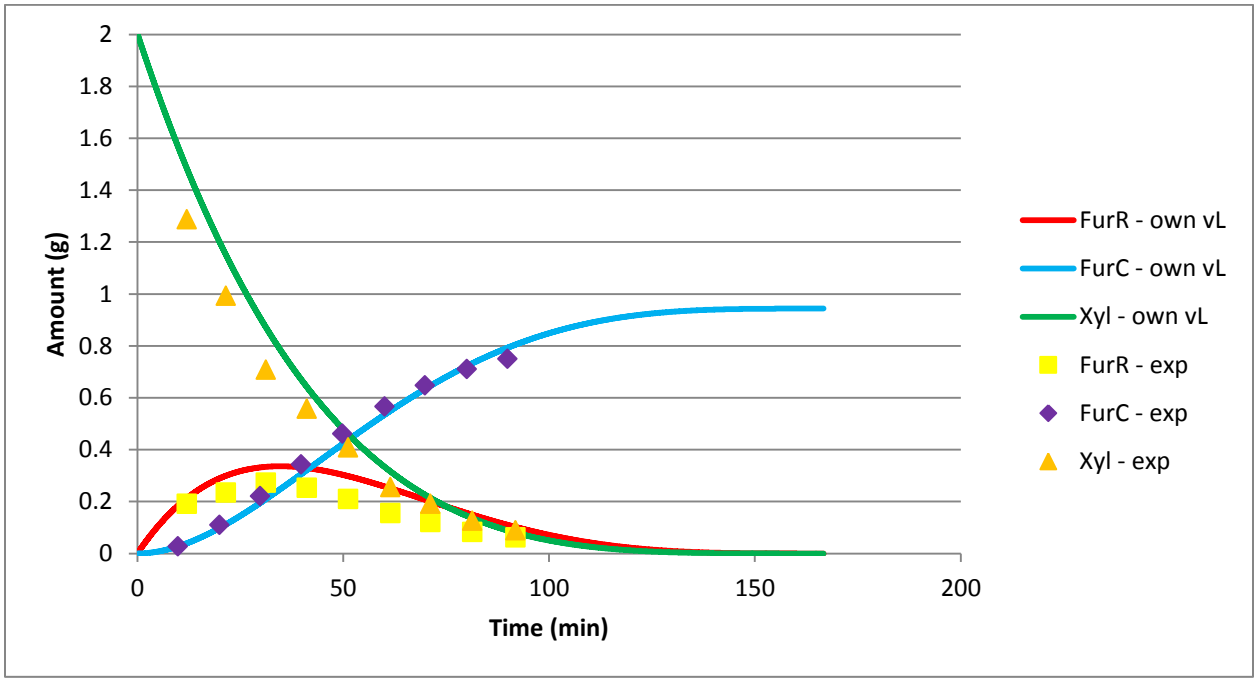

c) 1000 ml/min

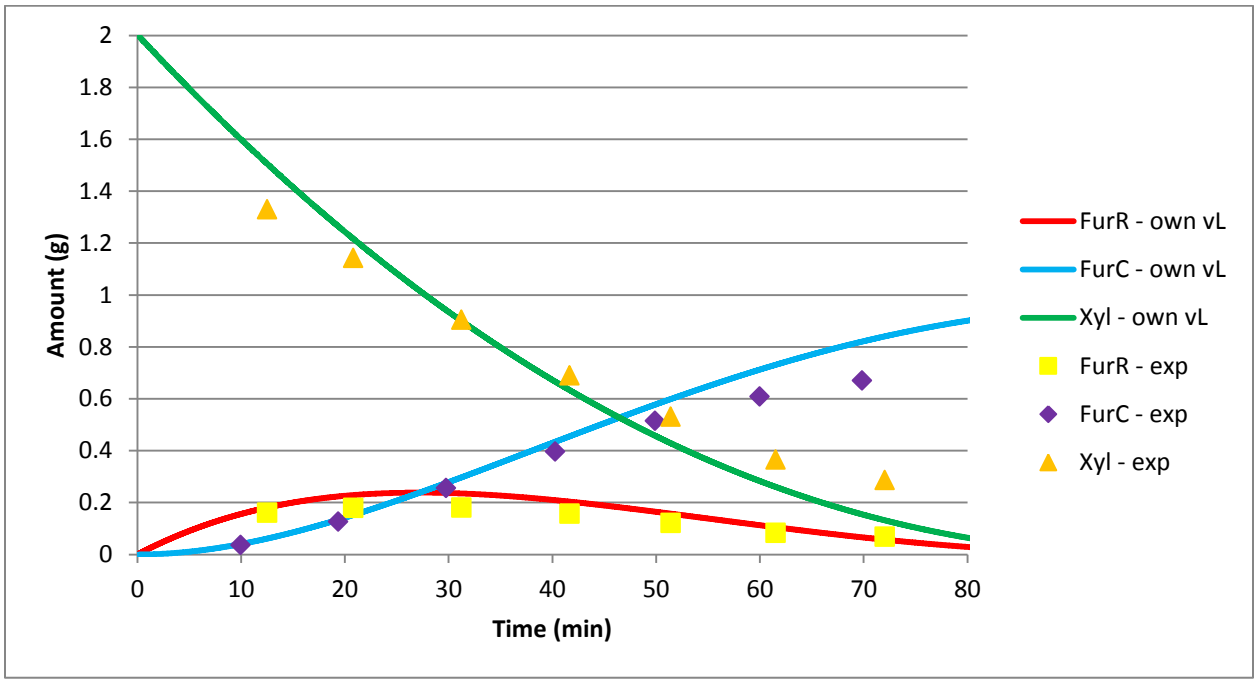

Amounts of furfural in the reactor (FurR), furfural in the condensate (FurC) and xylose (Xyl) for the other stripping rates are shown using Fele's NRTL parameters; at 170°C, 10 bar, 0.5 w% H_2SO_4 and 1 w% initial xylose.

a) 150 ml/min

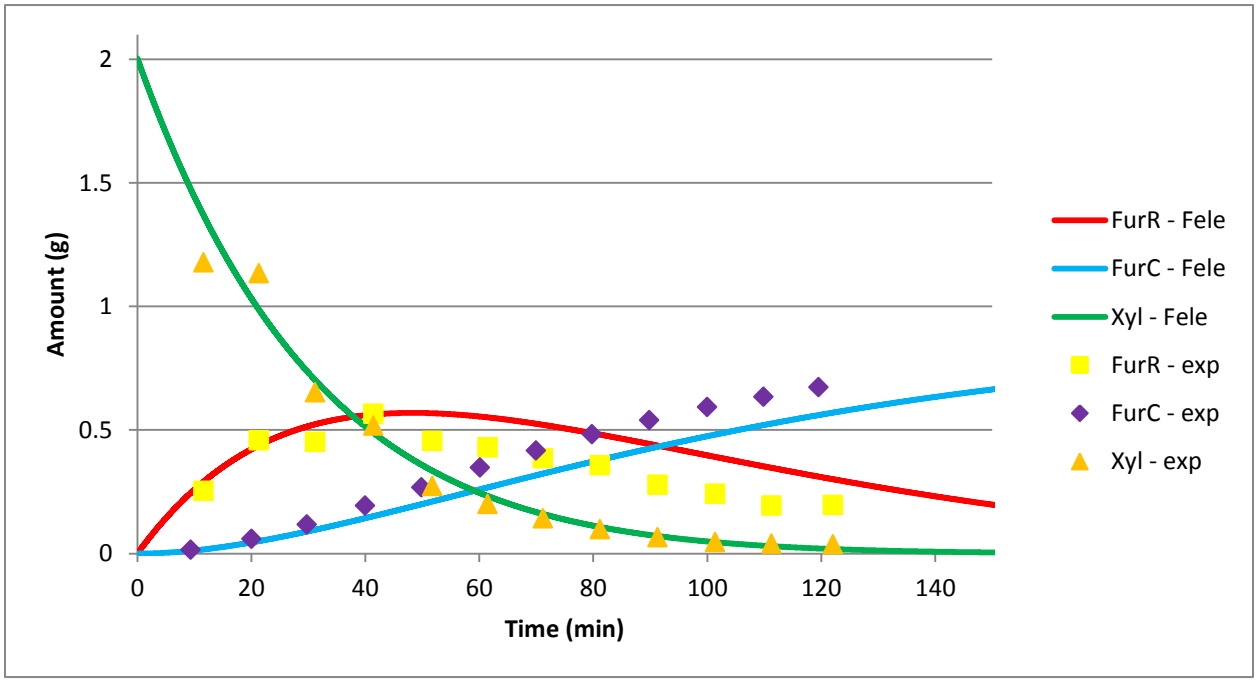

b) 300 ml/min

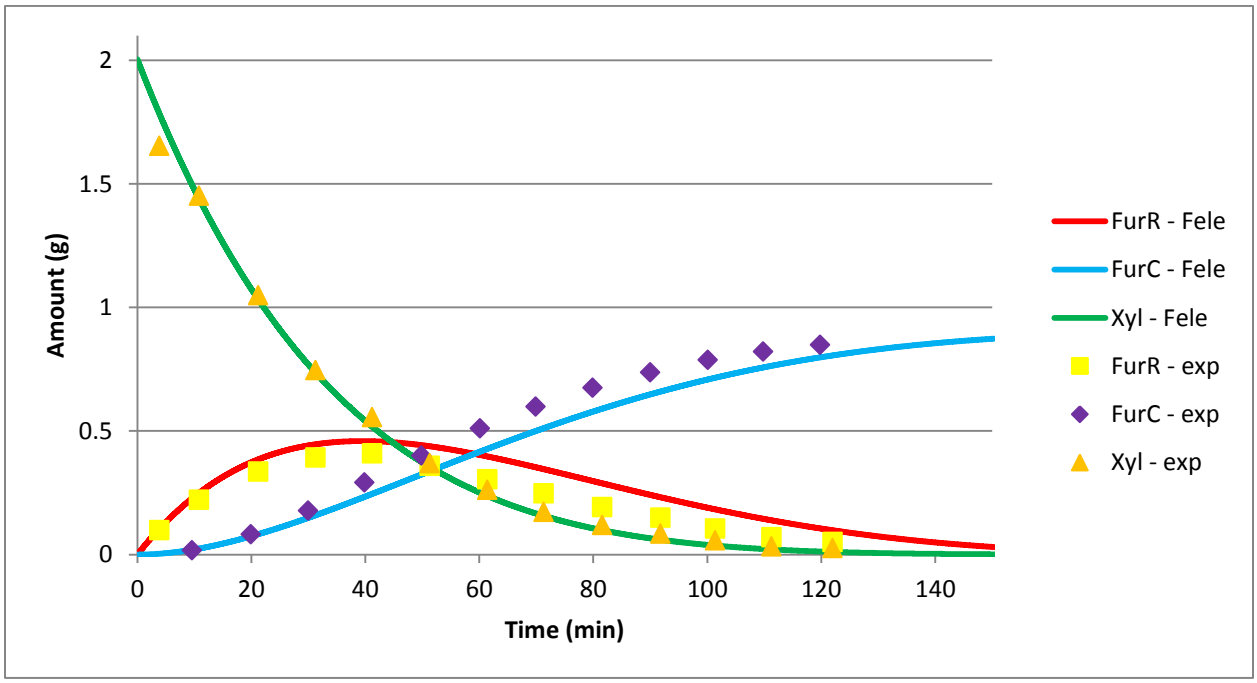

c) 500 ml/min

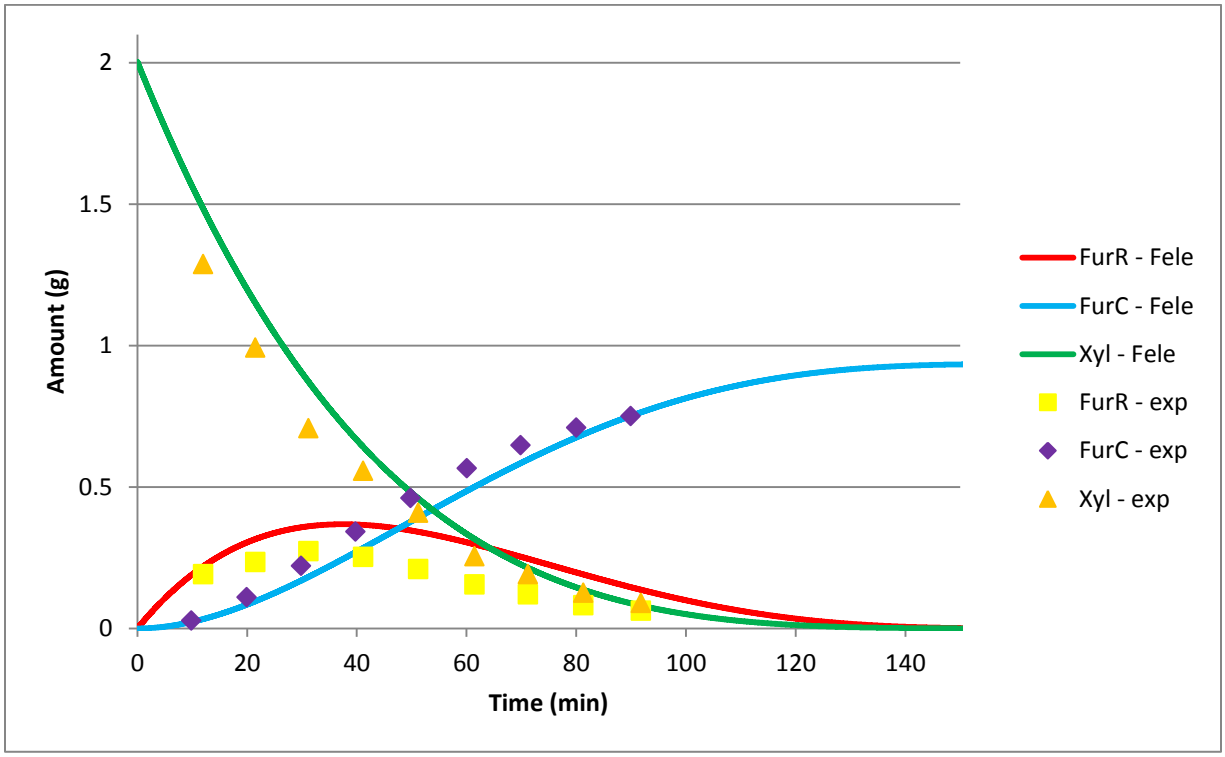
2
1.5
1
0.5
0
Amount (g)
0
20
40
60
80
100
120
140
Time (min)
FurR - Fele
FurC - Fele
Xyl - Fele
FurR - exp
FurC - exp
Xyl - exp

A comparison in the amounts of furfural in the reactor (FurR), furfural in the condensate (FurC) and xylose (Xyl) are shown for the different ASPEN NRTL parameters; at 170°C, 10 bar, 0.5 w% H_2SO_4, 1 w% initial xylose and 150 ml/min N_2 stripping rate.

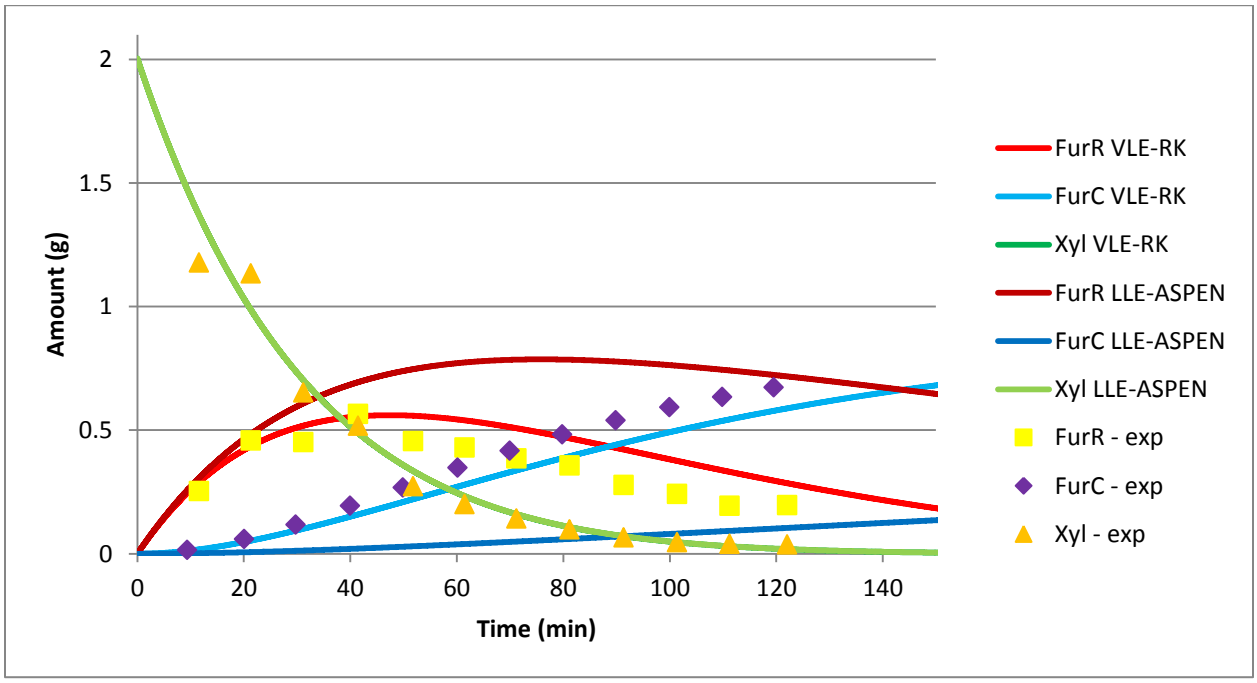

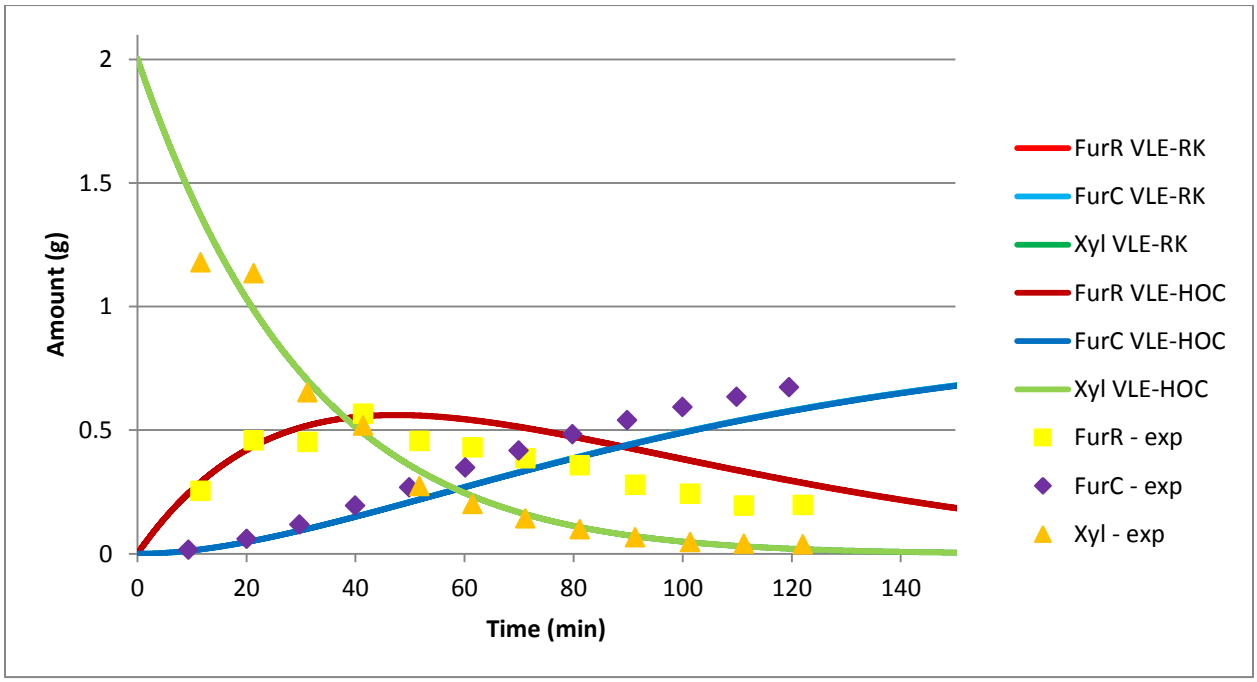

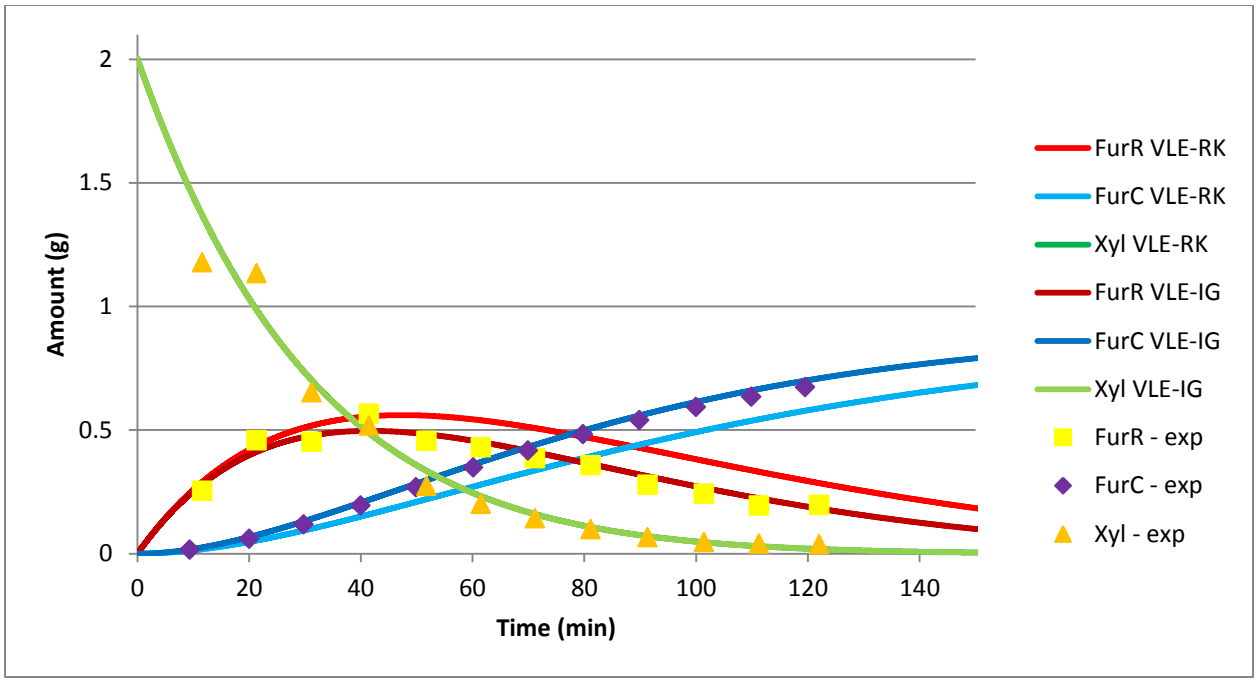
Amount (g)
Time (min)
0
0.5
1
1.5
2
0
20
40
60
80
100
120
140
FurR VLE-RK
FurC VLE-RK
Xyl VLE-RK
FurR VLE-IG
FurC VLE-IG
Xyl VLE-IG
FurR - exp
FurC - exp
Xyl - exp

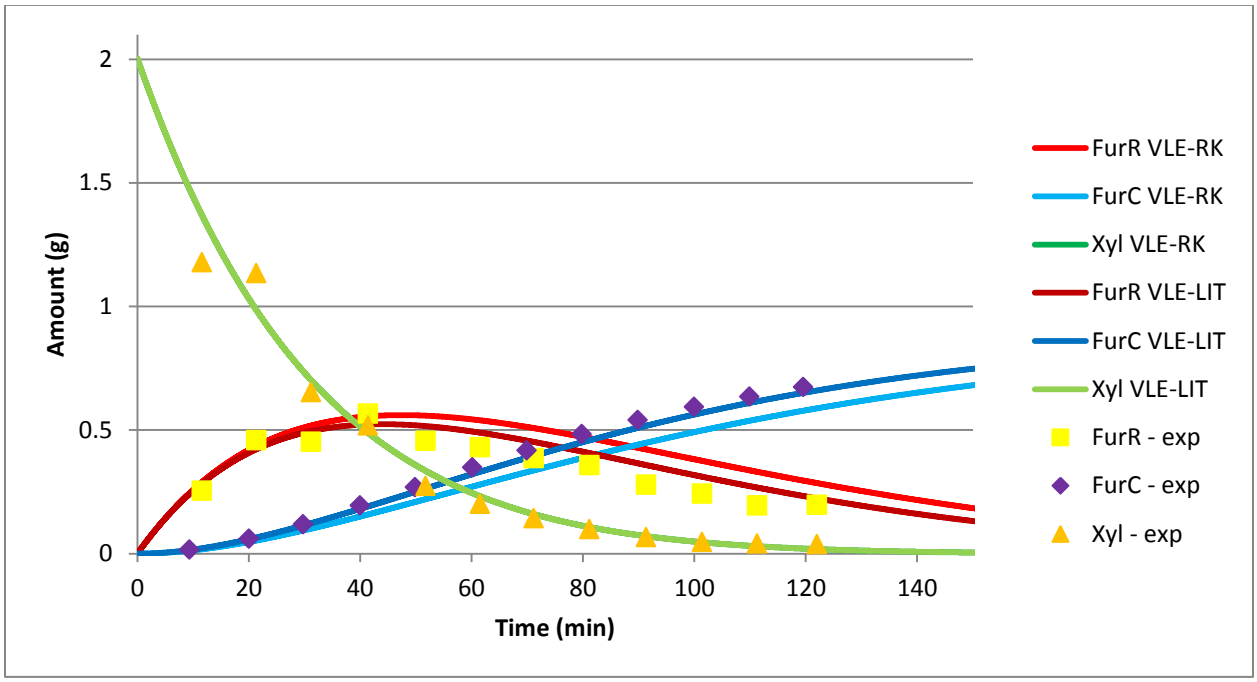
Amount (g)
Time (min)
0
0.5
1
1.5
2
0
20
40
60
80
100
120
140
FurR VLE-RK
FurC VLE-RK
Xyl VLE-RK
FurR VLE-LIT
FurC VLE-LIT
Xyl VLE-LIT
FurR - exp
FurC - exp
Xyl - exp

A comparison in the amounts of furfural in the reactor (FurR), furfural in the condensate (FurC) and xylose (Xyl) are shown for the different VLE-IG and own fitted binary interaction parameters; at 170°C, 10 bar, 0.5 w% H_2SO_4, 1 w% initial xylose and all N_2 stripping rates.

a) 150 ml/min

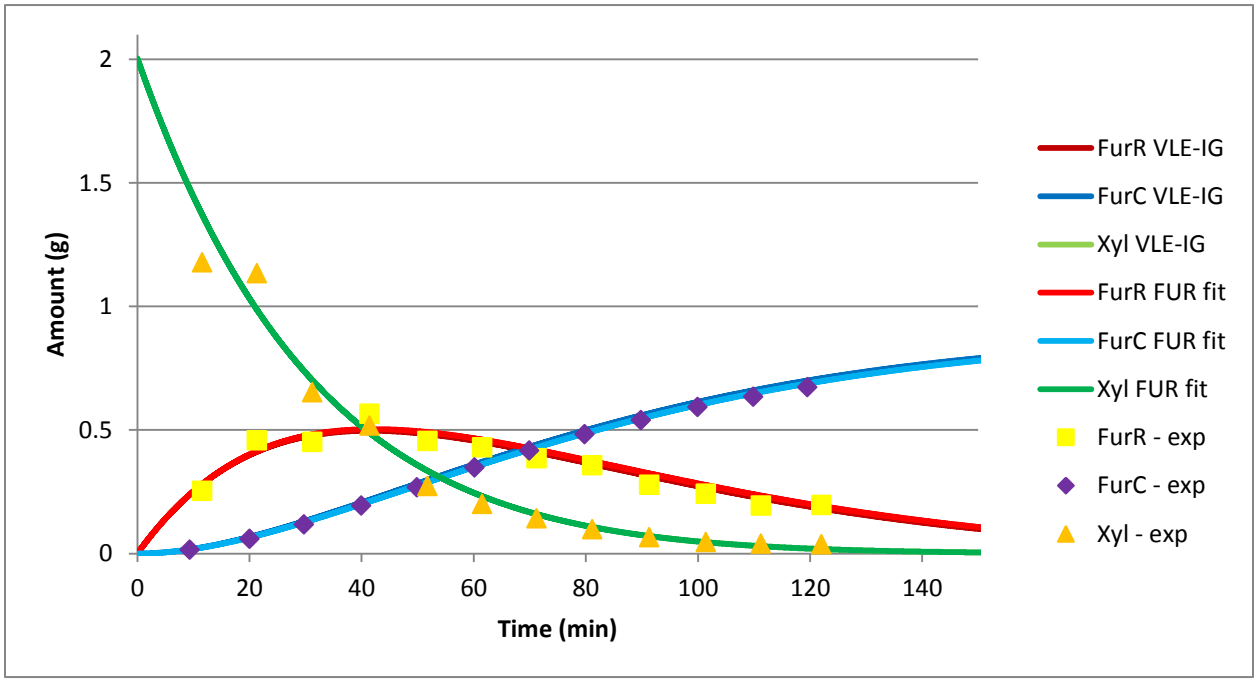

b) 300 ml/min

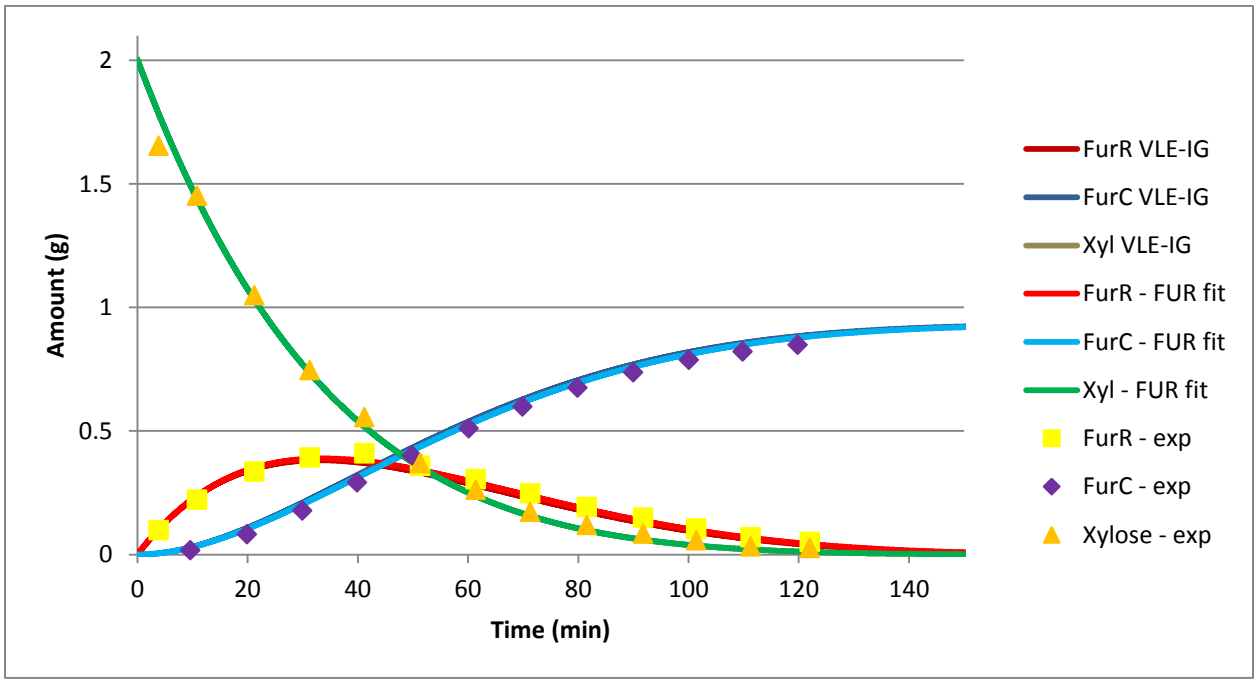

c) 500 ml/min

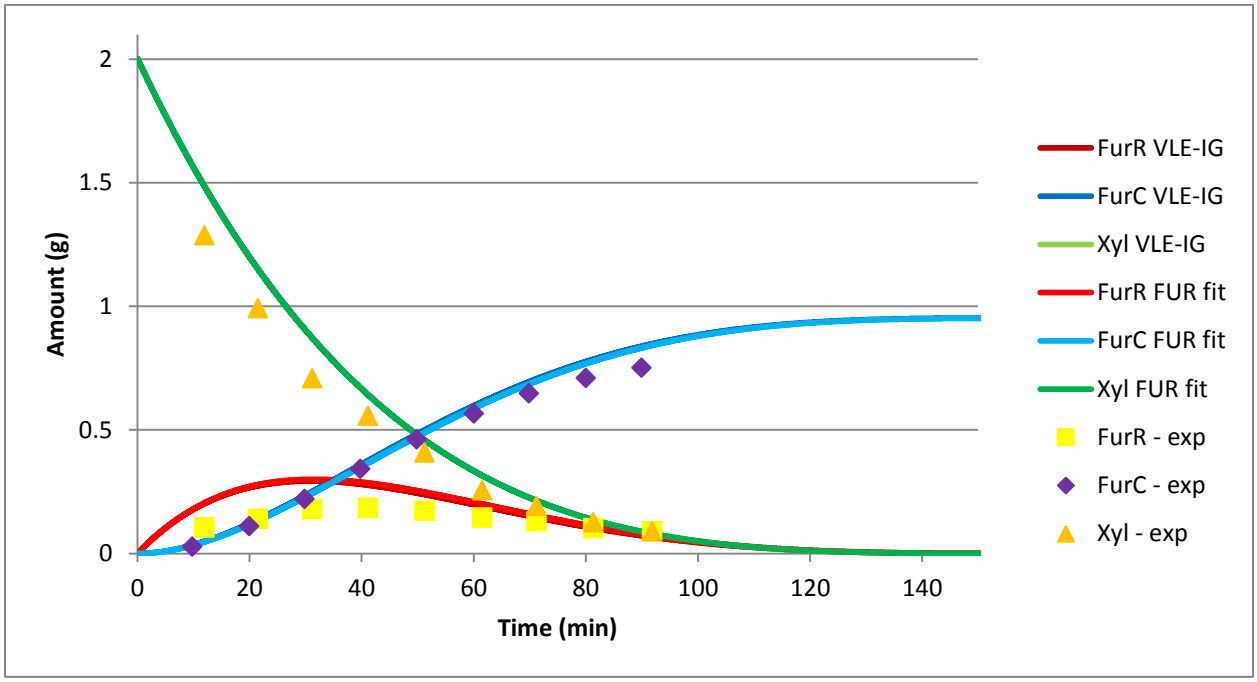

d) 1000 ml/min

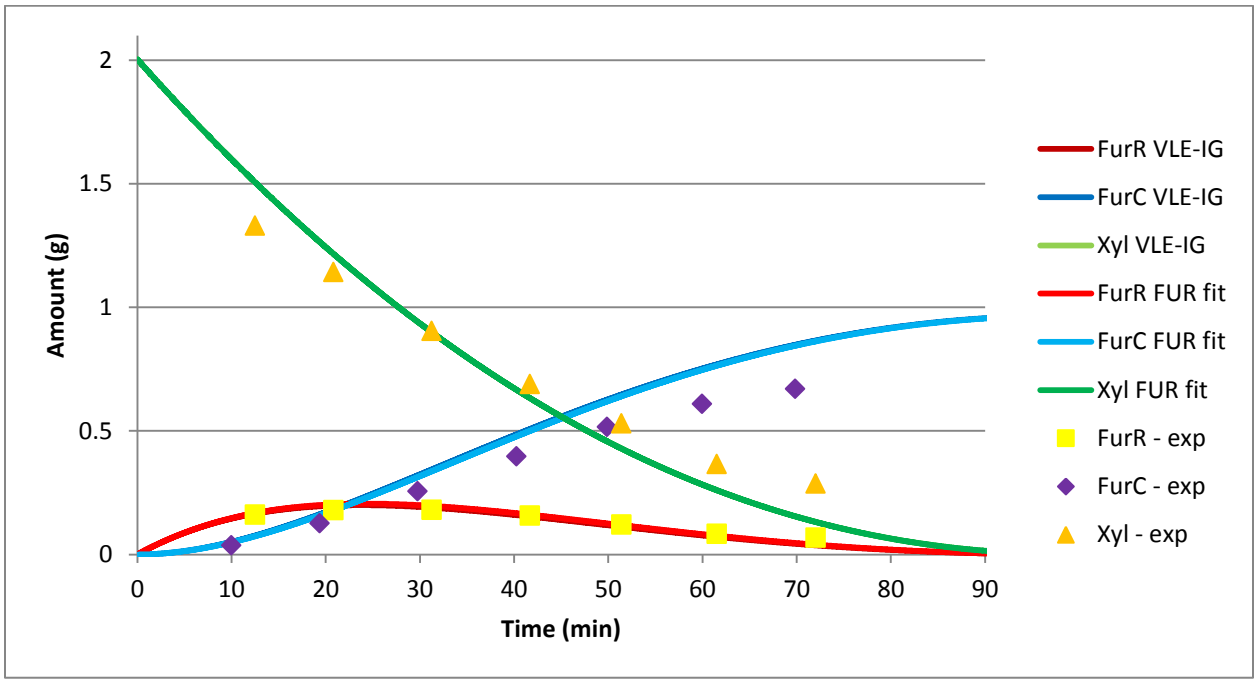

A comparison in the amounts of furfural in the reactor (FurR), furfural in the condensate (FurC) and xylose (Xyl) are shown for the addition of sulfuric acid and xylose binary interaction parameters; at 170°C, 10 bar, 0.5 w% H_2SO_4, 1 w% initial xylose and 1000 ml/min N_2 stripping rate.

a) Addition of binary interaction parameters for water/H_2SO_4

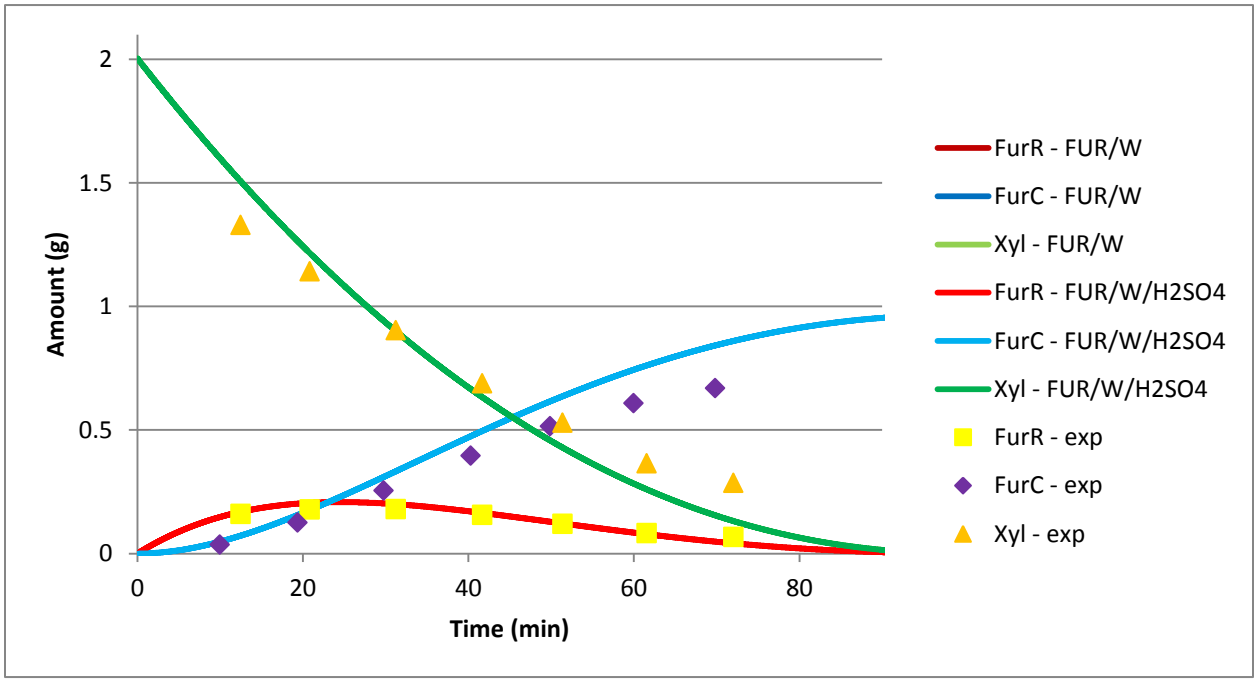

b) Addition of binary interaction parameters for water/xylose

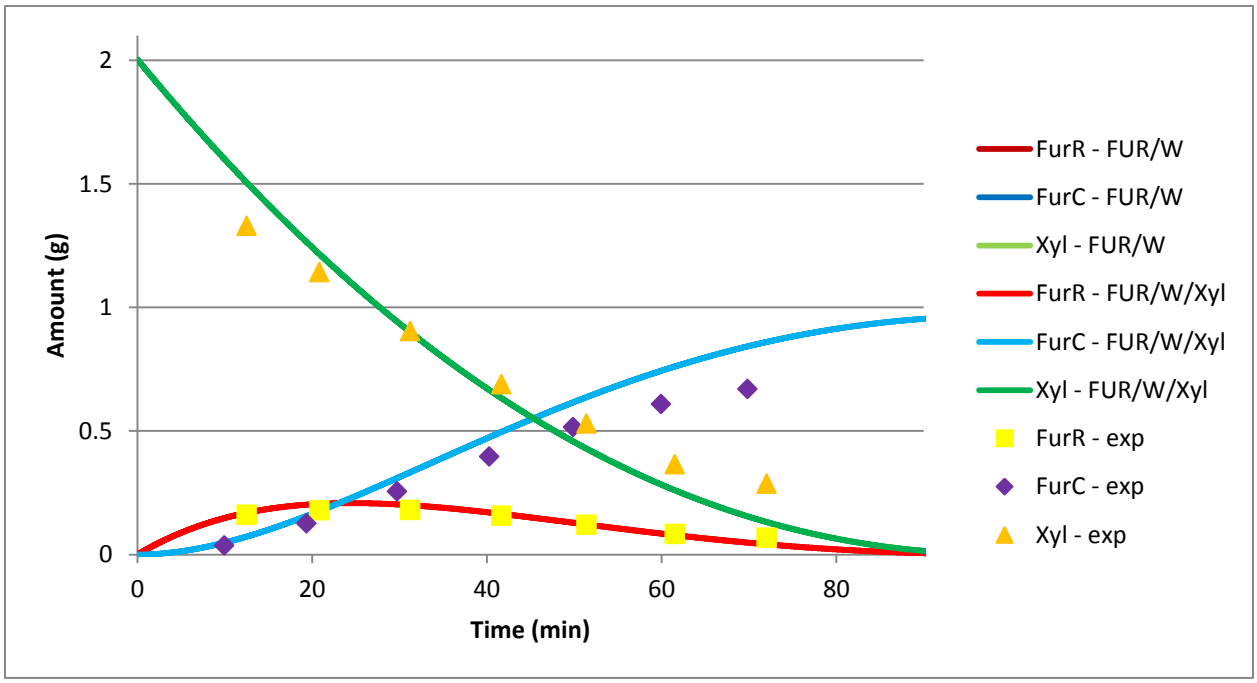

The conversion, furfural yield, concentration of furfural in the reactor (FurR) and in the condensate (FurC) are shown for the outlook acid concentration range 0.5 – 10 w%; at 170°C, 10 bar, 1 w% initial xylose and 500 ml/min N_2 stripping rate.

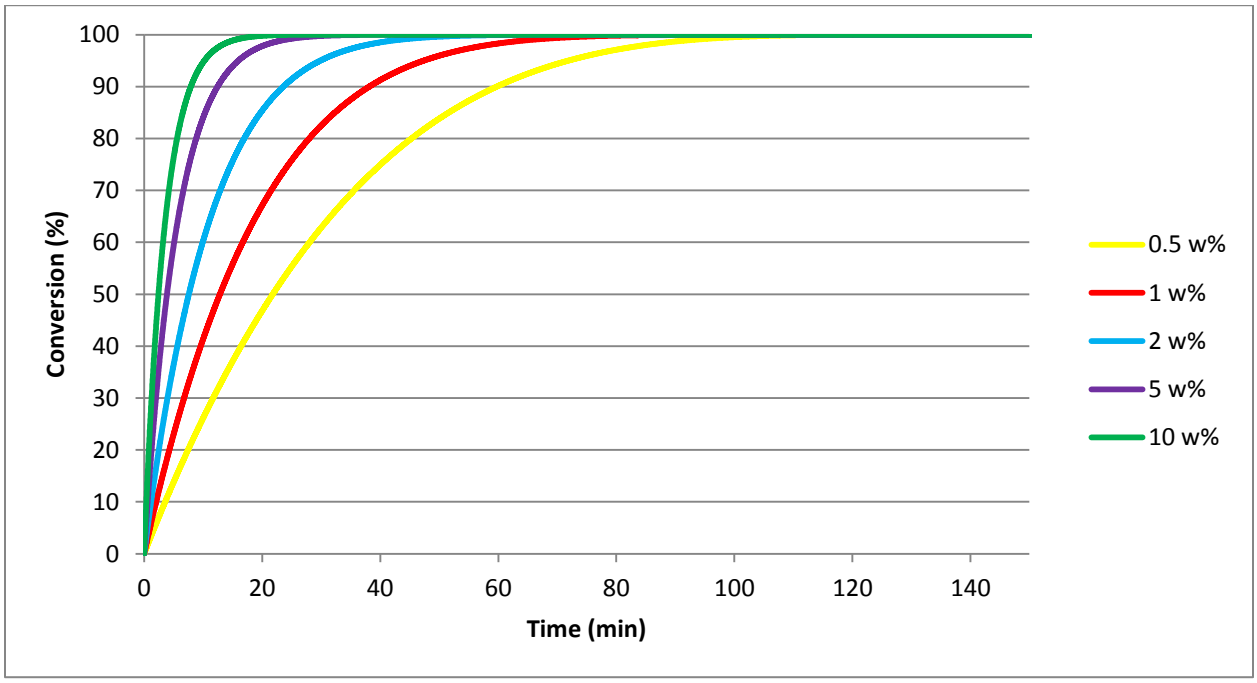

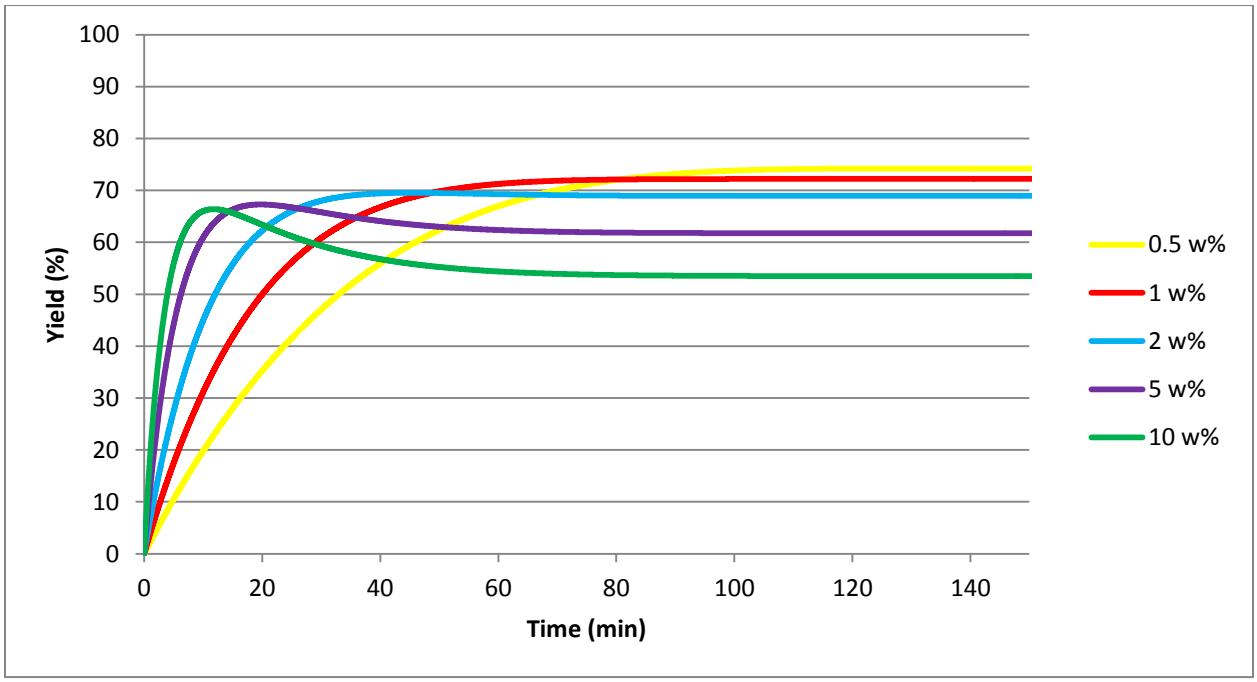

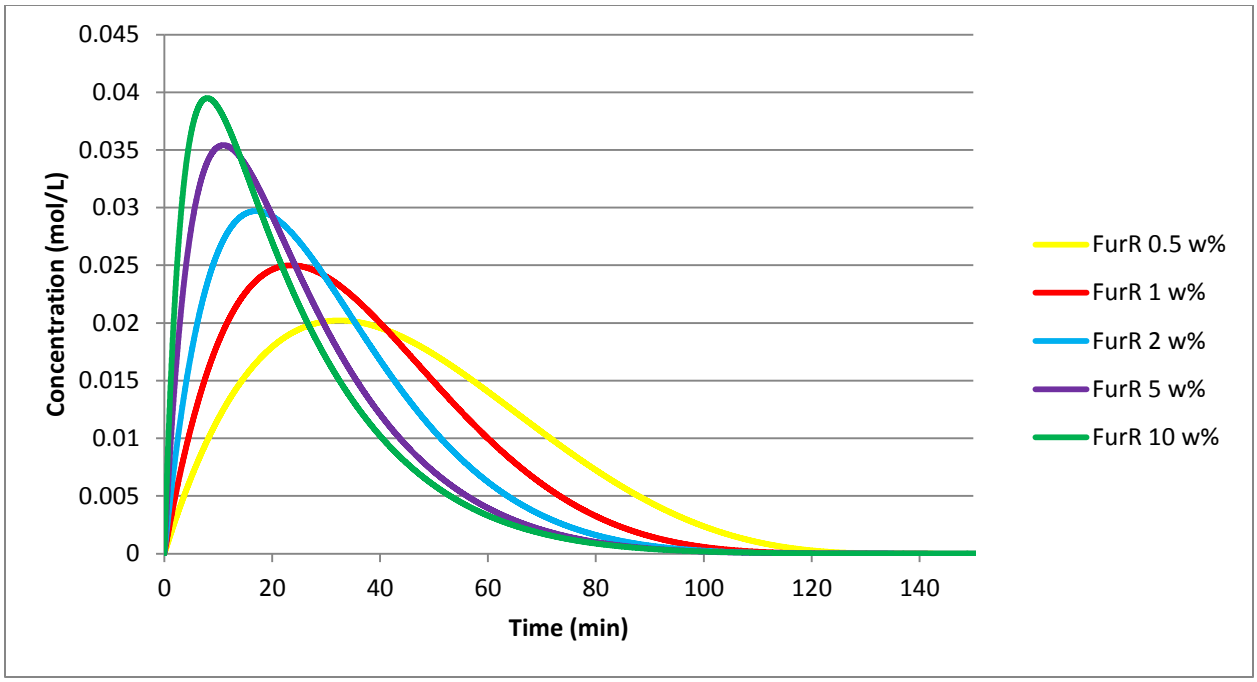
0.045
0.04
0.035
0.03
0.025
0.02
0.015
0.01
0.005
0
Concentration (mol/L)
0
20
40
60
80
100
120
140
Time (min)
FurR 0.5 w%
FurR 1 w%
FurR 2 w%
FurR 5 w%
FurR 10 w%

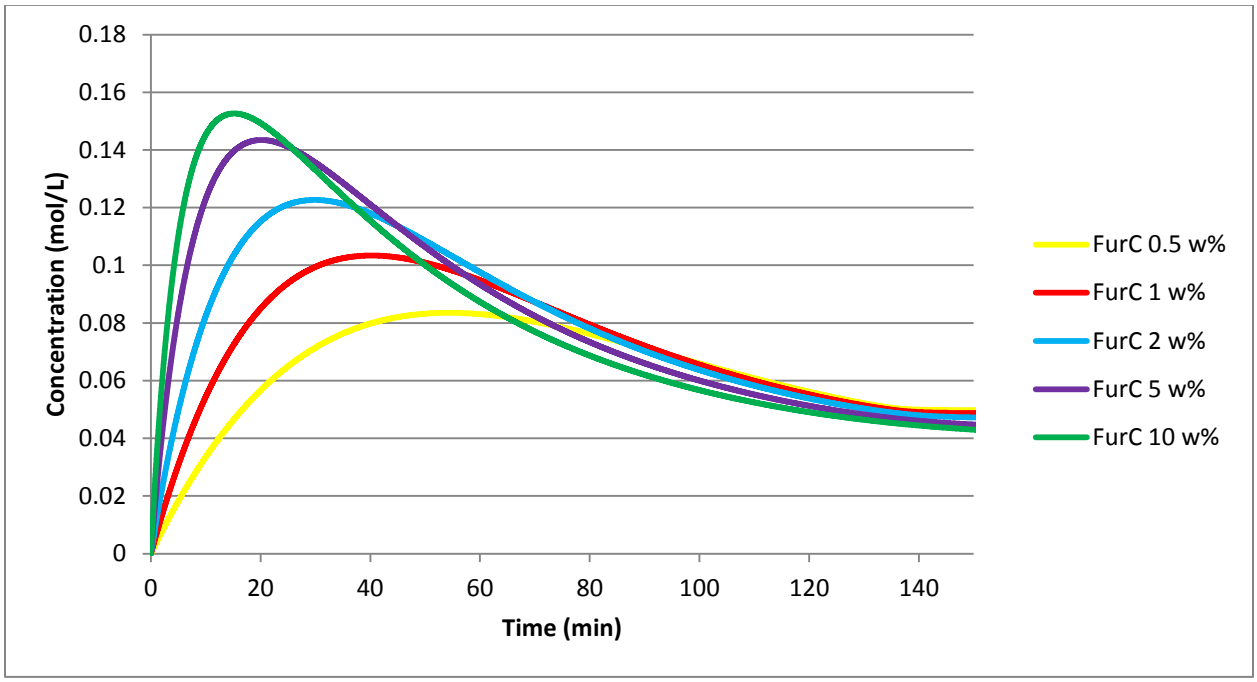
0.18
0.16
0.14
0.12
0.1
0.08
0.06
0.04
0.02
0
Concentration (mol/L)
0
20
40
60
80
100
120
140
Time (min)
FurC 0.5 w%
FurC 1 w%
FurC 2 w%
FurC 5 w%
FurC 10 w%

The furfural yield, concentration of furfural in the reactor (FurR) and in the condensate (FurC) are shown for the outlook xylose concentration range 0.5 – 10 w%; at 170°C, 10 bar, 0.5 w% H_2SO_4 and 500 ml/min N_2 stripping rate.

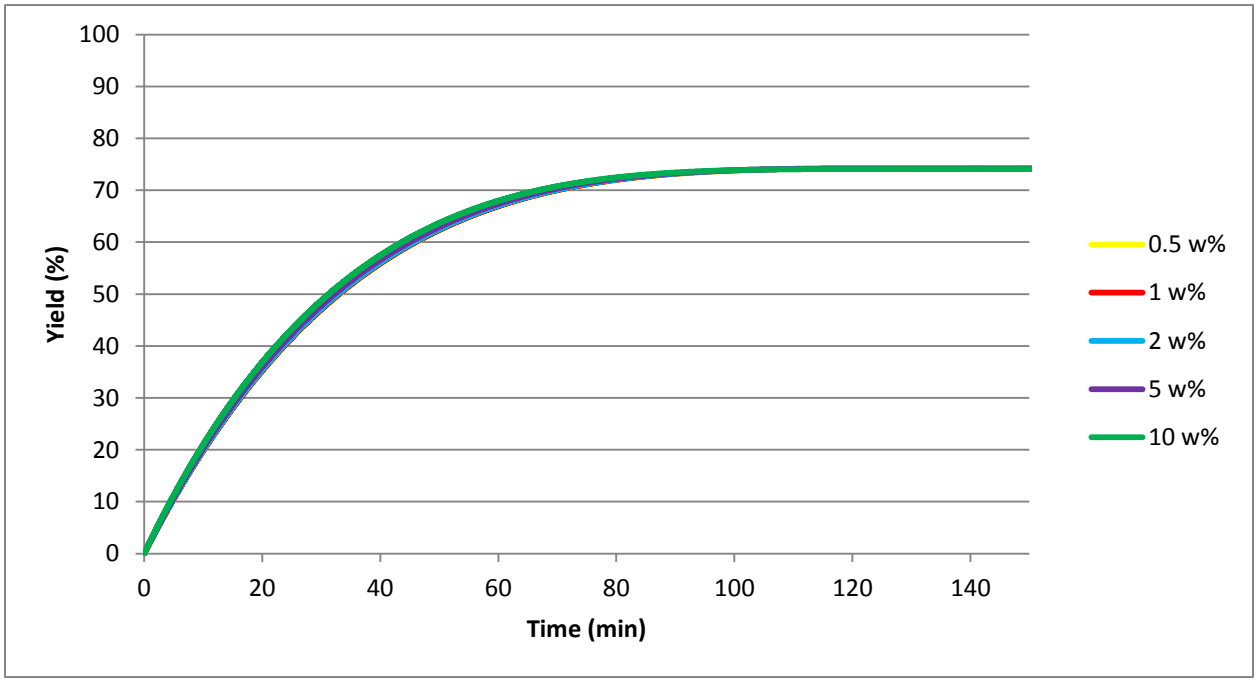

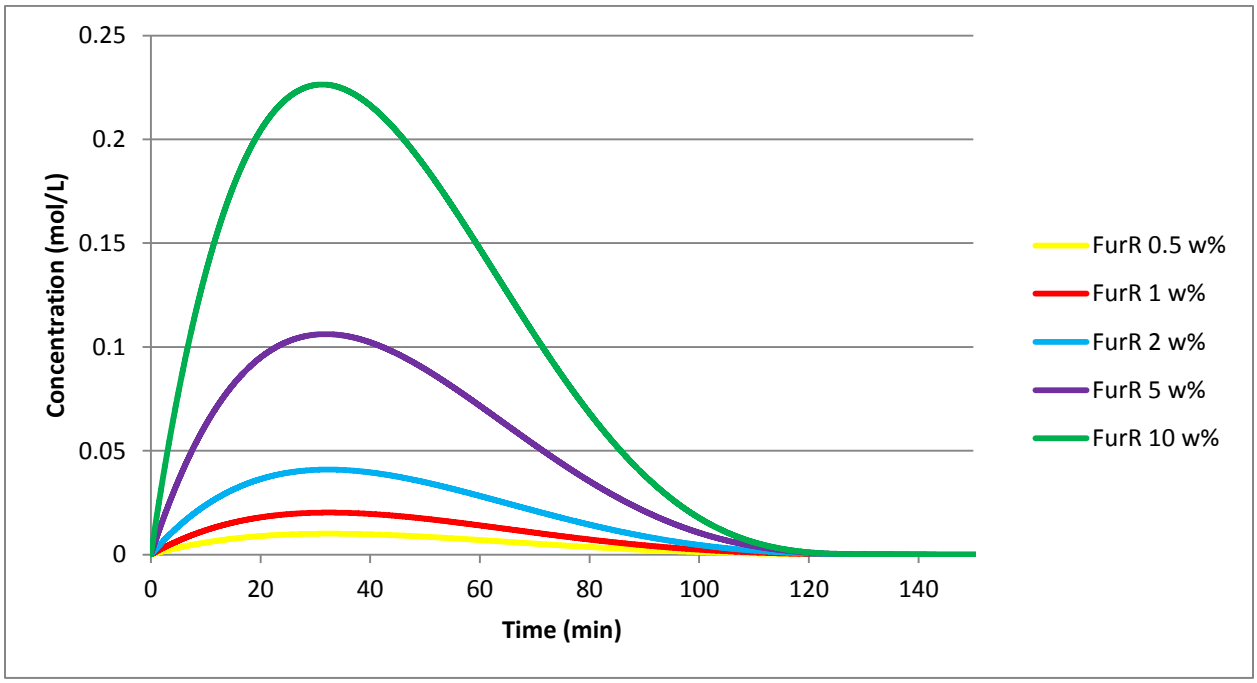

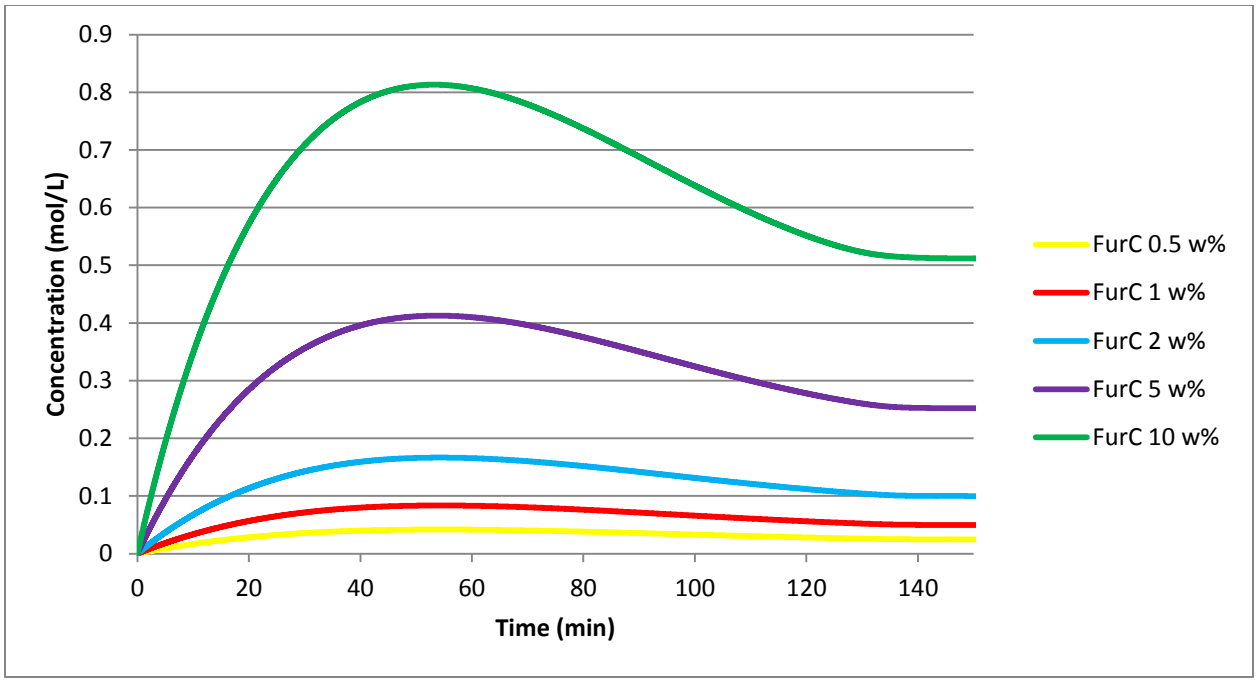
0.9
0.8
0.7
0.6
0.5
0.4
0.3
0.2
0.1
0
Concentration (mol/L)
0
20
40
60
80
100
120
140
Time (min)
FurC 0.5 w%
FurC 1 w%
FurC 2 w%
FurC 5 w%
FurC 10 w%

The conversion, furfural yield, concentration of furfural in the reactor (FurR) and in the condensate (FurC) are shown for the outlook temperature range 150 - 200°C; at 10 bar, 0.5 w% H_2SO_4, 1 w% initial xylose and 500 ml/min N_2 stripping rate.

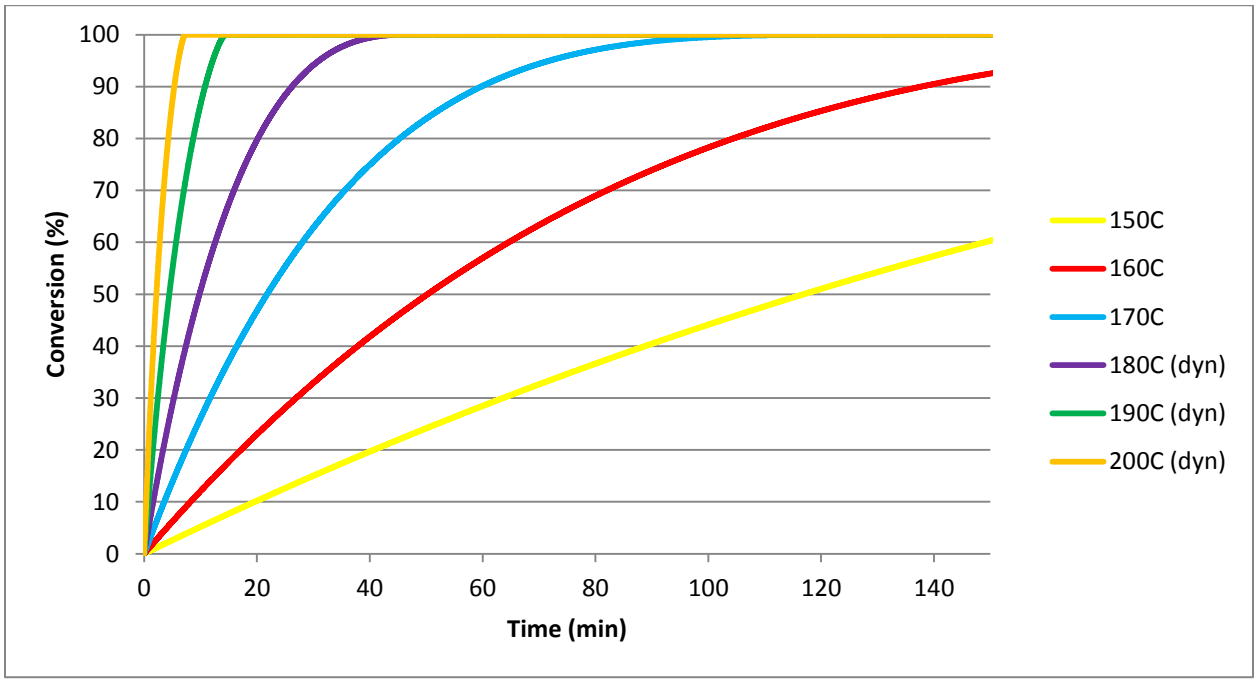

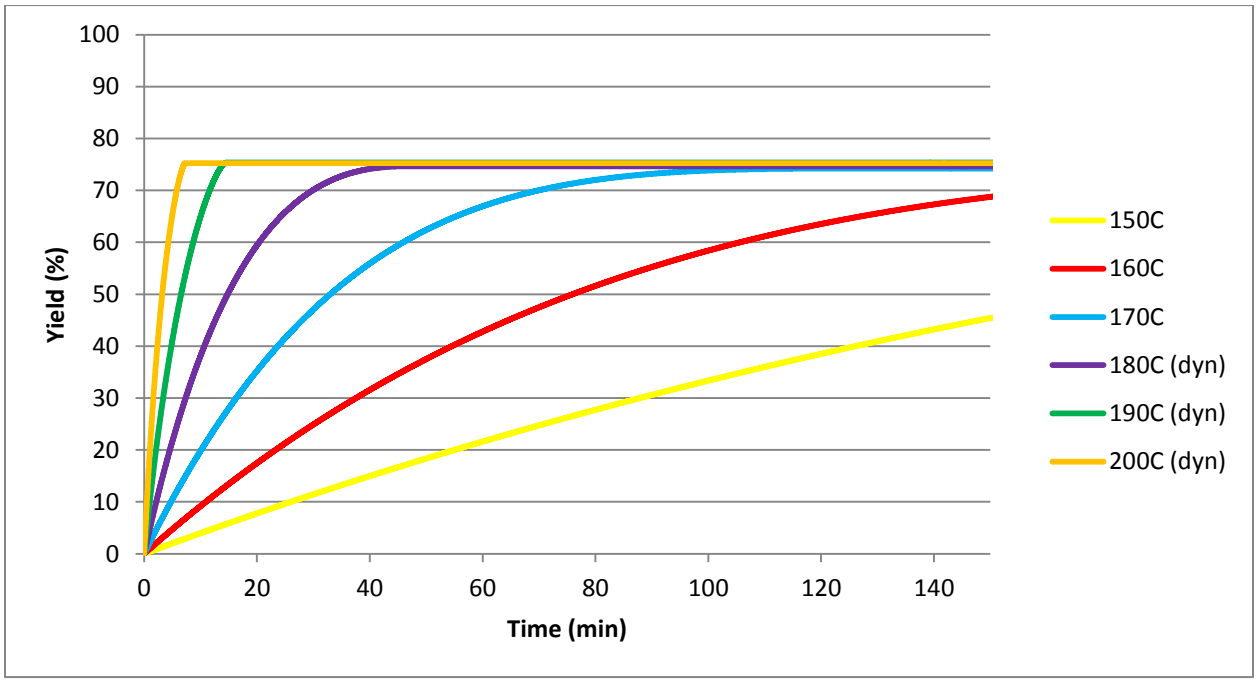

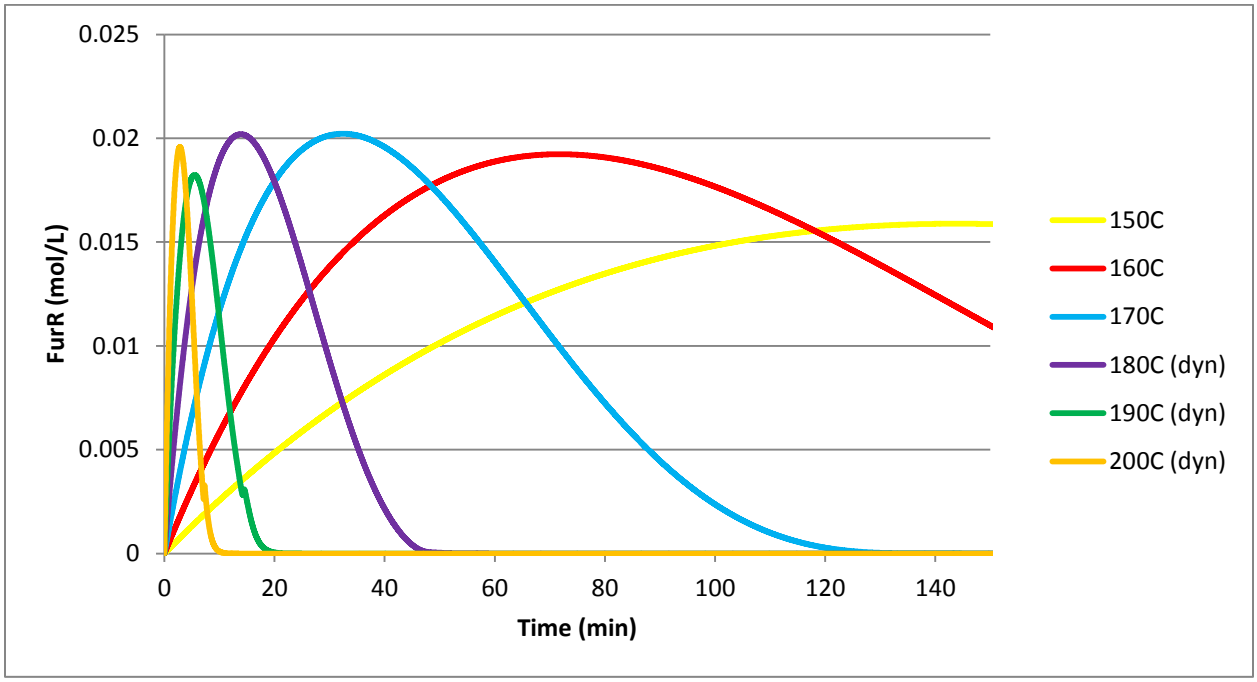
0.025
0.02
0.015
0.01
0.005
0
FurR (mol/L)
0
20
40
60
80
100
120
140
Time (min)
150C
160C
170C
180C (dyn)
190C (dyn)
200C (dyn)

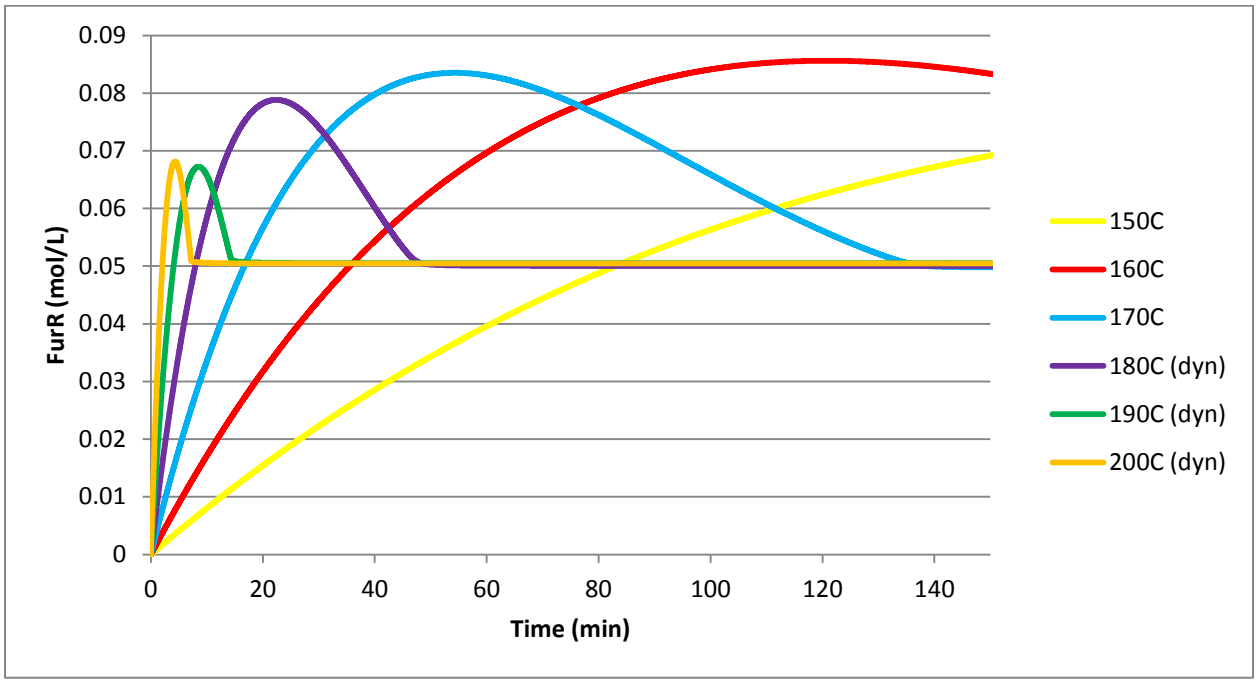
0.09
0.08
0.07
0.06
0.05
0.04
0.03
0.02
0.01
0
FurR (mol/L)
0
20
40
60
80
100
120
140
Time (min)
150C
160C
170C
180C (dyn)
190C (dyn)
200C (dyn)

The concentration of furfural in the condensate (FurC) is shown for the different operating pressures 10 and 20 bar; at 170°C/200°C, 0.5 w% H_2SO_4, 1 w% initial xylose and 500 ml/min N_2 stripping rate.

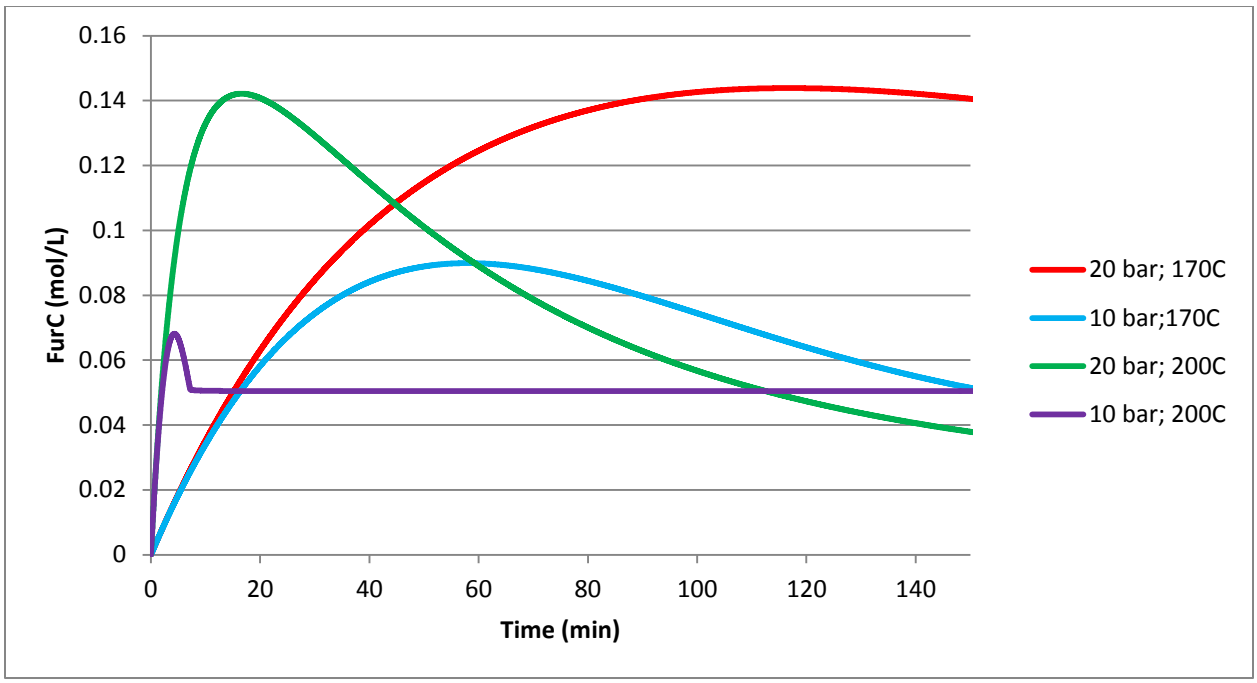

The expression for the saturation temperature is fitted from the following experimental data .

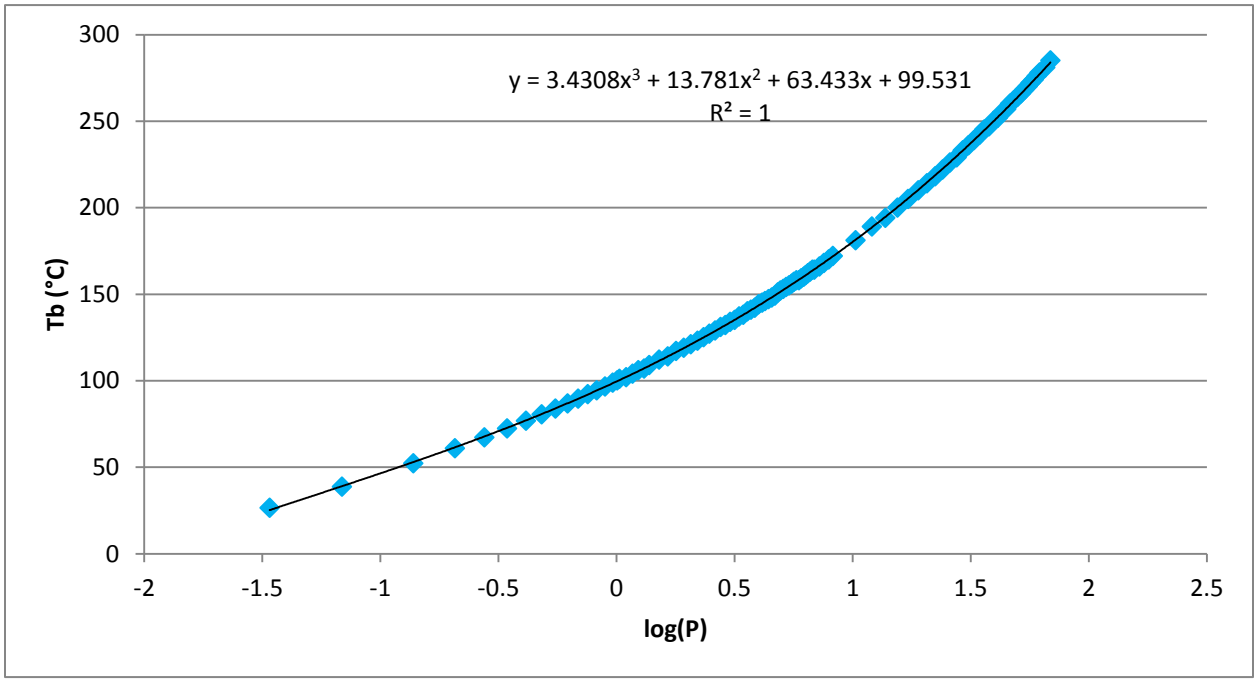

Appendix C: Model explanation and scripts

In the script *CSTRpar* all parameters, both physical and operating, are given/ estimated. Also the correlations to calculate parameter estimations are included in this script.

The operating conditions, such as temperature (*p.T*), pressure (*p.P_in*) and stripping rate (*p.FN2_in*) could be specified in this script. For continuous operating also the feed rate of the xylose-solution (*p.FX_in*) has to be given.

To specify the initial conditions the amount of xylose(*p.NX0*), water (*p.NH2O0*) and sulfuric acid (*p.Nacid*) need to be given. (Of course also valid for other components.) In the case of continuous operation the xylose concentration of the feed solution (*p.CX_in*) and its density (*p.rhoXyl*) are important as well.

The previously mentioned kinetic parameter correlations are defined is this script as well. These correlations, described by Marcotulio et al., are shown below:

$$\ln(k_x^*) = 31.86 - \frac{133.3\ 10^3\ [\frac{J}{mol}]}{RT}$$

$$\ln(k_3^*) = 26.64 - \frac{125.1\ 10^3 [\frac{J}{mol}]}{RT}$$

$$k = k^*\ C_{acid}\ \gamma_{acid}\ [s^{-1}]$$

For the activity coefficient of sulfuric acid γ values from literature could be used. Also a correlation is defined, based on data available from Marcotulio et al. and Staples [7] [33] , for a concentration range till 10 w% at a temperature of 170°C.

The fraction parameter f_k that splits the rate constant for the conversion of xylose into a constant for the formation of furfural and a constant leading to loss products, is optimized and assumed to be 0.77.

Activity coefficients

The thermodynamic models are based on the implementation of activity coefficients for the components in the reaction mixture.

The activity coefficients could be implemented as constants in the *CSTRpar script* (by *p.gammaF* and *p.gammaH*).

Also two methods are used to calculate the activity coefficients, by implementing the van Laar equations or NRTL model equations.

The model based on the van Laar equations defined the activity coefficients for furfural and water as follows in the model script:

```
gammaF = 10^((par.B*XH2O*XH2O)/((XH2O+(par.B/par.A)*XFUR)^2));
gammaH = 10^((par.A*XFUR*XFUR)/((XH2O*(par.A/par.B)+XFUR)^2));
```

The second thermodynamic model, based on the use of the NRTL local compositions model, calculated the activity coefficients by the following equations:

```
gammaH =
exp((XFUR*XFUR)*((par.tau21*((par.G21/(XH2O+XFUR*par.G21))^2))+(par.tau12*par
.G12/((XFUR+XH2O*par.G12)^2))));
gammaF =
exp((XH2O*XH2O)*((par.tau12*((par.G12/(XFUR+XH2O*par.G12))^2))+(par.tau21*par
.G21/((XH2O+XFUR*par.G21)^2))));
```

For four components in the reaction mixture (water, furfural, xylose and sulfuric acid) activity coefficient calculations could be done including the multiple components in the NRTL modeling. For a component in a four component mixture a calculation is described as follows:

```
gamma(1) =
exp((par.tau(1,1)*par.G(1,1)*X(1)+par.tau(2,1)*par.G(2,1)*X(2)+par.tau(3,1)*p
ar.G(3,1)*X(3)+par.tau(4,1)*par.G(4,1)*X(4))/(par.G(1,1)*X(1)+par.G(2,1)*X(2)
+par.G(3,1)*X(3)+par.G(4,1)*X(4)) +
(X(1)*par.G(1,1))/(par.G(1,1)*X(1)+par.G(2,1)*X(2)+par.G(3,1)*X(3)+par.G(4,1)
*X(4))*(par.tau(1,1)-
((X(1)*par.tau(1,1)*par.G(1,1)+X(2)*par.tau(2,1)*par.G(2,1)+X(3)*par.tau(3,1)
*par.G(3,1)+X(4)*par.tau(4,1)*par.G(4,1))/(par.G(1,1)*X(1)+par.G(2,1)*X(2)+pa
r.G(3,1)*X(3)+par.G(4,1)*X(4))) +
(X(2)*par.G(1,2))/(par.G(1,2)*X(1)+par.G(2,2)*X(2)+par.G(3,2)*X(3)+par.G(4,2)
*X(4))*(par.tau(1,2)-
((X(1)*par.tau(1,2)*par.G(1,2)+X(2)*par.tau(2,2)*par.G(2,2)+X(3)*par.tau(3,2)
*par.G(3,2)+X(4)*par.tau(4,2)*par.G(4,2))/(par.G(1,2)*X(1)+par.G(2,2)*X(2)+pa
r.G(3,2)*X(3)+par.G(4,2)*X(4))) +
(X(3)*par.G(1,3))/(par.G(1,3)*X(1)+par.G(2,3)*X(2)+par.G(3,3)*X(3)+par.G(4,3)
*X(4))*(par.tau(1,3)-
((X(1)*par.tau(1,3)*par.G(1,3)+X(2)*par.tau(2,3)*par.G(2,3)+X(3)*par.tau(3,3)
*par.G(3,3)+X(4)*par.tau(4,3)*par.G(4,3))/(par.G(1,3)*X(1)+par.G(2,3)*X(2)+pa
r.G(3,3)*X(3)+par.G(4,3)*X(4))) +
(X(4)*par.G(1,4))/(par.G(1,4)*X(1)+par.G(2,4)*X(2)+par.G(3,4)*X(3)+par.G(4,4)
*X(4))*(par.tau(1,4)-
((X(1)*par.tau(1,4)*par.G(1,4)+X(2)*par.tau(2,4)*par.G(2,4)+X(3)*par.tau(3,4)
*par.G(3,4)+X(4)*par.tau(4,4)*par.G(4,4))/(par.G(1,4)*X(1)+par.G(2,4)*X(2)+pa
r.G(3,4)*X(3)+par.G(4,4)*X(4))));
```

For the van Laar equations there are two interaction parameters, A and B. These were implemented in several ways, by using values from literature, correlations from literatures and by developing own correlations. (see *CSTRpar %% van Laar parameters*) For the calculation of this last method experimental data of Curtis & Hatt were used. [26]

```
p.A = (-85.62/(p.Tsat+273.15)) + 0.6229;            % own correlation for van
Laar parameter
p.B = (799.73/(p.Tsat+273.15)) - 0.3366;            % own correlation for van
Laar parameter
```

For the correlations to calculate parameters A and B, the saturation temperature at the specific pressure was calculated as well. Using another correlation from literature:

```
p.Tsat = (3.43083*(p.logP)^3)+(13.781*(p.logP)^2)+63.433*(p.logP)+99.531; %
correlation made from lit data
```

Calculating the activity coefficients using the NRTL model, the parameters tau and G have to be given or calculated.

G is expressed as follows:

```
p.G12 = exp(-p.alpha*p.tau12);
p.G21 = exp(-p.alpha*p.tau21);
```
Where α is an constant, determined by the nonrandomness of a binary mixture.

Tau is defined by Sunder et al. [30]:

```
p.tau12 = p.g12/(p.R*p.T);          % Sunder
p.tau21 = p.g21/(p.R*p.T);          % Sunder
```
Here g is the energy of interaction between components.

By Fele et al. and other authors tau is expressed by [31]:

```
p.tau12 = p.a12 + (p.b12/p.T);       % Fele
p.tau21 = p.a21 + (p.b21/p.T);       % Fele
```

ASPEN expends these correlations, depending on the input used:

```
p.tau12 = p.a12 + (p.b12/p.T) + p.e12*log(p.T) + p.f12*p.T;       % ASPEN
p.tau21 = p.a21 + (p.b21/p.T) + p.e21*log(p.T) + p.f21*p.T;       % ASPEN
```

The values of a and b are fitted to experimental data for the binary interactions between water and furfural [26], water and xylose [34], water and sulfuric acid [35].

Recycle

To make the implementation of a recycle stream from the hydrogenation reaction of furfural possible, input parameters *p.FFurG_in* and *p.FH2OG_in* are added. (see CSTRpar2) In the balances *p.FFurG* and *p.FH2OG* are implemented as well.

ODEsolver

```
par = CSTRpar;

tspan = linspace(0,1e4,1e4);
init = [par.NX0 par.NF0 par.NF_G0 par.NH2O0 par.NH2O_G0 par.NS0 par.NH0
par.NF_C par.NH2O_C];
options = odeset ('RelTol', 1e-9, 'AbsTol', 1e-9);

tic
[t,Y] = ode15s (@CSTR, tspan, init, options, par);
toc

Z1 = [Y(:,1)];
Z2 = [Y(:,2)];
Z4 = [Y(:,4)];
Z6 = [Y(:,6)];
Z7 = [Y(:,7)];

Z8 = [Y(:,8)];
Z9 = [Y(:,9)];

tau = par.VR/par.FX;
A = linspace(0,tau,length(Z1));


Xx = (par.NX0-Y(:,1))/par.NX0;                                          % batch
%tx = par.CX_in*par.FX*1000*t;
%Xx = ((par.NX0+tx)-Y(:,1))./(par.NX0+tx);
% CSTR
Yf = (Y(:,2)+Y(:,8))/(par.NX0);
Yf2 = Y(:,2)./(par.NX0-Y(:,1));                                         % batch
%Yf = Y(:,2)./(par.NX0+tx);
% CSTR
%Yf2 = Y(:,2)./((par.NX0+tx)-Y(:,1));
%Yf3 = (Y(:,2)+Y(:,8))./(par.NX0+tx);
% stripping yield
Ys = Y(end,6)/(par.NX0);                                                % batch
%Ys = Y(:,6)./(par.NX0+tx);                                                    %
CSTR
Yh = Y(end,7)/(3*par.NX0);                                              % batch
%Yh = Y(:,7)./(3*(par.NX0+tx));
% CSTR

VL = (Y(:,4)*par.MH2O/par.rhoH2O) + (Y(:,2)*par.MF/par.rhoF) +
(par.Nacid*par.Macid/par.rho_acid);
VL_condens =(Y(:,9)*par.MH2O/par.rhoH2O) + (Y(:,8)*par.MF/par.rhoF);
```

CSTR model (van Laar)

```
function dN = CSTR(t,N,par)
%% Including van Laar


%% Differentials

VL = (N(4)*par.MH2O/par.rhoH2O) + (N(2)*par.MF/par.rhoF) +
(par.Nacid*par.Macid/par.rho_acid);
VG = par.VR*1000-VL;
CX = N(1)/VL;
CF = N(2)/VL;
Cacid = par.Nacid/VL;

XFUR = N(2)/(N(2)+N(1)+N(4)+par.Nacid+N(6)+N(7));
XH2O = N(4)/(N(2)+N(1)+N(4)+par.Nacid+N(6)+N(7));

gammaF = 10^((par.B*XH2O*XH2O)/((XH2O+(par.B/par.A)*XFUR)^2));
gammaH = 10^((par.A*XFUR*XFUR)/((XH2O*(par.A/par.B)+XFUR)^2));

yFUR = gammaF*XFUR*par.PFUR/par.P;
yH2O = gammaH*XH2O*par.PH2O/par.P;

dN(1) = (par.FX*1000*par.CX_in-(par.k1+par.k2)*CX*Cacid*VL);
dN(2) = (par.k1*CX*Cacid*VL-par.k3*CF*Cacid*VL-
(gammaF*XFUR*par.PFUR*VG/(1000*par.R*par.T)-N(3)));
dN(3) = ((gammaF*XFUR*par.PFUR*VG/(1000*par.R*par.T)-N(3))-(par.FN2_m/(1-
yFUR-yH2O)*yFUR));
dN(4) = (par.FH2O+3*par.k1*CX*Cacid*VL-
(gammaH*XH2O*par.PH2O*VG/(1000*par.R*par.T)-N(5)));
dN(5) = ((gammaH*XH2O*par.PH2O*VG/(1000*par.R*par.T)-N(5))-(par.FN2_m/(1-
yFUR-yH2O)*yH2O));

dN(6) = (par.k2*CX*Cacid*VL);
dN(7) = (1/3*par.k3*CF*Cacid*VL);

dN(8) = (par.FN2_m/(1-yFUR-yH2O)*yFUR);
dN(9) = (par.FN2_m/(1-yFUR-yH2O)*yH2O);

dN = dN';
```

CSTR model (multicomponent NRTL)

```
%% NRTL multicomponent (including Hydrogenation recycle)


%% Differentials

VL = (N(4)*par.MH2O/par.rhoH2O) + (N(2)*par.MF/par.rhoF) +
(par.Nacid*par.Macid/par.rho_acid);
VG = par.VR*1000-VL;
CX = N(1)/VL;
CF = N(2)/VL;
Cacid = par.Nacid/VL;

X(1) = N(4)/(N(2)+N(1)+N(4)+par.Nacid+N(6)+N(7)); %Water
X(2) = N(2)/(N(2)+N(1)+N(4)+par.Nacid+N(6)+N(7)); %Furfural
X(3) = N(1)/(N(2)+N(1)+N(4)+par.Nacid+N(6)+N(7)); %Xylose
X(4) = par.Nacid/(N(2)+N(1)+N(4)+par.Nacid+N(6)+N(7)); %H2SO4

gamma(1) =
exp((par.tau(1,1)*par.G(1,1)*X(1)+par.tau(2,1)*par.G(2,1)*X(2)+par.tau(3,1)*p
ar.G(3,1)*X(3)+par.tau(4,1)*par.G(4,1)*X(4))/(par.G(1,1)*X(1)+par.G(2,1)*X(2)
+par.G(3,1)*X(3)+par.G(4,1)*X(4)) +
(X(1)*par.G(1,1))/(par.G(1,1)*X(1)+par.G(2,1)*X(2)+par.G(3,1)*X(3)+par.G(4,1)
*X(4))*(par.tau(1,1)-
((X(1)*par.tau(1,1)*par.G(1,1)+X(2)*par.tau(2,1)*par.G(2,1)+X(3)*par.tau(3,1)
*par.G(3,1)+X(4)*par.tau(4,1)*par.G(4,1))/(par.G(1,1)*X(1)+par.G(2,1)*X(2)+pa
r.G(3,1)*X(3)+par.G(4,1)*X(4)))) +
(X(2)*par.G(1,2))/(par.G(1,2)*X(1)+par.G(2,2)*X(2)+par.G(3,2)*X(3)+par.G(4,2)
*X(4))*(par.tau(1,2)-
((X(1)*par.tau(1,2)*par.G(1,2)+X(2)*par.tau(2,2)*par.G(2,2)+X(3)*par.tau(3,2)
*par.G(3,2)+X(4)*par.tau(4,2)*par.G(4,2))/(par.G(1,2)*X(1)+par.G(2,2)*X(2)+pa
r.G(3,2)*X(3)+par.G(4,2)*X(4)))) +
(X(3)*par.G(1,3))/(par.G(1,3)*X(1)+par.G(2,3)*X(2)+par.G(3,3)*X(3)+par.G(4,3)
*X(4))*(par.tau(1,3)-
((X(1)*par.tau(1,3)*par.G(1,3)+X(2)*par.tau(2,3)*par.G(2,3)+X(3)*par.tau(3,3)
*par.G(3,3)+X(4)*par.tau(4,3)*par.G(4,3))/(par.G(1,3)*X(1)+par.G(2,3)*X(2)+pa
r.G(3,3)*X(3)+par.G(4,3)*X(4)))) +
(X(4)*par.G(1,4))/(par.G(1,4)*X(1)+par.G(2,4)*X(2)+par.G(3,4)*X(3)+par.G(4,4)
*X(4))*(par.tau(1,4)-
((X(1)*par.tau(1,4)*par.G(1,4)+X(2)*par.tau(2,4)*par.G(2,4)+X(3)*par.tau(3,4)
*par.G(3,4)+X(4)*par.tau(4,4)*par.G(4,4))/(par.G(1,4)*X(1)+par.G(2,4)*X(2)+pa
r.G(3,4)*X(3)+par.G(4,4)*X(4))));

gamma(2) =
exp((par.tau(1,2)*par.G(1,2)*X(1)+par.tau(2,2)*par.G(2,2)*X(2)+par.tau(3,2)*p
ar.G(3,2)*X(3)+par.tau(4,2)*par.G(4,2)*X(4))/(par.G(1,2)*X(1)+par.G(2,2)*X(2)
+par.G(3,2)*X(3)+par.G(4,2)*X(4)) +
(X(1)*par.G(2,1))/(par.G(1,1)*X(1)+par.G(2,1)*X(2)+par.G(3,1)*X(3)+par.G(4,1)
*X(4))*(par.tau(2,1)-
((X(1)*par.tau(1,1)*par.G(1,1)+X(2)*par.tau(2,1)*par.G(2,1)+X(3)*par.tau(3,1)
*par.G(3,1)+X(4)*par.tau(4,1)*par.G(4,1))/(par.G(1,1)*X(1)+par.G(2,1)*X(2)+pa
r.G(3,1)*X(3)+par.G(4,1)*X(4)))) +
(X(2)*par.G(2,2))/(par.G(1,2)*X(1)+par.G(2,2)*X(2)+par.G(3,2)*X(3)+par.G(4,2)
*X(4))*(par.tau(2,2)-
((X(1)*par.tau(1,2)*par.G(1,2)+X(2)*par.tau(2,2)*par.G(2,2)+X(3)*par.tau(3,2)
```

```
*par.G(3,2)+X(4)*par.tau(4,2)*par.G(4,2))/(par.G(1,2)*X(1)+par.G(2,2)*X(2)+pa
r.G(3,2)*X(3)+par.G(4,2)*X(4))) +
(X(3)*par.G(2,3))/(par.G(1,3)*X(1)+par.G(2,3)*X(2)+par.G(3,3)*X(3)+par.G(4,3)
*X(4))*(par.tau(2,3)-
((X(1)*par.tau(1,3)*par.G(1,3)+X(2)*par.tau(2,3)*par.G(2,3)+X(3)*par.tau(3,3)
*par.G(3,3)+X(4)*par.tau(4,3)*par.G(4,3))/(par.G(1,3)*X(1)+par.G(2,3)*X(2)+pa
r.G(3,3)*X(3)+par.G(4,3)*X(4))) +
(X(4)*par.G(2,4))/(par.G(1,4)*X(1)+par.G(2,4)*X(2)+par.G(3,4)*X(3)+par.G(4,4)
*X(4))*(par.tau(2,4)-
((X(1)*par.tau(1,4)*par.G(1,4)+X(2)*par.tau(2,4)*par.G(2,4)+X(3)*par.tau(3,4)
*par.G(3,4)+X(4)*par.tau(4,4)*par.G(4,4))/(par.G(1,4)*X(1)+par.G(2,4)*X(2)+pa
r.G(3,4)*X(3)+par.G(4,4)*X(4))));

gamma(3) =
exp((par.tau(1,3)*par.G(1,3)*X(1)+par.tau(2,3)*par.G(2,3)*X(2)+par.tau(3,3)*p
ar.G(3,3)*X(3)+par.tau(4,3)*par.G(4,3)*X(4))/(par.G(1,3)*X(1)+par.G(2,3)*X(2)
+par.G(3,3)*X(3)+par.G(4,3)*X(4)) +
(X(1)*par.G(3,1))/(par.G(1,1)*X(1)+par.G(2,1)*X(2)+par.G(3,1)*X(3)+par.G(4,1)
*X(4))*(par.tau(3,1)-
((X(1)*par.tau(1,1)*par.G(1,1)+X(2)*par.tau(2,1)*par.G(2,1)+X(3)*par.tau(3,1)
*par.G(3,1)+X(4)*par.tau(4,1)*par.G(4,1))/(par.G(1,1)*X(1)+par.G(2,1)*X(2)+pa
r.G(3,1)*X(3)+par.G(4,1)*X(4))) +
(X(2)*par.G(3,2))/(par.G(1,2)*X(1)+par.G(2,2)*X(2)+par.G(3,2)*X(3)+par.G(4,2)
*X(4))*(par.tau(3,2)-
((X(1)*par.tau(1,2)*par.G(1,2)+X(2)*par.tau(2,2)*par.G(2,2)+X(3)*par.tau(3,2)
*par.G(3,2)+X(4)*par.tau(4,2)*par.G(4,2))/(par.G(1,2)*X(1)+par.G(2,2)*X(2)+pa
r.G(3,2)*X(3)+par.G(4,2)*X(4))) +
(X(3)*par.G(3,3))/(par.G(1,3)*X(1)+par.G(2,3)*X(2)+par.G(3,3)*X(3)+par.G(4,3)
*X(4))*(par.tau(3,3)-
((X(1)*par.tau(1,3)*par.G(1,3)+X(2)*par.tau(2,3)*par.G(2,3)+X(3)*par.tau(3,3)
*par.G(3,3)+X(4)*par.tau(4,3)*par.G(4,3))/(par.G(1,3)*X(1)+par.G(2,3)*X(2)+pa
r.G(3,3)*X(3)+par.G(4,3)*X(4))) +
(X(4)*par.G(3,4))/(par.G(1,4)*X(1)+par.G(2,4)*X(2)+par.G(3,4)*X(3)+par.G(4,4)
*X(4))*(par.tau(3,4)-
((X(1)*par.tau(1,4)*par.G(1,4)+X(2)*par.tau(2,4)*par.G(2,4)+X(3)*par.tau(3,4)
*par.G(3,4)+X(4)*par.tau(4,4)*par.G(4,4))/(par.G(1,4)*X(1)+par.G(2,4)*X(2)+pa
r.G(3,4)*X(3)+par.G(4,4)*X(4))));

gamma(4) =
exp((par.tau(1,4)*par.G(1,4)*X(1)+par.tau(2,4)*par.G(2,4)*X(2)+par.tau(3,4)*p
ar.G(3,4)*X(3)+par.tau(4,4)*par.G(4,4)*X(4))/(par.G(1,4)*X(1)+par.G(2,4)*X(2)
+par.G(3,4)*X(3)+par.G(4,4)*X(4)) +
(X(1)*par.G(4,1))/(par.G(1,1)*X(1)+par.G(2,1)*X(2)+par.G(3,1)*X(3)+par.G(4,1)
*X(4))*(par.tau(4,1)-
((X(1)*par.tau(1,1)*par.G(1,1)+X(2)*par.tau(2,1)*par.G(2,1)+X(3)*par.tau(3,1)
*par.G(3,1)+X(4)*par.tau(4,1)*par.G(4,1))/(par.G(1,1)*X(1)+par.G(2,1)*X(2)+pa
r.G(3,1)*X(3)+par.G(4,1)*X(4))) +
(X(2)*par.G(4,2))/(par.G(1,2)*X(1)+par.G(2,2)*X(2)+par.G(3,2)*X(3)+par.G(4,2)
*X(4))*(par.tau(4,2)-
((X(1)*par.tau(1,2)*par.G(1,2)+X(2)*par.tau(2,2)*par.G(2,2)+X(3)*par.tau(3,2)
*par.G(3,2)+X(4)*par.tau(4,2)*par.G(4,2))/(par.G(1,2)*X(1)+par.G(2,2)*X(2)+pa
r.G(3,2)*X(3)+par.G(4,2)*X(4))) +
(X(3)*par.G(4,3))/(par.G(1,3)*X(1)+par.G(2,3)*X(2)+par.G(3,3)*X(3)+par.G(4,3)
*X(4))*(par.tau(4,3)-
((X(1)*par.tau(1,3)*par.G(1,3)+X(2)*par.tau(2,3)*par.G(2,3)+X(3)*par.tau(3,3)
*par.G(3,3)+X(4)*par.tau(4,3)*par.G(4,3))/(par.G(1,3)*X(1)+par.G(2,3)*X(2)+pa
```

```
r.G(3,3)*X(3)+par.G(4,3)*X(4))) +
(X(4)*par.G(4,4))/(par.G(1,4)*X(1)+par.G(2,4)*X(2)+par.G(3,4)*X(3)+par.G(4,4)
*X(4))*(par.tau(4,4)-
((X(1)*par.tau(1,4)*par.G(1,4)+X(2)*par.tau(2,4)*par.G(2,4)+X(3)*par.tau(3,4)
*par.G(3,4)+X(4)*par.tau(4,4)*par.G(4,4))/(par.G(1,4)*X(1)+par.G(2,4)*X(2)+pa
r.G(3,4)*X(3)+par.G(4,4)*X(4))));


% yFUR = gamma(2)*X(2)*par.PFUR/par.P;
% yH2O = gamma(1)*X(1)*par.PH2O/par.P;

Ntot = par.P*VG/(1000*par.R*par.T);
yFUR = N(3)/Ntot;
yH2O = N(5)/Ntot;

dN(1) = (par.FX*1000*par.CX_in-(par.k1+par.k2)*CX*Cacid*VL);
dN(2) = (par.k1*CX*Cacid*VL-par.k3*CF*Cacid*VL-
(gamma(2)*X(2)*par.PFUR*VG/(1000*par.R*par.T)-N(3)));
dN(3) = (par.FFurG+(gamma(2)*X(2)*par.PFUR*VG/(1000*par.R*par.T)-N(3))-
(par.FN2_m/(1-yFUR-yH2O)*yFUR));
dN(4) = (par.FH2O+3*par.k1*CX*Cacid*VL-
(gamma(1)*X(1)*par.PH2O*VG/(1000*par.R*par.T)-N(5)));
dN(5) = (par.FH2OG+(gamma(1)*X(1)*par.PH2O*VG/(1000*par.R*par.T)-N(5))-
(par.FN2_m/(1-yFUR-yH2O)*yH2O));

dN(6) = (par.k2*CX*Cacid*VL);
dN(7) = (1/3*par.k3*CF*Cacid*VL);

dN(8) = (par.FN2_m/(1-yFUR-yH2O)*yFUR);
dN(9) = (par.FN2_m/(1-yFUR-yH2O)*yH2O);


dN = dN';
```

Parameters

```
function p = CSTRpar
%% Physical parameters

p.MH2O = 18.02;
p.MF = 96.08;
p.Macid = 98.079;
p.MX = 150.13;
p.rhoH2O = 998;
p.rhoF = 1160;
p.rho_acid = 1840;
p.rhoX = 1525;

p.Vmn = 0.0224127224278312;              % m3/mol


%% Operating conditions

p.R = 8.314;                             % gas constant
p.T = 170+273.15;                        % K
p.P_in = 10;                             % bar
p.P = p.P_in*100000;                     % Pa
p.FN2_in = 500;                          % ml/min
p.FN2 = p.FN2_in/60/1e6;                 % m3/s
p.FFurG_in = 0;                          % recycle stream ml/min
p.FH2OG_in = 0;                          % recycle stream ml/min
p.FFurG = p.FFurG_in/(60*1e6*p.Vmn);     % recycle stream mol/s
p.FH2OG = p.FH2OG_in/(60*1e6*p.Vmn);     % recycle stream mol/s
p.FN2_m = (p.FN2/p.Vmn)+p.FFurG+p.FH2OG;% mol/s
p.FX_in = 0;                             % ml/min
p.FX = p.FX_in/60/1e6;                   % m3/s
p.VR = 300e-6;                          % reactor volume m3

p.PFUR = exp(78.653-8043/(p.T)-8.1424*log((p.T))+0.000004509*(p.T)^2); %Pa
p.PH2O = exp(77.345+(0.0057*(p.T))-(7235/(p.T)))/((p.T)^8.2); %Pa

p.wX = 1;                               % g Xylose/ml
p.rhoXyl = 1.00988;                      % g/ml Xyl-sol

p.FH2O = p.FX_in*(p.rhoXyl-p.wX)/60/p.MH2O;             % mol/s water in

p.CX_in = p.wX/p.MX*1000;                  % xylose initial concentration  in
M
%p.CH2O_in = 0;                           % water initial concentration  in M
p.CF_in = 0;                             % furfural initial concentration  in
M
p.CS_in = 0;                             % xylose side reactions initial
concentration  in M
p.CH_in = 0;                             % furfural side reactions initial
concentration  in M

p.NX0 = 2/p.MX;                 % values for initial condition
p.NF0 = zeros(1)/p.MF;
p.NF_G0 = zeros(1);
```

```
p.NH2O0 = 197/p.MH2O;
p.NH2O_G0 = zeros(1);
p.NS0 = zeros(1);
p.NH0 = zeros(1);

p.NF_C = zeros(1);
p.NH2O_C =zeros(1);

p.Nacid = 1/p.Macid;

%% Activity coefficients

p.gammaF = 26.68;                          % activity on furfural
p.gammaH = 0.999;                          % activity water

%% van Laar parameters

%%p.logP = log10(p.P_in);
%%p.Tsat = (3.43083*(p.logP)^3)+(13.781*(p.logP)^2)+63.433*(p.logP)+99.531; %
correlation made from lit data

%p.A = ((-0.20505*1000)/(p.Tsat+273.15)) + 0.9017;  % correlation for van
Laar parameter
%p.B = ((0.9091*1000)/(p.Tsat+273.15)) - 0.60886;   % correlation for van
Laar parameter
%%p.A = (-85.62/(p.Tsat+273.15)) + 0.6229;            % own correlation for
van Laar parameter
%%p.B = (799.73/(p.Tsat+273.15)) - 0.3366;            % own correlation for
van Laar parameter
%p.A = 0.4504;                        % van Laar parameter (10 atm)
%p.B = 1.392;                         % van Laar parameter (10 atm)
%p.A = 0.449376337;                   % correlation for van Laar parameter -
calc
%p.B = 1.396540839;                   % correlation for van Laar parameter -
calc

%% NRTL parameters
% water(1) furfural(2) xylose(3) H2SO4(4)

p.G = zeros(4,4);
p.tau = zeros(4,4);
p.alpha = zeros(4,4);

p.a = zeros(4,4);
p.b = zeros(4,4);
p.e = zeros(4,4);
p.f = zeros(4,4);

p.a(1,2) = -0.0619;                        % Furfural data fitted
p.a(2,1) = 31.91;
p.b(1,2) = 1468.8;
p.b(2,1) = -8114.8;

% p.a(1,2) = 7.1079;                        % ASPEN VLE-IG
```

```
% p.a(2,1) = -5.8732;
% p.b(1,2) = -1265.8367;
% p.b(2,1) = 2335.0493;

p.c = 0.3;
p.d = 0;

p.alpha(1,2) = p.c + p.d*(p.T-273.15);      % randomness parameter ASPEN
p.alpha(2,1) = p.c + p.d*(p.T-273.15);      % randomness parameter ASPEN

p.a(1,4) = 14.796;                          % Sulfuric acid BOSEN&ENGELS
p.a(4,1) = 1.391;
p.b(1,4) = -6518.3;
p.b(4,1) = -2639;
p.alpha(1,4) = -0.059;
p.alpha(4,1) = -0.059;

p.a(1,3) = -8.514803317;                    % Xylose fitted from data Comesana
p.a(3,1) = 53.42269308;
p.b(1,3) = -0.015817732;
p.b(3,1) = -7999.912573;
p.alpha(1,3) = 0.3;                         % fixed before fitting
p.alpha(3,1) = 0.3;


for i = 1:4
    for j = 1:4

p.tau(i,j) = p.a(i,j) + (p.b(i,j)/p.T) + p.e(i,j)*log(p.T) + p.f(i,j)*p.T;

p.G(i,j) = exp(-p.alpha(i,j)*p.tau(i,j));
p.G(1,1) = 1;
p.G(2,2) = 1;
p.G(3,3) = 1;
p.G(4,4) = 1;

    end
end

%p.g12 = 1683.3;                        % K %energy of interaction Sunder
%p.g21 = -463.5;                        % K %energy of interaction Sunder
% p.a21 = -3.1078;                        % Fele
% p.b21 = 964.0374;
% p.a12 = 4.4233;
% p.b12 = -95.0897;

% p.a12 = 4.2744;                         % ASPEN VLE-RK
% p.a21 = -4.7587;
% p.b12 = -273.1076;
% p.b21 = 1910.4714;
% p.c = 0.3;
% p.d = 0;
% p.e12 = 0;
% p.e21 = 0;
% p.f12 = 0;
```

```
% p.f21 = 0;

% p.a12 = 52.8289;                        % ASPEN LLE-ASPEN
% p.a21 = 112.55;
% p.b12 = -2808.5376;
% p.b21 = -4131.4375;
% p.c = 0.2;
% p.d = 0;
% p.e12 = -6.902;
% p.e21 = -17.3004;
% p.f12 = 0;
% p.f21 = 0;

% p.a12 = 4.2362;                         % ASPEN VLE-HOC
% p.a21 = -4.7563;
% p.b12 = -262.2408;
% p.b21 = 1911.4222;
% p.c = 0.3;
% p.d = 0;
% p.e12 = 0;
% p.e21 = 0;
% p.f12 = 0;
% p.f21 = 0;

% p.a12 = 7.1079;                         % ASPEN VLE-IG
% p.a21 = -5.8732;
% p.b12 = -1265.8367;
% p.b21 = 2335.0493;
% p.c = 0.3;
% p.d = 0;
% p.e12 = 0;
% p.e21 = 0;
% p.f12 = 0;
% p.f21 = 0;

% p.a12 = 0;                          % ASPEN VLE-LIT
% p.a21 = 0;
% p.b12 = 1309.6942;
% p.b21 = 219.8905;
% p.c = 0.3958;
% p.d = 0;
% p.e12 = 0;
% p.e21 = 0;
% p.f12 = 0;
% p.f21 = 0;

%p.alpha = 0.12;                        % randomness parameter Sunder
%p.alpha = 0.2;                          % randomness parameter Fele
%p.alpha = p.c + p.d*(p.T-273.15);       % randomness parameter ASPEN

%p.tau12 = p.g12/(p.R*p.T);             % Sunder
%p.tau21 = p.g21/(p.R*p.T);             % Sunder
%p.tau12 = p.a12 + (p.b12/p.T);          % Fele
%p.tau21 = p.a21 + (p.b21/p.T);          % Fele
% p.tau12 = p.a12 + (p.b12/p.T) + p.e12*log(p.T) + p.f12*p.T;       % ASPEN
% p.tau21 = p.a21 + (p.b21/p.T) + p.e21*log(p.T) + p.f21*p.T;       % ASPEN
```

```
% p.G12 = exp(-p.alpha*p.tau12);
% p.G21 = exp(-p.alpha*p.tau21);


%% Reaction parameters

%p.gamma = 0.67;
p.CH2SO4 = p.Nacid/(p.NH2O0*p.MH2O/p.rhoH2O);
p.gamma = -0.12246*log(p.CH2SO4)+0.34638; %at 170C

p.kX = p.gamma*exp(31.86-(133300/(p.R*p.T)));
p.fk = 0.77;

p.k1 = p.kX*p.fk;
p.k2 = p.kX-p.k1;
p.k3 = p.gamma*exp(26.64-(125100/(p.R*p.T)));

%% Mass transfer

p.kGLaBF = 0.1;
p.kGLaBH = 1/p.kGLaBF;
%p.kGLaB = 3.84E-02;
```

Appendix D: Other models

Several authors have investigated the production of furfural and tried to model their experimental results. [19] [8] Agirrezabal-Tellaria et al. studied the stripping of furfural formed from xylose using sulfonic ion-exchange resins (Amberlyst). [8] [16] [17] His model of the furfural stripping data involves a mass transfer constant or stripping diffusion constant K_S. The model is based on the equations given below:

$$\frac{dC_x}{dt} = -k_1' C_x - k_2' C_x C_{F,R}$$

$$\frac{dC_{F,R}}{dt} = k_1' C_x - k_2' C_x C_{F,R} - k_3' C_{F,R} - K_S \frac{C_{F,R}}{V_R} - \frac{C_{F,R} \frac{dV_R}{dt}}{V_R}$$

$$\frac{dC_{F,C}}{dt} = \frac{C_{F,R}}{V_C} - \frac{C_{F,C} \frac{dV_C}{dt}}{V_C}$$

Where the kinetic rate constants of the model described in this study are lumped with the sulfuric acid concentration/ apparent concentration, the constants from Telleria et al. are lumped with the amount of Amberlyst catalyst used.

From the equations… it could be seen that no direct loss of xylose is assumed, but a loss reaction of furfural with xylose. Other authors observed that the rate of xylose conversion does not change upon addition of furfural to the solution, which suggests that there is no reaction of xylose with furfural. [1] The decrease of furfural yield upon the addition of furfural to a xylose solution indicates possible reaction of furfural with intermediate products (condensation reactions). The loss by the formation of humins from furfural is modeled as well.

The stripping of furfural from the reactor is described by introducing a mass transfer/ stripping diffusion constant K_S, which needs to be fitted to the experimental data. Values of 0.039-0.049 L min^{-1} are reported for this constant.

Where Agirrezabal-Tellaria et al. were able to model estimations in good agreement with the experimental data, it was not possible to reproduce the model with the given information.

The use of a simple mass transfer constant instead of an activity coefficient model as developed in this study is investigated.

Unfortunately Agirrezabal-Tellaria et al. do not mention the handling of the largest component in the reaction mixture, water. From the vapor-liquid equilibrium data (Figure 20) it is clear that the constant for the stripping of water will not be the same as the constant for the stripping of furfural. The ratio of $K_{S,F}/K_{S,W}$ is estimated to be 26.6 based on the activity data.

No value for K_S could be found the fit both the conversion of xylose and formation of furfural (in reactor and condensate). A K_S value of 0.004 L min^{-1}, similar to the values reported in literature, results in a

reasonable fit of the amount of furfural in the reactor, both overestimates the other components. To describe the condensate better a lower of value of 0.0023 L min^{-1} is required. The conversion of xylose is never described well using a constant K_S, but significant higher values of about 0.05 L min^{-1} result in the best fit. The results for the best fitted values are shown below in Figure 42.

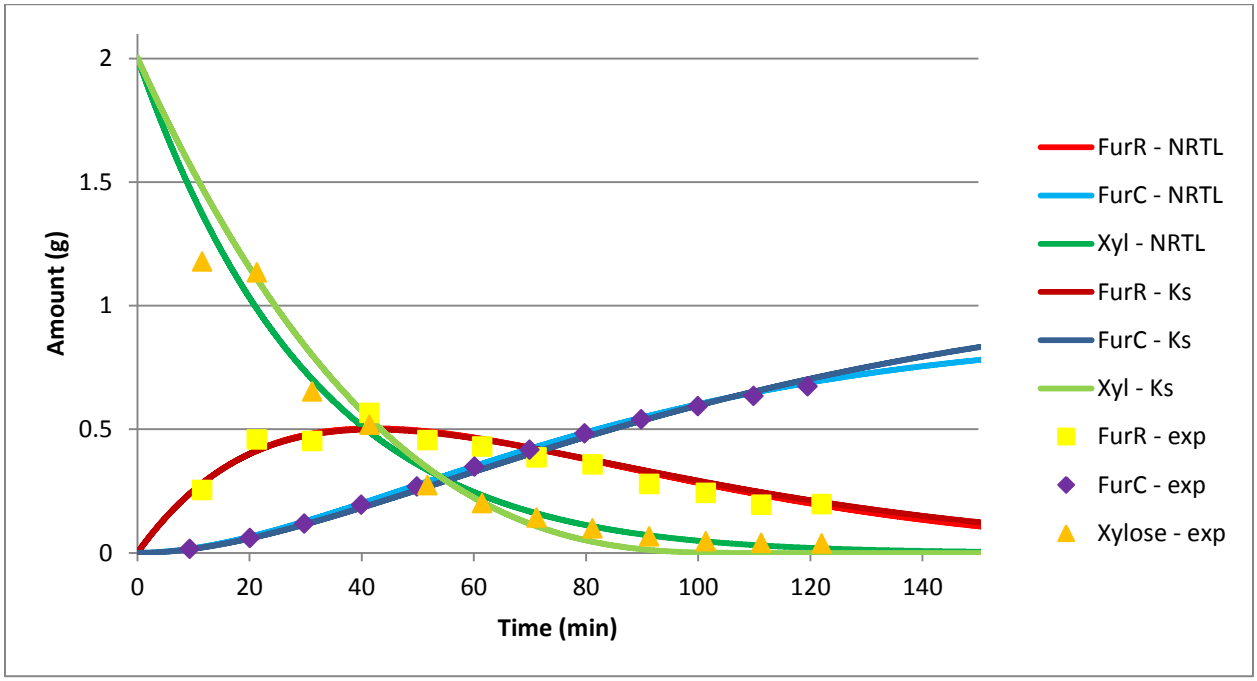

Figure 42: Three different Ks values are fitted to the experimental results for xylose and furfural; 170°C, 10 bar, 0.5 w% H_2SO_4, 1 w% initial xylose and 150 ml/min N_2 stripping stream.